

---

**lek. Albert Stachura**

**Wpływ N-acetylocysteiny na gojenie ran w zwierzęcym modelu  
cukrzycy**

**Rozprawa na stopień doktora nauk medycznych i nauk o zdrowiu  
w dyscyplinie nauki medyczne**

Promotor: prof. dr hab. n. med. Paweł Włodarski

Promotor pomocniczy: dr n. med. i n. o zdr. Wiktor Pascal

Zakład Metodologii Badań Naukowych



Obrona rozprawy doktorskiej przed Radą Dyscypliny Nauk Medycznych  
Warszawskiego Uniwersytetu Medycznego

Warszawa 2024 r.

*Paweł Włodarski*

---

**Słowa kluczowe:** N-acetylocysteina, gojenie ran, cukrzyca typu II, badanie *in vivo*, myszy db/db

**Keywords:** N-acetylcysteine, wound healing, type 2 diabetes mellitus, *in vivo* study, db/db mice

Rozprawa doktorska powstała w oparciu o wyniki projektu badawczego, który był finansowany z mini-grantu studenckiego nr 1MN/2/MG/N/20. Tytuł projektu badawczego: „Wpływ N-acetylocysteiny na gojenie ran chirurgicznych w modelu szczurów z cukrzycą streptozocynową”.

**Dedykacje:** Chciałbym zadedykować poniższą rozprawę wszystkim współautorom załączonych prac: Ishani Khannie, Piotrowi Krysiakowi, Profesorowi Marcinowi Sobczakowi, Karolinie Kędrze, Karolinie Kopce i Michałowi Kopce. W szczególności dziękuję moim promotorom Profesorowi Pawłowi Włodarskiemu i Doktorowi Wiktorowi Pascalowi, bez których wsparcia i zachęcenia nie postawiłbym kolejnych kroków na ścieżce rozwoju naukowego.

Ponadto pragnę podziękować moim rodzicom Kamilli i Albertowi Stachurom oraz przyjaciołom, których wsparcie było i pozostaje bezcenne: Roksanie, Zuzannie, Jakubowi W., Annie, Jakubowi P., Weronice, Marcie, Igorowi, Natalii.

**Wykaz publikacji stanowiących pracę doktorską:**

1. Stachura A, Khanna I, Krysiak P, Paskal W, Włodarski P. Wound Healing Impairment in Type 2 Diabetes Model of Leptin-Deficient Mice—A Mechanistic Systematic Review. *International Journal of Molecular Sciences*. 2022; 23(15):8621. <https://doi.org/10.3390/ijms23158621>
2. Stachura A, Sobczak M, Kędra K, Kopka M, Kopka K, Włodarski PK. The Influence of N-Acetylcysteine-Enriched Hydrogels on Wound Healing in a Murine Model of Type II Diabetes Mellitus. *International Journal of Molecular Sciences*. 2024; 25(18):9986. <https://doi.org/10.3390/ijms25189986>

---

## Spis treści

<b>1. Wykaz stosowanych skrótów</b> .....	<b>3</b>
<b>2. Streszczenie w języku polskim</b> .....	<b>4</b>
<b>3. Streszczenie w języku angielskim</b> .....	<b>4</b>
<b>4. Wstęp</b> .....	<b>5</b>
<b>5. Założenie i cel pracy</b> .....	<b>12</b>
5.1. Założenie i hipoteza badawcza.....	12
5.2. Cele pracy.....	12
<b>6. Kopie opublikowanych prac</b> .....	<b>12</b>
<b>7. Podsumowanie i wnioski</b> .....	<b>13</b>
<b>8. Opinia komisji etycznej</b> .....	<b>13</b>
<b>9. Oświadczenia współautorów publikacji</b> .....	<b>14</b>
<b>10. Referencje</b> .....	<b>15</b>

## 1. Wykaz stosowanych skrótów

AGE – zaawansowane produkty glikacji, ang. *advanced glycation end-products*

HBOT – tlenoterapia hiperbaryczna, ang. *hyperbaric oxygen therapy*

IL – interleukina

NAC – N-acetylocysteina

PDGF – płytkopochodny czynnik wzrostu, ang. *platelet-derived growth factor*

T.I.M.E.R.S. - *tissue debridement* – opracowanie tkanek, *infection and inflammation control* – kontrola infekcji i zapalenia, *moisture balance* – równowaga wilgoci, *epidermization stimulation* – pobudzenie naskórkowania, *repair and regeneration* – naprawa i regeneracja, *social and individual-related factors* – czynniki społeczne i indywidualne predyktory

TNF – czynnik martwicy nowotworu, ang. *tumor necrosis factor*

VAC – podciśnieniowa terapia ran, ang. *vaccum assisted closure*

---

## **2. Streszczenie w języku polskim**

Cukrzyca typu II jest powszechną chorobą cywilizacyjną. Jednym z najpoważniejszych powikłań tej choroby jest upośledzone gojenie ran, które w swojej zaawansowanej formie przybiera kliniczną postać owrzodzeń stopy cukrzycowej. Obecnie istnieje niewiele interwencji z udowodnioną skutecznością działania, które można by stosować lokalnie celem poprawy procesu gojenia ran cukrzycowych. Nowe interwencje powinny być testowane w pierwszej kolejności w badaniach przedklinicznych z zastosowaniem modelu jak najwierniej imitującego procesy zachodzące u człowieka. Myszim modele db/db i ob/ob polegają na upośledzeniu funkcjonowania leptyny. Konsekwencją jest fenotyp przypominający cukrzycę typu II, wynikający z nadmiernego łaknienia, wtórnej otyłości oraz powiązanych problemów metabolicznych, włączając w to opóźnione gojenie ran. W niniejszej rozprawie w systematyczny sposób podsumowałem literaturę dotyczącą mechanizmów upośledzonego gojenia ran w mysim modelu z dysfunkcją leptyny. Wykazałem, że pomimo niektórych ograniczeń, model ten w pewnym stopniu odzwierciedla patofizjologię gojenia ran cukrzycowych u ludzi oraz był dotychczas szeroko stosowany w literaturze. Ze względu na potrzebę identyfikacji łatwo dostępnych oraz tanich substancji, mogących wspomagać gojenie ran cukrzycowych, w rozprawie tej skupiłem się na badaniu N-acetylocysteiny. Cząsteczka ta miała dotychczas udowodnione korzystne działanie we wspomaganiu regeneracji ran w modelach zdrowych zwierząt oraz modelach imitujących fenotyp cukrzycy typu I. W drugiej części niniejszej rozprawy opisany został eksperyment z wykorzystaniem hydrożeli uwalniających N-acetylocysteinę w różnych stężeniach. Porównano skuteczność tych hydrożeli z placebo, pokazując, że 5% N-acetylocysteina uwalniana w obrębie rany mogła przyspieszyć gojenie na wczesnym etapie regeneracji w mysim modelu db/db. Dalsze badania są wskazane celem potwierdzenia dotychczasowych wyników, optymalizacji drogi podania oraz stężenia N-acetylocysteiny w kontekście gojenia ran cukrzycowych.

## **3. Streszczenie w języku angielskim**

Type II diabetes mellitus is a common disease. One of the most severe complications of this disease is impaired wound healing, which in its advanced form takes the clinical form of diabetic foot ulcers. Currently, there are few interventions with proven efficacy that can be applied locally to improve diabetic wound healing. New interventions should be tested first in preclinical setting using a model that mimics the human processes as closely as possible. db/db and ob/ob murine models rely on impaired leptin function. The consequence is a phenotype resembling type II diabetes, resulting in excessive craving, secondary obesity and associated



---

metabolic abnormalities, including delayed wound healing. In this thesis, I have systematically summarised the literature on the mechanisms of impaired wound healing in a murine model of leptin dysfunction. I have shown that, despite some limitations, this model reflects to some extent the pathophysiology of diabetic wound healing in humans and has been widely used in the literature to date. Due to the need to identify readily available and affordable substances that can promote diabetic wound healing, in this dissertation I focused on the study of N-acetylcysteine. This molecule has so far been shown to have beneficial effects in supporting wound regeneration in healthy animal models and models mimicking the phenotype of type I diabetes mellitus. In the second part of this dissertation, an experiment using hydrogels releasing N-acetylcysteine at different concentrations is described. The efficacy of these hydrogels was compared with placebo, showing that 5% N-acetylcysteine released within the wound was able to accelerate healing at an early stage of regeneration in a murine model of db/db. Further studies are indicated to confirm the current results, optimise the route of administration and the concentration of N-acetylcysteine in the context of diabetic wound healing.

## 4. Wstęp

Cukrzyca typu 2 charakteryzuje się hiperglikemią, insulinoopornością i względnym upośledzeniem wydzielania insuliny. Choroba ta jest powszechnym zaburzeniem, którego częstość występowania znacznie wzrasta wraz ze wzrostem stopnia otyłości i wieku.<sup>1</sup> Częstość występowania cukrzycy typu 2 wzrosła alarmująco w ciągu ostatniej dekady,<sup>2,3</sup> w dużej mierze w związku z tendencjami do otyłości i siedzącego trybu życia.<sup>4</sup> Według raportu Global Burden of Disease 2021 cukrzyca jest 10. główną przyczyną zgonów i 7. główną przyczyną obciążenia chorobami na całym świecie.<sup>5</sup> Ryzyko wystąpienia owrzodzenia stopy cukrzycowej u osób z cukrzycą wynosi od 19% do 34%.<sup>6</sup> Cukrzyca jest również często związana z powikłanym gojeniem się ran.<sup>7</sup> Chociaż chirurgiczne oczyszczenie rany pozostaje złotym standardem w leczeniu ran cukrzycowych, pilnie potrzebne są dodatkowe metody leczenia w celu poprawy wyników pacjentów.<sup>8</sup>

Jednym z głównych powikłań cukrzycy jest upośledzone gojenie ran.<sup>9</sup> Jest to związane z czynnikami zewnętrznymi i wewnętrznymi. Do pierwszych należą powtarzalne urazy, na które osoby z cukrzycą mogą być mniej uważne ze względu na zaburzenia czucia spowodowane neuropatią obwodową oraz zaburzeniem krążenia w małych naczyniach. Hiperglikemia może mieć szkodliwy wpływ na gojenie się ran poprzez tworzenie zaawansowanych końcowych produktów glikacji (AGE), które indukują produkcję cząsteczek zapalnych (TNF- $\alpha$ , IL-1) i zakłócają syntezę kolagenu.<sup>10</sup> Wysoki poziom glukozy jest także związany ze zmianami w

---

morfologii komórek, zmniejszoną proliferacją i nieprawidłowym różnicowaniem keratynocytów.<sup>11</sup> Zmieniona funkcja układu odpornościowego może również przyczyniać się do słabego gojenia się ran u pacjentów z cukrzycą. Zmniejszona chemotaksja, fagocytoza i zabijanie bakterii są związane z wczesną fazą gojenia się ran w cukrzycy.<sup>12</sup> Upośledzona infiltracja leukocytów i IL-6 w płynie z rany charakteryzują późne fazy zapalne gojenia się ran w cukrzycy.<sup>13</sup> Wydaje się zatem, że zmieniony wzór pojawiania się cytokin w środowisku rany może przyczyniać się do opóźnionego gojenia.

Badanie skuteczności nowych interwencji często zaczynają się od badań *in vitro* lub *in vivo*. Wybór modelu jest jednak kluczowy dla zwiększenia prawdopodobieństwa translacji wyników z etapu przedklinicznego do badań klinicznych. W szczególności w kontekście wieloczynnikowego procesu upośledzenia gojenia ran w cukrzycy typu II wybór odpowiedniego modelu zwierzęcego stanowi wyzwanie.

W poniższej rozprawie połączyłem dwie publikacje w jeden cykl tematyczny.<sup>14,15</sup> Pierwsza z nich to przegląd systematyczny, podsumowujący dotychczasową literaturę omawiającą mechanizmy upośledzenia gojenia ran w mysim modelu z deficytem leptyny (db/db lub ob/ob). Praca ta powstała z uwagi na potrzebę uporządkowania wiedzy w zakresie podobieństw i różnic pomiędzy gojeniem ran u pacjentów z cukrzycą oraz gojeniem ran w modelu, który mógłby imitować procesy, zachodzące u ludzi. Wybór modelu *in vivo*, który adekwatnie odwzorowałby ludzką dynamikę gojenia, stanowi wyzwanie.<sup>16</sup> Zrozumienie patofizjologii gojenia ran jest niezbędne do zbadania nowych interwencji terapeutycznych. W związku z tym opracowano kilka modeli eksperymentalnych, głównie zwierzęcych, stosowanych w celu zbadania odpowiedzi komórkowych i molekularnych w gojeniu ran. Właściwy wybór tych zwierzęcych modeli ma kluczowe znaczenie, ponieważ każdy model ma swoje zalety i wady.

Jednym z wyzwań doboru odpowiedniego modelu zwierzęcego jest wybranie gatunku. Możliwe jest przeprowadzenie badań na świniami, świnkach morskich, królikach, szczurach czy myszach.<sup>16</sup> Świński model jest uważany za standardowy przedkliniczny model gojenia się ran ze względu na uderzające podobieństwa do ran ludzkich, w tym reepitelializację zamiast obkurczania naskórka (jak u gryzoni). Anatomicznie, fizjologicznie i metabolicznie, świnie są bardziej podobne do ludzi na kilka sposobów, co czyni je lepszym wyborem w przypadku badania gojenia ran niż gryzoni.<sup>17</sup> Królik jest najpowszechniej wykorzystywanym zwierzęciem laboratoryjnym po myszach i szczurach. U królików ucho jest najbardziej preferowanym narządem wykorzystywanym do tworzenia ran niedokrwiennych w celu badania wpływu niedotlenienia na gojenie się ran. Powodem jego szerokiego zastosowania jest ubogie unaczynienie, które prowadzi do dominującego mechanizmu epitelializacji i ziarninowania w

---

celu gojenia się ran, a nie obkurczania skóry.<sup>18</sup> Co więcej, niedokrwienie jest odwracalne i trwa około 14 dni, aby rozwinąć krążenie oboczne. Ponadto model ten oferuje większą powierzchnię, na której można tworzyć analogiczne rany w tym samym uchu, a drugie ucho można wykorzystać jako grupę kontrolną.<sup>19</sup> Co więcej, model ucha królika został również wykorzystany do zbadania wpływu różnych miejscowych czynników wzrostu na gojenie się ran.

Szczur jest najczęściej wykorzystywanym modelem gryzonia, zwłaszcza w badaniach związanych z gojeniem się ran ostrych. Ponieważ są one stosunkowo mniejsze, łatwe w obsłudze i relatywnie tanie, mają przewagę w porównaniu z innymi zwierzętami. Co więcej, genetycznie zmodyfikowane szczury zostały opracowane w taki sposób, aby można je było wykorzystać do badania różnych szlaków i produktów pośrednich zaangażowanych w gojenie i reepitelializację. Jednak szczury mają inną fizjologię, krótszą żywotność i mniejsze rozmiary ciała niż ludzie. Nie są w stanie skutecznie odtworzyć pełnej patogenezy niektórych chorób, m. in. cukrzycy. Gojenie się ran u szczurów i ludzi ma podobne odrębne fazy złożonych zdarzeń komórkowych, takich jak zapalenie, proliferacja i przebudowa. Jednak pełne procesy molekularne nie są w pełni zrozumiałe. Chociaż szczur i ludzie mają podobne warstwy skóry, istnieje znaczna różnica w ich grubości. Ludzka skóra jest stosunkowo grubsza niż u jakiegokolwiek innego zwierzęcia, a skóra przylega do leżącej pod nią tkanki. Ludzki naskórek składa się z 5-10 warstw komórek. Z kolei skóra szczura jest delikatna i luźna. Naskórek szczura składa się z 2 lub 3 warstw. Co więcej, warstwa podskórna szczurów składa się z *panniculus carnosus*, który jest nieobecny w ludzkiej skórze. Ta cienka warstwa *panniculus carnosus* wpływa na biomechanizm gojenia poprzez promowanie szybszego kurczenia się ran o pełnej grubości u szczurów. Ludzka skóra właściwa jest przymocowana do warstwy podskórnej; w związku z tym rany pełnej grubości u ludzi goją się poprzez granulację i reepitelizację. Chociaż luźna skóra i skurcz utrudniają badanie zdarzeń zachodzących u ludzi, nie może to być powodem do wykluczenia modelu szczurzego w badaniach gojenia się ran, ale należy zachować ostrożność przy interpretacji wyników.<sup>20</sup>

Myszy są jednym z najczęściej wykorzystywanych modeli gryzoni do badania gojenia ran. Mają luźną skórę i warstwę *panniculus carnosus* podobną do szczurów, która sprawia, że gojenie odbywa się głównie poprzez skurcz, a nie reepitelializację. W kilku badaniach nad gojeniem się ran wykorzystano myszy jako model nie tylko ze względu na ich rozmiar, szeroką dostępność i większą zmienność genetyczną. Innym powodem jest dostępność szerokiej wiedzy zdobytej przez lata wcześniejszych badań. Co więcej, świnie nie są dobrze scharakteryzowane na poziomie komórkowym i fizjologicznym w porównaniu do myszy, a specyficzne odczynniki dla świń, takie jak przeciwciała i czynniki wzrostu, nadal nie są dostępne. Z tego powodu

---

zdecydowana większość badań dotyczących gojenia się ran skóry jest przeprowadzana na myszach i szczurach.<sup>16</sup>

Kolejnym istotnym aspektem doboru modelu zwierzęcego do badania gojenia ran w modelu cukrzycy jest odpowiedni dobór metody, odpowiedzialnej za wzrost glikemii u zwierzęcia. Metody takie jak indukcja alloxanem czy streptozotocyną prowadzą do uszkodzenia komórek  $\beta$  trzustki produkujących insulinę, wtórnego zmniejszenia wydzielania insuliny i zwiększenia glikemii.<sup>21</sup> Co istotne, upośledzenie gojenia ran nie jest skorelowane ze zwiększonym stężeniem glukozy w surowicy, ale raczej jest powiązane z metabolicznymi konsekwencjami otyłości.<sup>22</sup> W istocie modele zwierzęce, w których cukrzyca była indukowana substancjami (przypominając tym samym fenotyp cukrzycy typu I), wykazywały mniejsze upośledzenie gojenia ran niż modele imitujące cukrzycę typu II.<sup>23</sup> Wobec tego używanie modelu imitującego cukrzycę typu II wydaje się bardziej uzasadnione w kontekście eksperymentów badających opóźnione gojenie ran oraz potencjalne interwencje, mogące usprawniać ten proces.

Ze względu na dostępność, relatywnie niskie koszty zakupu i utrzymania oraz łatwość w obsłudze, gryzonie są chętniej wybieranym modelem zwierzęcym do badania gojenia ran. Wśród myszy, modele db/db oraz ob/ob są najczęściej używanymi zwierzętami, imitującymi fenotyp cukrzycy typu II. Pierwszy z nich polega na mutacji punktowej genu receptora dla leptyny, drugi zaś na mutacji punktowej genu odpowiedzialnego za ekspresję leptyny. Efektywnie, oba modele prowadzą do upośledzenia przekąźnictwa leptynowego, wtórnego odhamowania głodu oraz rozwoju otyłości ze wszystkimi konsekwencjami metabolicznymi, w tym upośledzonym gojeniem ran.<sup>14</sup>

Zrozumienie mechanizmów, które stoją za wadliwym procesem regeneracji skóry w tym modelu, jest niezbędne do prawidłowego planowania eksperymentów oraz interpretacji wyników badań, w których stosowane są nowe interwencje. W moim przeglądzie systematycznym podsumowałem dane dotyczące gojenia ran w modelach db/db oraz ob/ob, omawiając następujące aspekty:

- Fenotyp oraz dynamikę gojenia ran
- Czynniki wzrostu
- Angiogenezę
- Cytokiny i mechanizmy immunologiczne
- Funkcjonowanie makrofagów
- Konsekwencja dysfunkcji szlaku leptynowego
- Działanie insuliny

- 
- Zaawansowane produkty glikacji, ang. *Advanced Glycation End-Products* (AGEs)
  - Fibroblasty i macierz pozakomórkową
  - Apoptozę i autofagię
  - Mechanizm działania komórek macierzystych pochodzenia szpikowego
  - Rolę niekodujących fragmentów RNA (ang. *non-coding RNA*)
  - Funkcję bakterii i biofilmu

Ponadto omówiłem modyfikacje ww. modeli, które zostały opracowane przy okazji innych eksperymentów i służyły dopasowaniu do bardziej specyficznych pytań badawczych. Celem powyższego przeglądu było systematyczne przedstawienie mechanizmów, które zarządzają gojeniem ran w mysim modelu cukrzycy typu II, w którym upośledzony jest szlak leptynowy. Korzyścią tego badania dla badaczy jest to, że przy planowaniu swoich eksperymentów mogą posiłkować się zebraną literaturą, by planować dobór odpowiednich interwencji, a także wybierać pierwszo- oraz drugorzędowe punkty końcowe badań, które wykazałyby skuteczność stosowanych interwencji oraz tłumaczyły ich mechanizm działania. Przegląd też stanowił również wstęp do problemu adresowanego przez badanie oryginalne, które również stanowi część niniejszego cyklu.

Wiele publikacji było dotychczas poświęconych poszukiwaniu interwencji, która byłaby skuteczna w gojeniu ran cukrzycowych, w szczególności powikłania, jakim jest owrzodzenie stopy cukrzycowej. Jednak tylko kilka z nich przeszło fazę przedkliniczną i weszło do badań klinicznych na ludziach.<sup>14</sup> Płytkopochodny czynnik wzrostu (PDGF) był skuteczny w badaniach przedklinicznych, a jego rekombinowana forma, Becaplermin (REGRANEX® Gel), została zatwierdzona do miejscowego leczenia owrzodzeń neuropatycznych kończyn dolnych, które wykraczają poza tkankę podskórną.<sup>24</sup> Niestety, w 2008 r. do żelu dodano ostrzeżenie, ponieważ zaobserwowano zwiększony odsetek zgonów z powodu ogólnoustrojowych nowotworów złośliwych u pacjentów, którzy otrzymali trzy lub więcej dawek leku.<sup>25</sup>

Obecnie pierwszą linią leczenia ran cukrzycowych, w szczególności stopy cukrzycowej jest usunięcie tkanki martwiczej (debridement).<sup>26</sup> Częstotliwość oceny i właściwa opieka mogą mieć większy wpływ na gojenie się ran niż rodzaj oczyszczania. W przeglądzie, w którym badano opiekę nad ranami przewlekłymi wśród weteranów, szansa na wygojenie owrzodzenia cukrzycowego wzrosła 2,5-krotnie, gdy oczyszczenie rany było wykonywane podczas 80% wizyt i podwoiła się, gdy niedokrwienie zostało ocenione podczas pierwszej wizyty.<sup>27</sup>

---

Interwencje pomocnicze stosowane lokalnie w przypadku owrzodzenia stopy cukrzycowej są ograniczone. Jedną z nich jest podciśnieniowa terapia ran (VAC), która polega na zastosowaniu kontrolowanego podciśnienia na powierzchni owrzodzenia. Metoda ta poprawia gojenie poprzez zwiększenie perfuzji rany, zmniejszenie obrzęku, zmniejszenie miejscowego obciążenia bakteryjnego i zwiększenie tworzenia się tkanki ziarninowej.<sup>28</sup> Przeszczepy ludzkiej skóry i bioinżynieryjne substytuty skóry (np. Dermagraft, Apligraf, TheraSkin, Graftskin, EpiFix, Zelen, Graftjacket, Hyalograft 3D, Kaloderm, OrCel) były badane u osób z niezakażonymi, niedokrwiennymi przewlekłymi owrzodzeniami stopy cukrzycowej. Przegląd systematyczny 17 badań z randomizacją wykazał, że częstość występowania całkowitego zamknięcia owrzodzeń stopy cukrzycowej była znacznie lepsza w przypadku przeszczepów skóry lub substytutów w porównaniu ze standardową opieką.<sup>29</sup> Tlenoterapia hiperbaryczna (HBOT) może być związana z poprawą gojenia jako element leczenia owrzodzeń cukrzycowych, ale wskazania do HBOT w leczeniu niegojących się owrzodzeń stopy cukrzycowej pozostają niepewne. Większość meta-analiz sugeruje, że hiperbaryczna terapia tlenowa może przynieść korzyści w leczeniu owrzodzeń stopy cukrzycowej; jednak jakość badań włączonych do przeglądów systematycznych jest zróżnicowana.<sup>30,31</sup> Dostępne badania są ograniczone przez małą liczebność próby i niejednorodność leczonych ran (np. rozmiar owrzodzenia, głębokość owrzodzenia, środowisko mikrobiologiczne, obecność niedokrwienia). Wymienione opcje stanowią jednak formę wspomagającą terapii gojenia ran cukrzycowych.

Po prawidłowym oczyszczeniu rany kluczowe jest nałożenie odpowiedniego opatrunku. Niektóre opatrunki po prostu zapewniają ochronę, podczas gdy inne promują nawilżenie rany lub zapobiegają nadmiernej wilgoci. Często stosowane są opatrunki z solą fizjologiczną, ale mogą one usuwać zarówno martwą, jak i żywą tkankę, co może skutkować wyschnięciem rany. Inne opatrunki są impregnowane środkami przeciwdrobnoustrojowymi, aby zapobiec infekcji i tworzeniu biofilmu bakteryjnego. W przypadku leczenia owrzodzeń stóp u pacjentów z cukrzycą nie ma wysokiej jakości dowodów sugerujących jakiegokolwiek znaczące różnice w wynikach gojenia ran przy porównywaniu różnych rodzajów opatrunków.<sup>32</sup> Do najpopularniejszych typów opatrunków należą opatrunki żelowe, hydrokoloidowe, włókniste, z alginianu wapnia, kolagenowe, foliowe, zawierając związki srebra oraz siatkowe. Heterogenność w badaniach ran przewlekłych oraz brak konkluzyjnych wskazań optymalnych opatrunków wynika również ze złożonego procesu doboru opatrunków do etapu gojenia rany. W tym celu stosuje się zasady T.I.M.E.R.S (tissue debridement – opracowanie tkanek, infection and inflammation control – kontrola infekcji i zapalenia, moisture balance – równowaga wilgoci, epidermization stimulation – pobudzenie naskórkowania, repair and regeneration –

---

naprawa i regeneracja, social and individual-related factors – czynniki społeczne i indywidualne predyktory) celem indywidualizacji leczenia opatrunkowego.<sup>33</sup> Ze względu na światowe rozpowszechnienie cukrzycy oraz jej powikłań, istnieje potrzeba zidentyfikowania łatwo dostępnych substancji, które mogłyby być dodawane do opatrunków i byłyby skuteczne w poprawie gojenia ran cukrzycowych.

N-acetylocysteina (NAC) jest przeciwutleniaczem i pochodną cysteiny, który silnie uzupełnia wewnątrzkomórkowe poziomy glutationu.<sup>34</sup> Reguluje również ekspresję genów,<sup>35</sup> może zapobiegać apoptozie i promować przeżycie komórek oraz bezpośrednio zmniejszać aktywność wybranych białek.<sup>35</sup> Choć niespecyficzna, substancja ta była szeroko stosowana: jako środek mukolityczny, antidotum na zatrucie paracetamolem, środek przeciwdziałający kardiotoksyczności doksorubicyny lub zmniejszający uszkodzenie serca w wyniku niedokrwienia/reperfuzji.<sup>36</sup> Substancja ta była stosowana w dermatologii oraz testowana w psychiatrii.<sup>37,38</sup> Dawki i drogi podania różnią się znacznie w zależności od wskazania. Wysokie dawki do 3000 mg/dobę doustnie lub w stężeniu 20% stosowane miejscowo były stosowane u ludzi z dobrą tolerancją.<sup>39,40</sup>

Zastosowanie NAC było również badane w kontekście gojenia ran. Proces ten obejmuje cztery kolejne fazy: hemostazę, stan zapalny, proliferację i przebudowę.<sup>41</sup> Ponieważ NAC może zmniejszać dysfunkcję śródbłonna i stan zapalny, a także przyspieszać proliferację komórkową,<sup>35</sup> została uznana za kandydata do interwencji w celu poprawy gojenia ran. Miejscowo stosowana 3% NAC promowała ponowną epitelializację w szczurzym modelu ran oparzeniowych i, w tym samym stężeniu, poprawiała angiogenezę i szybkość gojenia ran w modelu rany wycięciowej.<sup>42,43</sup> Tsai i wsp. wykazali, że korzystny efekt NAC był zależny od dawki i osiągał maksimum przy stężeniu 3% (maksymalne testowane w ramach badania).<sup>42</sup> Pojedyncze wstrzyknięcie 0,03% NAC zmniejszyło obszar i szerokość blizny w modelu gojenia się rany nacięciowej szczura.<sup>44</sup>

W drugim badaniu w ramach niniejszej rozprawy wykazałem, że hydrożel wzbogacany 5% NAC przyspiesza gojenie rany wycięciowej na wczesnym etapie u myszy z upośledzonym przekazywaniem leptynowym. Poprawa ta była powiązana ze zwiększonym obszarem intensywnej proliferacji w obrębie skóry właściwej, bezpośrednio przylegającej do rany.<sup>15</sup> Praca ta stanowi pierwszą na świecie, w której badano wpływ N-acetylocysteiny na gojenie ran w zwierzęcym modelu imitującym cukrzycę typu II.

---

## **5. Założenie i cel pracy**

### **5.1. Założenie i hipoteza badawcza**

Założeniem niniejszej rozprawy było to, że w świetle obecnie dostępnej literatury N-acetylocysteina ma obiecujący potencjał w zakresie wspomagania gojenia ran. Dotychczasowe prace były poświęcone badaniu ran u zdrowych zwierząt lub ran, które były tworzone u zwierząt z indukowaną substancjami imitacją cukrzycy typu I. Dane wskazywały na korzystny wpływ N-acetylocysteiny we wszystkich tych przypadkach. Założeniem pracy było zatem, że N-acetylocysteina powinna również mieć korzystny wpływ na gojenie ran w bardziej skomplikowanym modelu ran, mianowicie u myszy z deficytem leptynowym, imitującym fenotyp cukrzycy typu II. Hipotezą badawczą było to, że hydrożele z N-acetylocysteiną przyspieszą czas gojenia ran wycięciowych w mysim modelu db/db.

### **5.2. Cele pracy**

Pierwszorzędowym celem badawczym było określenie szybkości gojenia ran opatrzonych hydrożelami z różnym stężeniem N-acetylocysteiny (5%, 10%, 20%) lub placebo. Ten punkt końcowy był mierzony poprzez szacowanie obszaru rany co 3 dni od momentu wytworzenia ran na podstawie dokumentacji fotograficznej.

Drugorzędowymi celami badawczymi było:

- Określenie parametrów morfometrycznych preparatów histologicznych ran, barwionych hematoksyliną i eozyną. Miało to pozwolić określić zmiany zachodzące w obrębie rany na poziomie mikroskopowym.
- Określenie gęstości oraz dystrybucji włókien kolagenowych w obrębie ran.
- Określenie odsetka makrofagów o fenotypie M1, czyli prozapalnych oraz M2, które biorą udział w przebudowie macierzy pozakomórkowej na etapie remodelingu rany. Cel ten został obrany ze względu na opóźnione przejście fenotypu z M1 do M2 w przypadku ran cukrzycowych. Zastosowanie substancji łagodzącej proces zapalny teoretycznie mogło wspomóc ten proces.

## **6. Kopie opublikowanych prac**

Na kolejnej stronie w pierwszej kolejności przedstawiony jest opublikowany przegląd systematyczny, a po nim praca oryginalna.





Review

# Wound Healing Impairment in Type 2 Diabetes Model of Leptin-Deficient Mice—A Mechanistic Systematic Review

Albert Stachura <sup>1,2</sup>, Ishani Khanna <sup>1</sup>, Piotr Krysiak <sup>1</sup>, Wiktor Paskal <sup>1</sup> and Paweł Włodarski <sup>1,\*</sup>

<sup>1</sup> Center for Preclinical Research, Department of Methodology, Medical University of Warsaw, 02-091 Warsaw, Poland; albert.stachura@wum.edu.pl (A.S.); s079327@student.wum.edu.pl (I.K.); s082108@student.wum.edu.pl (P.K.); wikt.paskal@wum.edu.pl (W.P.)

<sup>2</sup> Doctoral School, Medical University of Warsaw, 02-091 Warsaw, Poland

\* Correspondence: pawel.wlodarski@wum.edu.pl

**Abstract:** Type II diabetes mellitus (T2DM) is one of the most prevalent diseases in the world, associated with diabetic foot ulcers and impaired wound healing. There is an ongoing need for interventions effective in treating these two problems. Pre-clinical studies in this field rely on adequate animal models. However, producing such a model is near-impossible given the complex and multifactorial pathogenesis of T2DM. A leptin-deficient murine model was developed in 1959 and relies on either dysfunctional leptin (*ob/ob*) or a leptin receptor (*db/db*). Though monogenic, this model has been used in hundreds of studies, including diabetic wound healing research. In this study, we systematically summarize data from over one hundred studies, which described the mechanisms underlying wound healing impairment in this model. We briefly review the wound healing dynamics, growth factors' dysregulation, angiogenesis, inflammation, the function of leptin and insulin, the role of advanced glycation end-products, extracellular matrix abnormalities, stem cells' dysregulation, and the role of non-coding RNAs. Some studies investigated novel chronic diabetes wound models, based on a leptin-deficient murine model, which was also described. We also discussed the interventions studied *in vivo*, which passed into human clinical trials. It is our hope that this review will help plan future research.

**Keywords:** diabetes; wound; leptin; wound healing; *db/db*; *ob/ob*; mice; wound healing in metabolic disease; wound healing in chronic disease; molecular mechanisms in wound healing



**Citation:** Stachura, A.; Khanna, I.; Krysiak, P.; Paskal, W.; Włodarski, P. Wound Healing Impairment in Type 2 Diabetes Model of Leptin-Deficient Mice—A Mechanistic Systematic Review. *Int. J. Mol. Sci.* **2022**, *23*, 8621. <https://doi.org/10.3390/ijms23158621>

Academic Editor: Desire' Pantalone

Received: 30 June 2022

Accepted: 29 July 2022

Published: 3 August 2022

**Publisher's Note:** MDPI stays neutral with regard to jurisdictional claims in published maps and institutional affiliations.



**Copyright:** © 2022 by the authors. Licensee MDPI, Basel, Switzerland. This article is an open access article distributed under the terms and conditions of the Creative Commons Attribution (CC BY) license (<https://creativecommons.org/licenses/by/4.0/>).

## 1. Introduction

Within the past three decades, the number of people with diabetes mellitus has multiplied exponentially, making it the ninth major cause of death. Type II Diabetes Mellitus (T2DM) leads to impaired wound healing and hence, diabetic foot ulcers are a leading cause of non-traumatic lower-limb amputations worldwide [1–3]. The lifetime risk of developing a diabetic foot ulcer is between 19% and 34% [4]. A variety of therapies have been suggested for the treatment of diabetic ulcers; however, there is still an on-going search for productive treatment. This may be due to the lack of knowledge regarding the complex mechanisms involved in the development of unhealed wounds in diabetes.

Considerable resources have been devoted to developing animal models in order to research wound healing in T2DM. Among the frequently used animal models are the diabetic rodent models: *db/db* and *ob/ob* mice. *Ob/ob* mice lack functional leptin due to a single autosomal recessive mutation on the obese gene (chromosome 6) whereas *db/db* mice lack functional leptin receptors due to a single autosomal mutation on the leptin receptor gene (chromosome 4). These rodent models classify diabetes as a monogenic disease in comparison to the etiology of the human T2DM, which is polygenic as well as multifactorial in nature. Thus, even though such models are useful for research purposes, the information obtained from studies utilizing them is of limited use [5].

The animal models available for diabetes research are most often more like maturity-onset diabetes in humans. The same initial sequence of events occurs in both strains, which includes hyperphagia that is followed by a further compensatory increase in insulin secretion, and by an expansion of the Beta-cell mass. The two strains chosen for this review differ in a subsequent manifestation of the db/db mutation. The C57BL/KsJ strain presents only primary and transient hyperinsulinemia, which completely reverses and leads to insulinopenia and hyperglycemia over time. This is caused by an expansion failure of Beta cells and results in islet atrophy. C57BL/6J strain, on the other hand, manifests the mutation with islet hyperplasia that causes permanent hyperinsulinemia. These metabolic irregularities in both strains lead to obesity, specifically in the C57BL/KsJ case. Because of a raised insulin level, we can observe increased activity of gluconeogenic enzymes. Both mutants are infertile and have defects in thermoregulation. One of the main differences between C57BL/KsJ and C57BL/6J strains is the intensity of developed diabetes, a mild one in the 6J case and severe in KsJ [6,7].

In this review, we analyze the molecular mechanics of wound healing within these leptin-deficient mice models. Though the models have been in use for decades, new data accumulated gradually over time and have not been systematically described or analyzed. This article is the first to provide a comprehensive overview of wound healing biology in ob/ob and db/db mice. It also discusses different variants of wound creation (including models of chronic infected wounds) and some interventions that have been studied using this model, which passed into clinical trials. Lastly, we underline some of the key limitations and points to be considered when interpreting studies utilizing these models or planning a new experiment.

## 2. Methods

This study was conducted in accordance with the Preferred Reporting Items for Systematic Reviews and Meta-Analyses (PRISMA) guidelines [8], using a previously designed protocol (Supplementary File S1). We searched for *in vivo* studies investigating leptin-deficient mice (db/db or ob/ob) with wounds or ulcers. These included studies assessing wound healing after an intervention or aimed to analyze the molecular mechanisms within the leptin-deficient mice model. All articles written in English were included, excluding reviews, letters, and editorials. Conference papers or papers without full text were excluded.

We searched using electronic databases: MEDLINE, EMBASE, Web of Science, and Scopus. To identify all relevant articles, we used prespecified search engines for each database (Supplementary File S1). On 5 May 2021, two independent reviewers (AS, IK) conducted a systematic search of the literature.

### 2.1. Study Selection

Each relevant publication was categorized using the PICO model. Articles were included based on predefined selection criteria, or the appropriate PICO: leptin-deficient mice and db/db or ob/ob with wounds or ulcers, with any possible interventions or comparisons, assessing wound healing. Wound healing was assessed macroscopically and histologically, or molecular analyses were conducted. Exclusion criteria were human studies, review letters and editorials, inadequate PICO, and a substantial lack of methodology.

Study eligibility was assessed by screening titles and if necessary, abstracts. Later, full texts were assessed for inclusion and exclusion criteria. All disagreements were resolved by a consensus between the two reviewers.

### 2.2. Data Extraction and Analyses

Studies were divided into two categories, intervention studies and model studies, i.e., studies aiming to identify the molecular mechanisms within the leptin-deficient mice model. The following information was extracted from each intervention study by IK and PK: animal strain, wounding model (excisional, incisional, ischemic), type of intervention, and the type of wound healing outcomes (macroscopic, histological, or molecular analyses).

The following information was extracted from each model study by AS: animal strain, age, and sex, as well as main outcomes. AS assessed the data extraction procedure and implemented necessary corrections.

We did not perform quantitative statistical analysis of the selected studies because of methodological heterogeneity. A systematic review of the methodology and outcomes was undertaken instead.

The primary search yielded 1433 scientific papers (Figure 1). Eventually, 105 model studies were included in this review. The most used interventions from 361 *in vivo* studies were summarized at the end of the literature review.

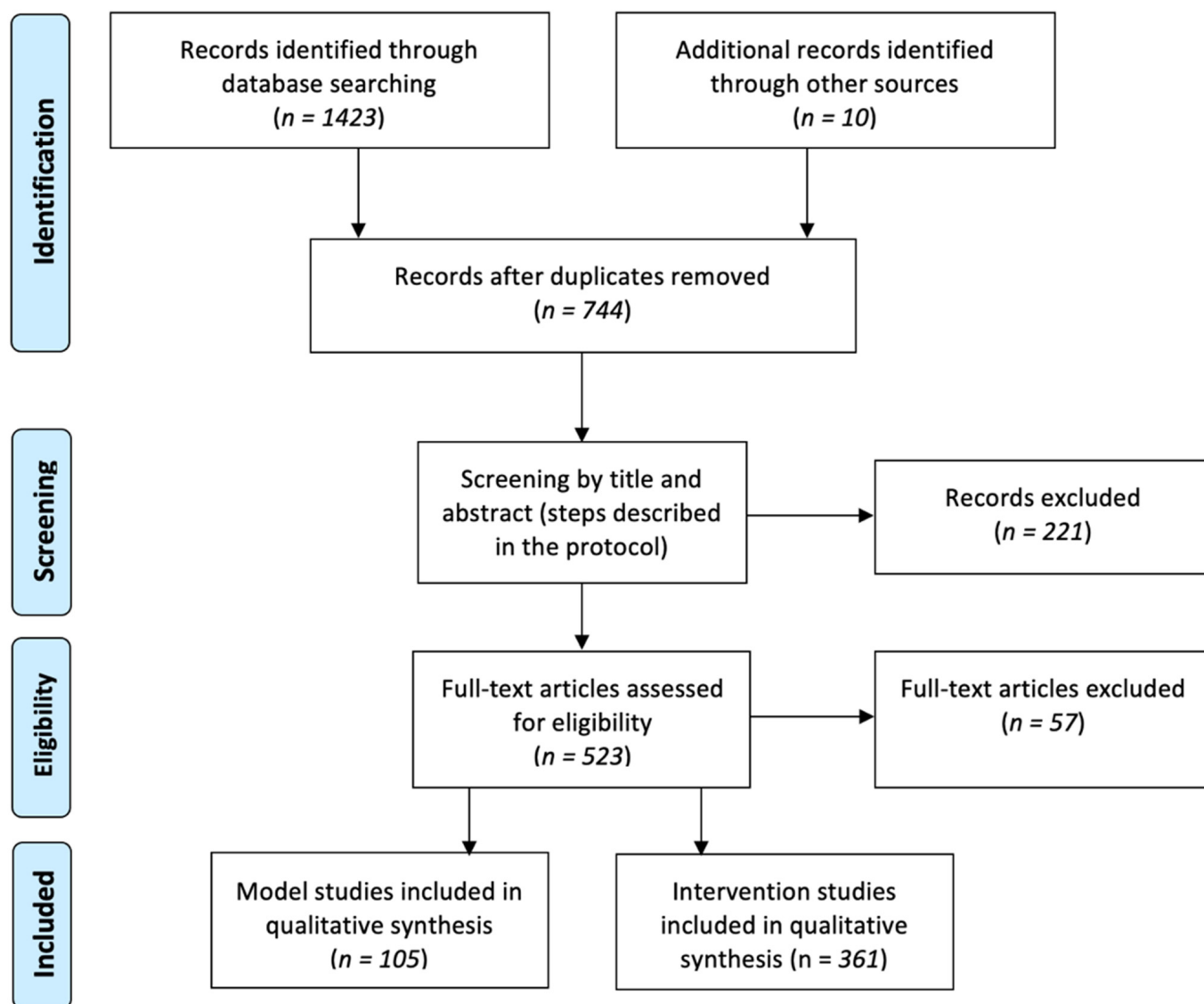


Figure 1. PRISMA flowchart of article selection.

### 3. Results and Discussion

#### 3.1. Literature Review

##### 3.1.1. Phenotype and Wound Healing Dynamics

Both leptin-deficient mice strains are characterized by a specific phenotype and wound healing dynamic. Animals have larger subdermal fat thicknesses and smaller dermal thicknesses. Reepithelialization plays a bigger role than contraction in wound healing [9]. Aged db/db have lower wound breaking strength and stiffness than younger db/db and healthy controls (young or aged). Hyperglycemia does not correlate with impaired wound

healing [10]. Topically applied substances do not spread to adjacent wounds in db/db mice when four 6 mm wounds are created on their backs [11]. Db/db strains do not differ in their susceptibility to I/R (ischemia/reperfusion) injury from the controls [12]. Neither fasting plasma glucose nor its change during the experimental process is a significant predictor of wound closure. However, an increase in body weight significantly and independently predicts wound closure [13].

Wounds become 10% larger after excision in db/db, and 16% smaller in healthy counterparts due to contraction. One study showed that semi-occlusive dressing prolongs wound closure (27.75 days vs. 13 days in db/db). No such differences were noted for healthy counterparts. Interestingly, no statistically significant difference in wound closure rates existed between uncovered wounds in db/db and healthy counterparts in this study. There were, however, significant differences between gross epithelization and histological assessment of epithelization [11]. Contrary to the previous study, Michaels et al. showed that db/db wound healing is significantly delayed compared with the Akita strain, mice with streptozotocin (STZ)-induced diabetes, and healthy controls. Mean wound areas were larger after day 8 at all time points. Db/db also exhibited less intense granulation tissue formation than other models. There was no difference in the epithelial gap or epithelialization rate between the 3 models. Less cluster of differentiation 31+ (CD31) cells were detected on day 14 compared with the Akita and STZ-induced diabetes model. Similarly, the Ki67 index was lower in db/db than in all other models [14]. Another study by Tkalcević et al. showed slower contraction, re-epithelialization rates and wound closure, as well as less intense granulation tissue formation in db/db compared with control [15]. Another study showed significantly delayed wound closure in db/db mice, caused mainly by impaired wound contraction, not by slow reepithelialization. This finding was associated with low transforming growth factor  $\beta$  receptor type I (TGF- $\beta$  RI) expression and attenuated small mothers against decapentaplegic 3 (SMAD3) nuclear translocation in the granulation tissue leading to impaired fibroblast-to-myofibroblast differentiation [16]. A transient increase in the wound volume appears in healthy mice due to early inflammation, which resolves during the first 7 days after wounding. In contrast, there is no such a transient increase in db/db mice due to prolonged inflammation and there is a significantly larger wound volume on days 10 and 14 post-op compared with healthy counterparts. Non-diabetic adult mice demonstrate full wound closure after 14 days, whereas in db/db animals, the wound bed shows persistent hypercellularity, indicative of prolonged inflammation, as shown by ultrasound examination [17]. Trousdale et al. found that by post-operative day 21, both wild-type and db +/- mice demonstrate complete wound closure. In db/db mice, open wounds were still present at post-operative day 21 with a range of percent wound closure from 24 to 81% with a mean of 55%. As in previous studies, no significant correlation between wound closure rate and severity of diabetes existed [18].

### 3.1.2. Growth Factors

During wound healing, a scab is formed. The scab serves as a source of bioactive mediators, such as growth factors [19]. Endogenous growth factors are essential for normal wound repair and compared to their healthy counterparts, db/db mice exhibit dysfunctional changes in growth factors' production (reduction and downregulation of their receptors), release, and distribution during wound healing. It prevents this process from its physiological course.

The fibroblast growth factor (FGF) family consists of at least nine different mitogens. A study investigating fibroblast growth factors found that the expression of keratinocyte growth factor (KGF) is reduced and delayed in its release in db/db mice when wounded. Basic FGF (bFGF) is released earlier, but with similar intensity in db/db mice compared to their normal counterparts. Interestingly, levels of bFGF are upregulated in the non-wounded skin. The receptors also tend to be dysfunctional in wound healing. The FGF receptor (FGFR), particularly its 2nd isoform that binds KGF and acidic FGF (aFGF), is

downregulated [20]. Both platelet-derived growth factor (PDGF) and its receptor are downregulated in db/db mice. PDGF receptor A (PDGFR $\alpha$ ) is downregulated in db/db mice in both non-wounded and wounded back skin. Furthermore, expression of the PDGFR $\beta$  is also reduced during the repair process [21]. Insulin-like growth factor (IGF) I affects tissue repair whereas IGF-II influences fetal development. IGF-I is downregulated, and its production is delayed upon wounding. IGF-II peaks higher in healthy animals than in db/db mice during wound healing [22]. Hypoxia-inducible factor 1 alpha (HIF- $\alpha$ ) plays a significant role in wound healing and hyperglycemia in db/db mice and impairs the stability of HIF-1 $\alpha$  and vascular endothelial growth factor (VEGF). The latter enhances the permeability of local blood vessels. When destabilized, VEGF, a classical target gene for HIF, is no longer modulated by hyperglycemia as the expression of Von Hippel-Lindau (VHL) protein is downregulated. Similarly, another study found that there are decreased levels of VEGF mRNA in db/db mice during the period of granulation tissue formation [23,24]. Destabilization of HIF-1 $\alpha$  may also lead to downregulation of its target genes. When hydroxylase inhibitors such as dimethylxalylglycine (DMOG) and the iron chelator deferoxamine (DFX) were used, they stabilized the HIF-1 $\alpha$  pathway, prompting the production of granulation tissue, total vessels number, and increasing cytokine receptors' expression in endothelial precursor cells: CXC receptor 4 (CXCR4), C-Kit, Tie-2 [23]. Pigment epithelium-derived factor (PEDF) levels are elevated in type II diabetic patients with diabetic foot ulcer (DFU) as well as db/db mice. It has been proposed that overexpression of PEDF suppresses the Wnt signaling pathway in the wounded skin. When PEDF was neutralized, wound healing was accelerated, angiogenesis increased, and functions and numbers of endothelial progenitor cells (EPCs) improved [25].

### 3.1.3. Angiogenesis

A central component of normal wound healing is angiogenesis. This process is significantly impaired in db/db mice by numerous pathological states, such as dysfunctional receptors, reduction in the number of essential ligands or cells, and epithelial to mesenchymal transition (EMT) failure (reducing the angiogenic capability).

Angiopoietins (Ang 1 through 4) target the vascular endothelium via their receptors, Tie-1 and Tie-2. Levels of Ang 1 through 4 as well as their receptors Tie-1 and Tie-2 are dysfunctional during angiogenesis in db/db mice. Both normal and db/db mice tend to have a constitutive expression of Ang-1 and upon injury, levels of Ang-2 increase. After 7 days, levels of Ang-2 begin to decrease in normal mice, however, keep on increasing in db/db mice. This overexpression of Ang-2 and the decreased levels of VEGF result in fewer endothelial cells. Similarly, Tie-1 expression is induced during wound healing and is excessively prolonged in db/db mice whereas the expression of Tie-2 is completely absent [26]. Similar to blood vessels, lymphatic vessels are necessary during wound healing. The reduction of macrophages in db/db mice may result in a significant reduction in lymphatic structures in the granulation tissue. These macrophages also show impaired recruitment via lower expressions of VEGFR3 mRNA and its ligands VEGF-C and -A. Macrophages usually express markers for lymphatic endothelium, including Lymphatic Vessel Endothelial Receptor 1 (LYVE-1), podoplanin, and Prox-1. The reduction of macrophages results in reduced lymphatic markers and hence, fewer lymphatic vessels are produced. In the normal counterpart of db/db mice, lymphatic vessels are produced de novo on day 5 after injury [27]. Wound margin keratinocytes tend to have an increase in Akt1 phosphorylation; however, this phosphorylation is dysfunctional in ob/ob mice. Insulin-mediated VEGF synthesis in keratinocytes is controlled by a Phosphoinositide 3-kinases (PI3K)/Akt/mammalian target of rapamycin (mTOR)-dependent post-transcriptional regulatory mechanism. Hence, decreased Akt1 phosphorylation will lead to poor phosphorylation of the eukaryotic initiation factor 4E-binding protein 1 (4E-BP1) and reduced levels of VEGF protein in chronic wounds of diabetic ob/ob mice. Thus, the post-transcriptional control of insulin-stimulated VEGF expression via Akt1 suggests a role of insulin in the control of keratinocyte angiogenic potential in wound healing [28]. The wound margin in db/db shows a prolonged



upregulation of CXC ligans (CXCL2, CXCL5) and colony stimulating factor 3 (CSF3), TGF $\alpha$ , and matrix metalloproteinase 9 (MMP9), leading to a decreased expression of CD31 on days 2 and 7 after wounding [29]. Peroxisome proliferator-activated receptor  $\gamma$  (PPAR $\gamma$ ) agonists improve the functions of endothelial cells and have been used as insulin sensitizers in diabetic patients. Db/db mice tend to have a reduced angiogenic potential as evidenced by isolated endothelial cells (ECs) and bone marrow-derived proangiogenic cells (PACs). This effect was partially rescued by incubation of cells with rosiglitazone (PPAR $\gamma$  activator). However, this effect did not manifest *in vivo*. Hence, db/db PACs have a decreased level of PPAR $\gamma$  and dysfunctional expression of PPAR $\gamma$  regulated genes compared with their normal counterparts [30]. Langer et al. established a model which allows high resolution *in vivo* imaging of functional angiogenesis in diabetic wounds compared with wild-type (WT) mice or BALB/c mice. They showed that db/db mice have a lower functional capillary density (FCD) and lower angiogenesis positive area (APA) compared with the BALB/c and WT mice [31]. Another study used a microCT analysis to visualize the 3D architecture of the capillary bed in db/db mice. They have a significantly decreased vessel surface area, branch junction number, total vessel length, and total branch number. They also have increased capillary permeability and decreased pericyte coverage of capillaries. Similarly, db/db mice tend to have a dysfunctional expression of factors associated with vascular regrowth, maturity, and stability. Specifically, the expression of VEGF-A, Sprouty2, PEDF, low-density lipoprotein receptor-related protein 6 (LRP6), Thrombospondin 1, CXCL10, CXCR3, PDGFR- $\beta$ , heparin-binding EGF-like growth factor (HB-EGF), EGFR, TGF- $\beta$ 1, Sema-phorin3a, Neuropilin 1, angiopoietin 2, neural/glial antigen 2 (NG2), and regulator of G protein signaling 5 (RGS5) are down-regulated in diabetic wounds [32]. Hypoxia (1% O<sub>2</sub>) does not increase VEGF and heme oxygenase 1 (HO1) mRNA in db/db mice, unlike in control. HIF-1 $\alpha$  is stable in mature db/db adipocytes *in vitro*, but not *in vivo*. This suggests that abnormal adipocyte response to hypoxia may play a role in the pathogenesis of T2DM [33].

One more molecule plays a role in diabetic angiogenesis. ZEB1 (Zinc finger E-box binding homeobox 1) is responsible for epithelial to mesenchymal transition (EMT)—a key process in wound healing—and its levels in the skin of db/db mice are particularly high. Successful depletion of ZEB1 in db/db mice improves perfusion and increases vasculature density, as well as promotes EMT. Both improved angiogenesis and EMT are associated with better wound closure. In epithelial cells, ZEB1 induces EMT toward wound reepithelialization. Hyperglycemia impairs this process. Excessive ZEB1, under diabetic conditions, may also contribute to persistent inflammation [34].

#### 3.1.4. Cytokines and Immunological Apparatus

Inflammation is the key component of wound healing, and its proper resolution is necessary for regeneration. In leptin-deficient diabetes, the course of inflammation is disturbed by an increased level of many inflammatory cytokines and elongation of their function. Upon wounding, expression of interleukin 18 (IL-18) (mainly unprocessed form) is prolonged and strongly elevated. This is associated with a longer infiltration of lymphocytes Th CD4<sup>+</sup> and macrophages [35]. Other molecules also show prolonged expression upon wounding: IL-1 $\beta$ , tumor necrosis factor  $\alpha$  (TNF- $\alpha$ ), as well as Macrophage inflammatory protein-2 (MIP-2), and Monocyte Chemoattractant Protein-1 (MCP-1). The last two are strongly associated with a prolonged infiltration of polymorphonuclear leukocytes (PMNs) gathering below the epithelium with macrophages encircling them. CXCR2 and C-C chemokine receptor type 2 (CCR2) in turn show lower expression compared with healthy counterparts [36]. PMNs-rich wounds of ob/ob mice also show strong oncostatin M mRNA and protein upregulation, suggesting the role of this molecule in cellular infiltration. Systemic leptin administration decreases oncostatin M level, as well as PMNs count [37]. Leptin-deficient mice show low expression of IL-1 $\beta$ , VEGF and TNF- $\alpha$  compared with control, when stimulated with lipopolysaccharide + interferon  $\gamma$ . (LPS + IFN- $\gamma$ ). Nitric oxide (NO<sup>2-</sup>) levels, on the contrary, are higher than in control. Such a stimulus does

not alter the respiratory burst in macrophages; however, they appear more rounded and clustered [38].

On day 5, inflammation decreases, and tissue healing begins. On day 8, new matrix formation is evident. There are relatively small changes between db/db and control in mRNA expression of IL-6, IL-1, MIP-2, and MCP-1. On day 8, extracellular matrix (ECM) is five-fold more abundantly present in control than in db/db mice [39]. Wound margin tissue shows strong and prolonged upregulation of CXCL2, CXCL5, CSF3, TGF $\alpha$ , and MMP9 [29].

Db/db mice suffer from neutrophil persistence impairing healing—treatment with Cellular Communication Network Factor 1 (CCN1) accelerates neutrophil clearance [40]. Transcription factors Forkhead Box M1 (FOXM1) and STAT3, which function to activate and promote the survival of immune cells, are inhibited in DFUs. Similar inhibition of FOXM1 is seen in db/db, resulting in delayed wound healing and decreased neutrophil and macrophage recruitment in diabetic wounds *in vivo* [41].  $\gamma\delta$  T cells are normally responsible for producing cytokines and growth factors in response to damage. They become dysfunctional in ob/ob mice, as hyperglycemia disturbs their proliferation due to altered STAT5 signaling, diminishing their numbers in the epidermis. Those residing in the skin are unresponsive to epithelial cell damage due to chronic inflammatory mediators, including TNF $\alpha$ . Neutralizing this cytokine partially restores  $\gamma\delta$  T cells' function [42]. Taylor et al. also showed that  $\gamma\delta$  T cells are unable to properly regulate keratinocytes' homeostasis in obesity, which also impairs cell–cell adhesion [43].

Both leptin-deficient and healthy mice exhibit high expression of cyclooxygenase-1 (COX-1) and nearly absent COX-2 in non-wounded skin. Upon wounding, COX-1 expression declines, whereas COX-2 expression increases. On day 13 post-wounding, COX-1 expression is still reduced, and COX-2 is drastically over-expressed in db/db and ob/ob, compared with control. Systemic leptin treatment in ob/ob mice normalizes glycemia, body weight, and wound healing. It also restores COX-1 expression in wound margin keratinocytes and decreases COX-2 expression in the wound bed to levels comparable to healthy counterparts. Macrophages in the wound bed express inducible nitric oxide synthase (iNOS) and COX-2 [44]. Proper keratinocyte regeneration is associated with an increased production of prostaglandins E2 (PGE2) and D2 (PGD2), mediated by normalized COX-1 expression [45].

Upon wounding, several dysregulations occur in ob/ob mice: there are high levels of lysozyme m and lipocalin mRNA, strong long-lasting macrophage signals, and high MIP-2 levels (preceding cellular infiltration)—especially on days 5 and 7. IL-1 $\beta$  induced upon wounding persists over 7 days. COX-2 expression, as mentioned earlier, is markedly prolonged until at least 11 days. Importantly, even though Akt does not activate properly, nuclear factor of kappa light polypeptide gene enhancer in B-cells inhibitor, alpha (I $\kappa$ B $\alpha$ ) degrades, thus further activating the nuclear factor kappa-light-chain-enhancer of activated B cells) NF $\kappa$ B pathway even in late wounds, prolonging inflammation [46].

Chronic inflammatory signals and endoplasmic reticulum-specific stress are associated with unfolded protein response (UPR). Wounds of ob/ob mice showed sustained induction of UPR associated with an increased expression of MIP-2. Moreover, prolongation of UPR impairs the angiogenic capacity of wound macrophages [47].

### 3.1.5. Macrophages

In non-diabetic mice on day 5, post-injury macrophages exhibit a pro-inflammatory phenotype, manifesting itself with high expression of IL-1 $\beta$ , MMP9, and iNOS. This phenotype normally subsides by day 10. In db/db, however, the pro-inflammatory phenotype persists through day 10 and is associated with decreased expression of IGF-1, TGF- $\beta$ 1, and VEGF [48]. Such macrophages (as in humans) exhibit high expression and secretion of IL-1 $\beta$ . Blocking the IL-1 $\beta$ -mediated pathway increases the level of growth factors, as well as improves healing [49]. Rodero et al. identified a noninflammatory subset of macrophages (Ly6c<sup>lo</sup>MHCII<sup>hi</sup>), which increases gradually during normal wound healing, but is missing in ob/ob mice. Moreover, they pointed to IL-17 as a key factor inhibiting nor-

mal wound closure. Blocking IL-17 markedly improved wound healing in leptin-deficient animals [50]. Ob/ob mice also show an increased and prolonged (up until 13 days) expression of protein Ym1—a marker of the IL-4-mediated alternatively activated macrophage phenotype. Interestingly, it seems that wound macrophages take up this protein from neutrophils, which carry it to the wound bed. This represents another mechanism of macrophages' phenotype polarisation in the healing environment, possibly contributing to inhibiting regeneration [51]. Another study presented an epigenetic mechanism skewing macrophage polarization towards the M1 phenotype and is associated with fewer wound macrophages. Hematopoietic stem cells (HSCs) derived from db/db mice exhibit markedly elevated oxidative stress levels decreasing microRNA let-7d-3p, which in turn leads to hypermethylation of genes responsible for macrophages' differentiation [52].

Early after injury, the diabetic wound exhibits a significant delay in macrophage infiltration resulting from reduced CCL2 expression. Treatment with CCL2 stimulates healing in diabetic wounds by restoring the macrophage response. The early diabetic wound exhibits a decrease in essential macrophage response, rather than hyperactive inflammation [53]. Peritoneal macrophages exhibit impaired macropinocytosis, mediated partially by a hyperglycemia-induced decrease in AMP-activated protein kinase (AMPK) activity [54]. Macrophages isolated both from diabetic humans and db/db mice show sustained high inflammasome activity due to a lack of endogenous inflammasome inhibitors, debilitating the switch from pro-inflammatory macrophages to healing-associated phenotype [55].

### 3.1.6. Leptin

Upon wounding, a rapid spike in leptin mRNA level is observed in db/db mice. However, leptin protein is decreased after injury, but its level comes back to normal in the period between the 3rd and the 13th day. After the injury, the functional leptin receptor subtype (obRb) declines, but comes back to normal on the 13th day. Leptin acts as a mitogen for primary epidermal keratinocytes (Figure 2) [56].

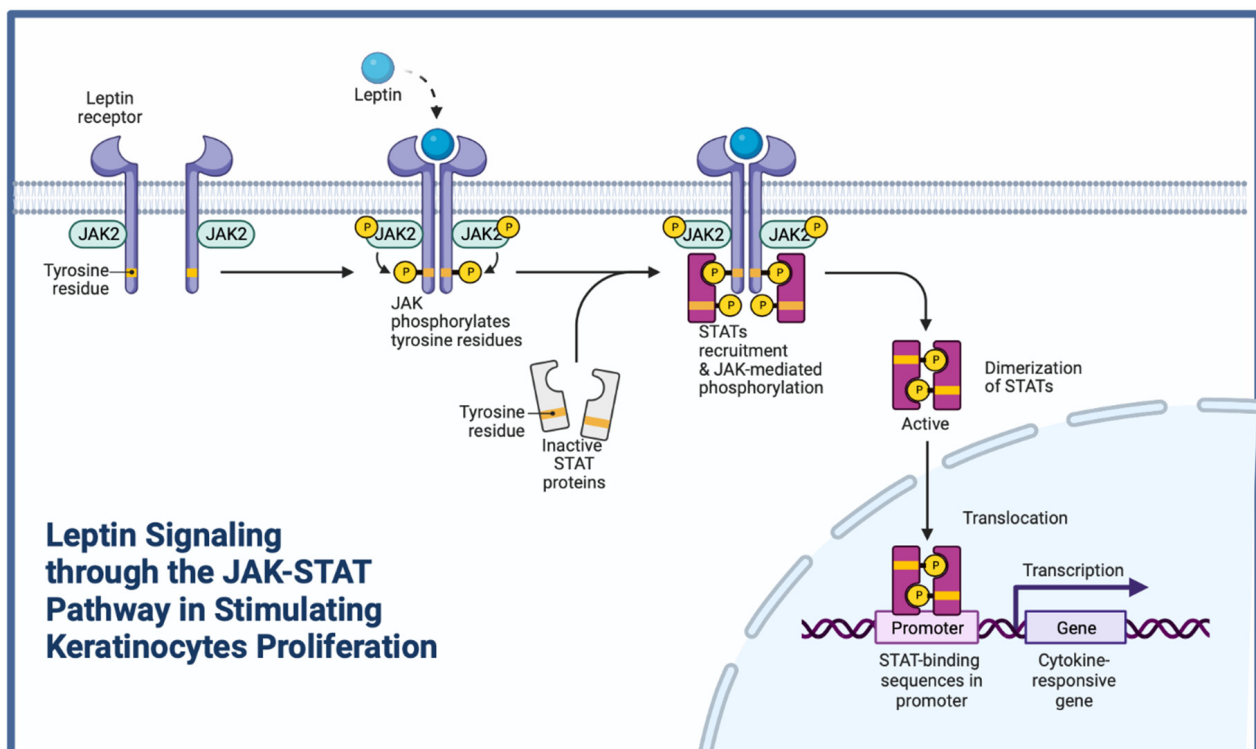


**Figure 2.** Leptin acting as a mitogen in wound healing. JAK-STAT—Janus kinase-signal transduction and transcription activation.



Leptin, not caloric deficit, improves wound healing [19]. It activates c-fos via the obRb leptin receptor in healthy keratinocytes, further signaling via Janus kinase (JAK) family kinases and Signal Transducer and Activator of Transcription (STAT). JAK-2 is the only kinase associated with leptin signaling. Its phosphorylation, however, differs between species and remains unclear. Protein Tyrosine Phosphatase 1B (PTP1B) is a negative regulator of leptin signaling (it dephosphorylates JAK-2). Moreover, PTP1B dephosphorylates VEGFR2, which suppresses proliferation, migration, and tube formation of vascular endothelial cells. Inhibiting this phosphatase rescues wound healing in ob/ob mice [57]. As mentioned earlier, systemic leptin treatment in ob/ob mice normalizes COX-1 and -2 expression, as well as PGE2/PGD2 biosynthesis [45]. Upon wounding and systemic leptin administration, there is a higher phosphorylation of STAT-3 (Y705) in wound tissue. This mechanism is noted both in human and murine keratinocytes [58]. Expression of VEGF protein upon injury is reduced (30 to 40%) in ob/ob mice compared with wild-type C57BL/6 animals. Systemic and topical administration of leptin reconstitutes normal wound VEGF expressions but fails to reverse the strongly reduced angiogenic response in ob/ob mice (wound vessel density) [56]. Moreover, neither systemic nor topical leptin administration induces any significant changes in hemoglobin level. It suggests that leptin accelerates wound repair by a mechanism other than stimulation of angiogenesis [59]. Immunohistochemistry confirms that the epithelium and blood vessels located in the granulation tissue express the functional leptin receptor obRb isoform during skin repair [56]. Systemic treatment of diabetic ob/ob mice with leptin blunts PMNs influx, but not macrophage influx into the wound site. Closed wounds of leptin-administered mice are characterized by tremendous numbers of macrophages within the granulation tissue. Differential effects of leptin on PMN and macrophage axes of inflammation must be indirect, as topical administration of leptin onto wounds of ob/ob mice does not reduce PMN influx into the wounded areas [19]. In the human study, from the DU group (diabetic ulcer), NDU group (not diabetic ulcer), and NC group (normal control), 10 biopsies each were examined. The cuticle thickness was significantly greater, and the epidermal layer was significantly lesser in the DU and NDU groups. Leptin protein expression was significantly higher in the DU and NDU than in the NC group ( $p < 0.001$ ), whereas OB-RL (leptin receptor-long form) mRNA and protein expressions were significantly lower in the DU group and significantly higher in the NDU group. Diabetic foot ulcer duration was negatively correlated with OB-RL protein expression [60].

Ob/ob mice exhibit a marked overexpression of arginase-1 post-wounding with subsequent inactivity of iNOS, leading to impaired NO production. Systemic leptin treatment readjusts enzymatic expression and improves healing conditions [61].

### 3.1.7. Insulin

In leptin-deficient mice, obesity impairs wound contraction and lowers collagen accumulation in the wound bed, regardless of the insulin treatment or diet restriction [62]. There are, however, severe dysregulations in insulin physiology in these models. Upon wounding, insulin receptor (InsR) and Glucose transporter type 4 (Glut-4) mRNA levels are significantly reduced in ob/ob mice compared with control. Protein tyrosine phosphatase 1B (PTP-1B), Insulin receptor substrate 1 (IRS-1), and IRS-2 mRNA expression profiles are not changed. However, InsR and PTP-1B protein levels decrease. Similarly, IRS-1 and IRS-2 proteins are less detectable in skin and wounds of ob/ob mice. This suggests a post-transcriptional blockade in the insulin signaling. Phosphorylated Glycogen synthase kinase-3 alpha (GSK3- $\alpha$ ) and GSK3- $\beta$  are almost completely absent in ob/ob (normally gradually increasing). No phosphorylation of GS in ob/ob is noticed, as opposed to normal mice. Glut-4 is downregulated in leptin-deficient animals. InsR is normally expressed in wound margin and in granulation tissue in healthy animals on day 5 post-wounding. On the contrary, a barely detectable signal is observed in ob/ob mice. Systemic leptin treatment restores IRS-1 and IRS-2 expression, as well as GSK3- $\beta$  and GS phosphorylation, and reduces TNF- $\alpha$  mRNA and protein levels. Topical leptin does not improve healing,

unlike systemic administration. Protein expression of the InsR, IRS-1, PTP-1B, Glut-4, and phosphorylation of GSK3- $\alpha$  and GS increase after leptin treatment in non-wounded skin also. This study suggests that impaired insulin signaling in obese animals is linked to increased levels of TNF- $\alpha$ , which in turn enhances inflammation and reduces peripheral uptake of glucose. This process is similar to the one seen in humans as human adipocytes constitutively express TNF- $\alpha$  [63]. Importantly, InsR downregulation plays a key role in debilitating cellular response to insulin in leptin-deficient model. This impairment, however, seems to result from a systemic, rather than local mechanism, as evidenced by no improvement after topical leptin administration [64]. It has been suggested that knockout of GM3S (ganglioside GM3 synthase), which is upregulated in ob/ob mice skin, may result in improved proliferation, migration, and activation of insulin receptor and IGF-1 receptor [65].

### 3.1.8. Advanced Glycation End-Products (AGEs)

AGEs are heterogeneous moieties endogenously produced from the glycation of proteins, lipids, and nucleic acids. Db/db mice have an accumulation of AGEs within the wound area. A high AGE concentration delays wound closure, cellularity, and inflammation at the early stages of wound healing (Figure 3). On the 14th day after wound injury, there is impaired reepithelialization, granulation, angiogenesis, and cell infiltration. The inflammation is prolonged until the 21st day post-wound injury [66]. The receptors for advanced glycation end-products (RAGE) are also dysfunctional in diabetic wound specimens. F4/80-positive macrophages and Heat shock protein 47 (HSP47)—positive fibroblasts are the major cell populations expressing RAGE during diabetic wound healing. Furthermore, diabetic wounds tend to have an increased expression of RAGE in fibroblasts and macrophages during the last stage of the repair. Thus, these results may indicate that elevated RAGE levels in diabetic wounds are associated with prolonged inflammation and deficient healing [67]. One study aimed to elucidate the skin barrier impairment in patients with T2DM and found this linked to AGEs. Murine models of diabetes presented with severe hyperglycemia, impaired skin barrier hemostasis, decreased epidermal proliferation and lipid synthesis, and decreased lamellar bodies (LB) and epidermal antimicrobial peptides (AMPs). In these animals, there is an increase in receptors for advanced glycation end-product (RAGE) in the epidermis as well as an increased serum AGE levels [68]. Db/db mice tend to have an increased expression of both RAGE and AGEs. One study attempted to support this hypothesis by blockade of RAGE using soluble RAGE (sRAGE). Administration of sRAGE accelerated the development of inflammatory cell infiltration and activation in wound foci. Cytokines such as TNF- $\alpha$ , IL-6, and MMP-2, -3 and -9 were suppressed. Thick, well-vascularized granulation tissue was enhanced as well as increased levels of PDGF-B and VEGF. Thus, blockade of this receptor may be a possible strategy to restore effective wound repair [69].

### 3.1.9. Fibroblasts and Extracellular Matrix (ECM)

Fibroblasts play a pivotal role in wound healing by secreting numerous growth factors, including VEGF. Fibroblasts cultured from db/db mice have impaired migration compared with wild-type mice. Hypoxia upregulates wild-type fibroblast migration—an effect not seen in the db/db mice. Db/db-derived fibroblasts have a greater activity and concentration of MMP-9, however, no differences in MMP-2. Fibroblasts cultured from db/db mice produce 13% of normally produced VEGF—the expression not increased by hypoxia. Despite these impairments, the proliferation and senescence of fibroblasts are normal in db/db mice [70]. In this strain, a higher rate of fibroblast-specific apoptosis is seen compared with wild-type mice. This is attributed to enhanced levels of activated caspase-3 and coincides with diminished expression of collagen I and III. Hence, db/db mice tend to have a lower fibroblasts' density and less ECM compared with wild type mice [39]. When treated with a TNF- $\alpha$  inhibitor (etanercept), caspase-3 levels decrease, alleviating fibroblasts' apoptosis and increasing ECM production [71]. The pro-apoptotic transcription factor

FOXO1 is excessively activated in db/db mice. Blocking TNF normalizes FOXO1 action, decreasing fibroblasts' apoptosis, and alleviating inflammation (measured with PMNs count). In vitro analyses show that TNF- $\alpha$  enhances the expression of genes related to apoptosis including Akt and p53, as well as those involved in inflammation, cytokines, toll-like receptors, and NF- $\kappa$ B pathways [72]. Db/db mice show insufficient FGF-7 induction compared with wild-type mice, leading to a reduced wound contraction rate [73]. Substance P is an amino acid peptide, which stimulates the mobilization of bone marrow-derived mesenchymal stem cells into the bloodstream. It improves wound healing in both db/db and wild-type mice. In db/db mice, it decreases fibroblasts' apoptosis and increases their proliferation by increasing the expressions of VEGF and stromal cell-derived factor-1 (SDF-1) [74]. Db/db-derived dermal fibroblasts have lower expression levels of IGF-1, SDF-1, connective tissue growth factor, and TGF- $\beta$ . Yes-associated protein (YAP) is a mediator of mechanotransduction in dermal fibroblasts and compared to wild-type fibroblasts, db/db-derived fibroblasts have a lower expression of this protein [75].

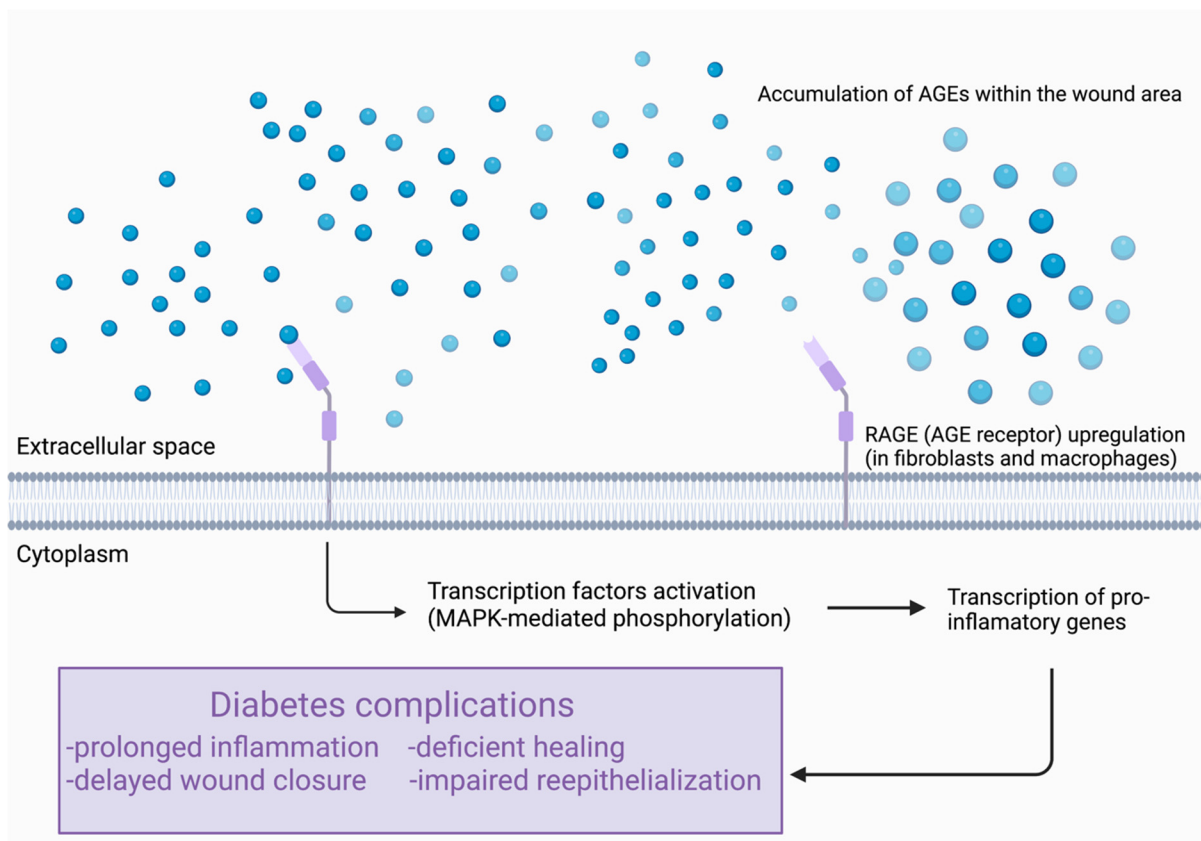


**Figure 3.** Effect of AGEs (advanced glycation end-products) on wound healing process. MAPK—mitogen-activated protein kinase.

### 3.1.10. Apoptosis and Autophagy

Db/db mice have higher levels of apoptotic fibroblasts after a bacterial-induced wound. This is primarily due to enhanced expression of pro-apoptotic factors, such as caspase 9 (CASP9), FAS, Fas Associated Via Death Domain (FADD), and TNF- $\alpha$ . Compared with the wild type mice, db/db mice have a two-fold increase in CASP3 activity. CASP 3, 8, and 9 activity remains high in db/db mice even eight days after wound induction. When treated with a pan caspase inhibitor, a number of fibroblasts, expression of collagen I and III, and ECM increase [76].

Another study showed that on day 4 post-wounding, TNF $\alpha$  mRNA and protein levels are increased in db/db wounds. Higher caspase-3/7 activity is also detected, followed by more pronounced fibroblast apoptosis. Antagonizing TNF $\alpha$  enhances healing in db/db

from day 5 to 9, decreasing fibroblast apoptosis. TNF- $\alpha$  significantly increases mRNA levels of genes involved in apoptosis by increasing apoptosis, Akt, and p53 gene sets but not mitochondrial or cell-cycle gene sets [72].

Autophagy is associated with increased light chain 3 (LC3) protein levels. Enhanced autophagy (increased LC3 levels) within db/db mice impairs the cutaneous healing process. If autophagy is inhibited by 3-Methyladenine (3-MA), proper healing is restored. The major cell type undergoing autophagy in wound healing are macrophages and it is the increased autophagy in db/db mice that induces the mobilization of macrophages. Hence, due to enhanced autophagy, db/db mice have increased expression of M1 macrophages with elevated CD11c population and gene expressions of proinflammatory cytokines. Interferon regulatory factor 8 (IRF8) is a mediator of autophagy and macrophage polarization and administration of certain AGEs results in a two-fold increase of IRF8. Subsequently, autophagic activity, and M1 macrophage polarization increase. Hence, modulating IRF8 activity could be a potential intervention for db/db mice [77].

Normally, apoptosis is limited to the wound edge and follows the advancing epithelial edge towards the center of the wound as healing progresses. Db/db mice have significant delays in the appearance of apoptotic patterns. This dysfunction is reversed after the topical application of growth factors such as IGF-II and PDGF [78].

#### 3.1.11. Stem Cells (Bone Marrow)

Stem cells also play a role in the impaired wound healing that occurs in diabetic mice (Figure 4). The following section includes a discussion of mesenchymal stem cells (MSCs), bone marrow progenitor cells (BM PCs), particularly the CXCR4-CXCL12 axis and Nicotinamide phosphoribosyltransferase—Nicotinamide adenine dinucleotide (NAMPT-NAD) pool, as well as the increased myelopoiesis in db/db mice.

Diabetic animals possess fewer MSCs than their healthy counterparts. In addition to the limited number of MSCs, their proliferation and survival are impaired. Furthermore, after wounding, significantly fewer endogenous MSCs are mobilized to the injury site. Direct application of MSCs does not accelerate wound closure in diabetic and healthy animals. However, there is a higher therapeutic outcome in healthy animals compared with diabetic animals [79].

When diabetic mice are wounded, endogenous BM-PCs are naturally mobilized. Wound re-epithelialization is the main mechanism contributing to wound closure when high levels of BM-PCs occur. The CXCR4-CXCL12 axis enhances the mobilization of diabetic BM-PCs. Treating mice with a CXCR4 antagonist increases the numbers of HSCs and EPCs in the wound bed compared with non-treated mice, as well as improves vascularization. As the CXCR4 antagonist increases, the release of these BM PCs wounds obtained from the treated animals show higher levels of phosphorylated MAPK (pMAPK), i.e., a marker of effective cell migration and activation. Further solidifying the role of the CXCR4-CXCL12 axis, when mice are treated with a c-Kit antibody (ACK2), which abrogates BM PCs mobilization, the number of HSCs and EPCs in the wound bed decreases [80].

The CXCR4 ligand—CXCL12, also known as SDF-1 $\alpha$ , plays a role in wound closure. Unexpectedly, wild-type mice have fewer progenitor cells (PCs) than diabetic mice. However, after cutaneous wounding, the wild-type bone marrow PC number increases markedly. This does not happen in diabetic mice as the SDF-1 $\alpha$  switch is dysfunctional. In wild-type mice, bone marrow SDF-1 $\alpha$  increases over time as opposed to diabetic mice, where it remains constant. Thus, the mobilization of vasculogenic PCs into the circulation is impaired. Upon treating diabetic mice with plerixafor, which restores the SDF-1 $\alpha$  switch, diabetic PC mobilization and wound closure improve [81].

Seven days post treatment with an SDF-1 $\alpha$  inhibitor, the volume of granulation tissue decreases, similar to the number of CD31+ cells and vessel density, and the number of CD45+ cells (leukocytes) increases. There is a high expression of IL-6 in the db/db treated with the SDF-1 $\alpha$  inhibitor on day 3 but not on day 7. However, there are higher levels of



MIP-2 on day 7. Inhibition of SDF-1 $\alpha$  also leads to a dose-dependent reduced migration of splenic leukocytes [82].

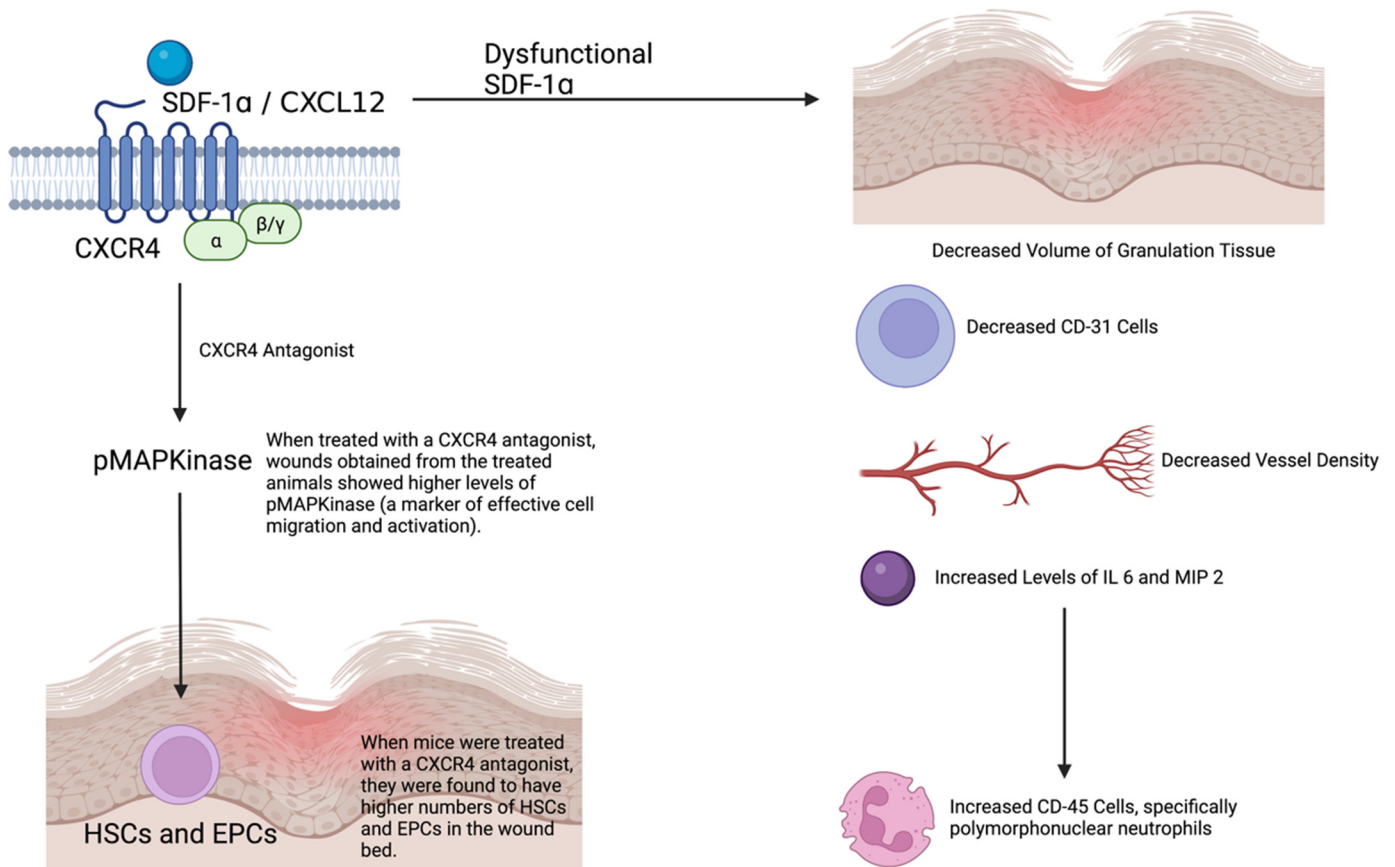


**Figure 4.** CXCR4/CXCL12-dependent stem cell function in wound healing. HSCs—hemapoietic stem cells, EPCs—endothelial progenitor cells, pMAPK—phosphorylated mitogen-activated protein kinase, CXCR—CXC chemokine receptor, SDF—stromal cell-derived factor, CXCL—CXC chemokine ligand, CD—cluster of differentiation, IL-6—interleukin 6, MIP 2—macrophage inflammatory protein 2.

NAMPT is the rate-limiting enzyme for the synthesis of NAD. NAMPT regulates neovascularization after hind-limb ischemia by controlling the function of EPCs. It also modulates the Notch 1 intracellular domain deacetylation in a sirtuin 1 (SIRT1)-dependent manner. The concentration of NAD and the expression of NAMPT are significantly decreased in EPCs in db/db mice. When the NAD pool is enhanced, the number of circulating EPCs increases, and post-ischemic wound healing and blood reperfusion improve. Normally, SDF-1 $\alpha$  is downregulated and endothelial NOS (eNOS) is upregulated in the bone marrow of wild-type mice. In db/db mice, this pathway works conversely. Treatment with nicotinamide and enhancing the NAD pool restores the proper pathway needed for wound healing. Additionally, enhancing the NAD pool inhibits the Poly (ADP-ribose) polymerase (PARP) and caspase-3 activates in db/db mice bone marrow. Thus, the intracellular NAMPT-NAD pool is positively associated with blood EPCs [83].

Diabetic mice have enhanced myeloid cell production after skin wounding. This is due to alterations in bone marrow progenitors present in db/db mice compared with their non-diabetic counterparts. Db/db mice have greater numbers of Lin<sup>−</sup>Sca-1+cKit<sup>+</sup> (LSK<sup>+</sup>) cells and an increased density of MyP cells in their bone marrow compared with wild-type mice. Among the MyP subsets, only the granulocyte macrophage progenitors are significantly increased in db/db mice. Hence, the increased frequency of LSK and MyP shows that db/db mice have an increased myeloid lineage commitment at the progenitor level. The levels of mRNA for critical transcription factors and growth factor receptors

associated with myeloid differentiation are upregulated in the LSK cells derived from db/db compared with WT mice. Furthermore, the expression of CSF1 receptor (CSF1R) and CSF2R alpha subunit (CSF2R $\alpha$ ) in the DB LSK cells is increased. Db/db mice have a significantly higher presentation of both neutrophils and Ly6Chi macrophages in the circulation and spleen, however not in the bone marrow. Thus, these findings suggest that stem cells in db/db mice may be intrinsically modified to produce myeloid lineage commitment by upregulation of critical transcription factors and receptors associated with myeloid differentiation [84].

Another study supports the claim that diabetic mice have enhanced myeloid cell production particularly due to HSCs proliferation. Cxc112 is a retention factor that promotes HSC quiescence. Endothelial cells in diabetic mice express fewer Cxc112, leading to excessive HSC proliferation. Mice with a specific endothelial-specific deletion of EGFR (Cdh5Cre Egfrfl/fl) were generated. These mice with the deletion had enhanced HSC proliferation and increased myeloid cell production. Reduced EGFR signaling decreases the expression of HSC retention factor angiopoietin-1. Inflammatory myeloid cells accumulate in skin wounds of diabetic Cdh5Cre Egfrfl/fl mice, significantly delaying wound closure. Cdh5Cre Egfrfl/fl mice also have increased atherosclerotic lesions in the aorta. Mice with hypercholesterolemia tend to have increased LSK proliferation, indicating that hypercholesterolemia may be the main driver of increased hematopoiesis in db/db mice. On the other hand, hyperglycemia may be a main driver of myelopoiesis in the STZ- and high-fat diet model [85].

Methylglyoxal (MGO) is a highly reactive dicarbonyl species that is formed during the metabolism of glucose and fructose. It converts proteins, lipids, and DNA to AGEs, which leads to cell dysfunction and organ damage. Thus, diabetic mice tend to have higher levels of methylglyoxal (MGO) due to hyperglycemia. Glyoxalase 1 (GLO1) is an MGO scavenger which reverses BMPCs dysfunction. It increases the expression of inositol-requiring enzyme 1a (IRE1a), an endoplasmic reticulum stress sensor. When diabetic mice were manipulated to augment tissue GLO1 expression, angiogenesis was enhanced, resulting in improved wound closure. Hence, GLO1 rescues BMC dysfunction and reverses MGO-induced impairment of IRE1a expression and activity [86].

### 3.1.12. Non-Coding RNAs

MicroRNAs are small, noncoding RNAs that bind to the 3'-untranslated region and interfere with mRNA translation. Several reports have identified the role of microRNAs in the angiogenic response of wounds in db/db mice.

There is a decreased expression of miR-27b in bone marrow-derived angiogenic cells (BMAC) of db/db mice, leading to dysfunctional angiogenesis. Normally, miR-27b is required to enhance BMAC function. Firstly, miR-27b suppresses antiangiogenic molecules such as Thrombospondin-1 (TSP-1) and Semaphorin 6A (Sema 6A). TSP-1 is an extracellular glycoprotein required to modulate cell-to-cell interactions. Hyperglycemia decreases the expression of miR-27b leading to increased expression of TSP-1. Secondly, miR-27b suppresses p66shc, which is a pro-oxidant protein and hence, contributes to the protection of bone marrow aspirate concentrate (BMAC) function by preventing mitochondrial oxidative stress. When miR-27b is given to db/db mice, BMAC function improves, including proliferation, adhesion, tube formation, and delayed apoptosis, and hence, partly improved wound healing [87]. Another study revealed that miR-26a is induced in db/db mice due to the increased concentration of glucose in endothelial cells. MiR-26a in the wounds of db/db mice is elevated compared with WT mice. Inhibiting miR-26a increases angiogenesis, and granulation tissue thickness and accelerates wound thickness. MiR-26a enhances bone morphogenetic protein (BMP)/SMAD1 signaling by decreasing the expression of SMAD1 and its downstream regulator inhibitor of DNA binding 1 (ID1), and further on, increases the expression of cell cycle inhibitor p27. The use of the miR-26a inhibitor reverses this effect [88]. Db/db mice also have reduced levels of miR-132, which plays an important role in inhibiting inflammation and promoting the growth of epidermal keratinocytes. TGF- $\beta$

plays a major role in wound healing and regulates the expression of miR-132; when dysfunctional, it reduces miR-132 levels. miR-132 also suppresses the NF- $\kappa$ B signaling pathway and affects other inflammation-related signaling pathways, including the NOD-like receptor, Toll-like receptor, and TNF signaling pathways [89]. Db/db mice also have an increased expression of miR-615-5p within their wounds. It inhibits the VEGF-Akt/eNOS signaling pathway in endothelial cells. Specifically, miR-615-5p targets IGF2 and the Ras-association domain family 2 (RASSF2) which decrease the VEGF-AKT/eNOS signaling, impairing angiogenesis. Furthermore, miR-615-5p inhibits the release of nitric oxide, which drives endothelial cell angiogenic responses. Endothelial cell proliferation and migration are reduced in db/db mice. Neutralization of the microRNA by local delivery of its inhibitors increases angiogenesis and granulation tissue thickness enhancing wound closure [90].

### 3.1.13. Bacterial Burden and Biofilm

On average, 40 times more bacteria colonize db/db mice skin than healthy counterparts, which is also associated with a greater variety of species. The genera *Staphylococcus* and *Aerococcus* are present more abundantly, whereas *Streptococcus*, *Lachnospiraceae*, *Incertae*, and *Sedis* are scarce in db/db skin as compared with db/+ skin. Upon wounding, the bacterial load increases, and the species' colonizing skin changes. Gene transcripts were compared between db/db and control with a punch biopsy at baseline and subsequent days, showing little differences at day 0. Later, however, the gene expression seems to be delayed in db/db mice compared with the control group. This finding is correlated with the selective *Staphylococcal* shift [91]. Biofilm within the wound promotes chronicity as bacteria express genes associated with cellular growth, thus exhausting oxygen resources in the wound bed. Additionally, they promote immune cells' migration to the wound site. These in turn use oxygen for defense-related processes (such as oxidative burst performed by PMNs). Overall, these effects lead to diminishing oxygen tensions and a prolonged healing duration [92]. Importantly, a state of lasting hypoxia is present in db/db mice even without any bacterial burden. Though it is difficult to assess it in an excisional wound (as measurements are highly influenced by atmospheric oxygen), a more accurate measurement is possible in pedicled flaps [93].

Db/db mice have an impaired ability to clear the wound of bacteria at days 5 and 10. Additionally, 12 h after inoculation, the db/db inflammatory response is greater than in healthy animals, and they also exhibit a higher myeloperoxidase (MPO) activity, which normalizes by 24 h. The early inflammatory response in db/db is non-effective as the bactericidal activity of neutrophils is reduced, an effect not mediated directly by hyperglycemia. PMNs present reduced respiratory bursts. Interestingly, bone-marrow derived neutrophils showed no difference in bactericidal activity between the groups [94].

Some changes in the dermal connective tissue are noted between db/db and control mice upon bacterial infiltration. On day 1, inflammation develops in both db/db and control with comparable TNF- $\alpha$  levels between the groups. On day 3, inflammation is prolonged in db/db with more PMNs, whereas it resolves in control. At the same time, the expression of TNF- $\alpha$ , MIP-1, and MCP-1 is prolonged in the former group [95].

### 3.1.14. Models of Chronic Diabetic Wounds

Some authors attempted to modify the original leptin-deficient murine model to reflect more accurately clinical situations such as infected diabetic wounds (Table 1). Zhao et al. challenged the wounds with *P. aeruginosa* biofilm two days post-wounding. This resulted in prolonged epithelialization, more extensive inflammation, tissue necrosis, and epidermal hyperplasia adjacent to wounds. The model proved reproducible and had low mortality rates [96,97]. Their follow-up study showed deficient vascularization in the same model, with HIF expression markedly elevated. Such wounds heal in approximately 6 weeks [98]. Later, Chen et al. showed that inoculating DB/db wounds with *P. aeruginosa* increased the ratio of pro-inflammatory cytokines to anti-inflammatory cytokines, and increased

numbers of both M1 and M2 macrophages with greater wound persistence in the former group [99].

**Table 1.** Modifications of leptin-deficient mice models.

Animal Model	Modification	Ref.
db/db (BKS) 11 weeks old, females	<i>Pseudomonas aeruginosa</i> biofilm challenge	[97,98]
db/db (C57BL/6)/db/db (BKS) 5–6 months old/db/db 11 weeks old, males	Increasing oxidative stress via blocking catalase and glutathione peroxidase	[100–102]
db/db (BKS) 12 weeks old, males	Wound splinting to prevent contraction	[103]

Another group challenged db/db mice wounds with excess oxidative stress by blocking catalase and glutathione peroxidase. After such an intervention, the biofilm developed within the wound spontaneously, rendering the wound chronic. Treatment with antioxidants  $\alpha$ -tocopherol and N-acetylcysteine reduced oxidative stress, and the biofilms had increased sensitivity to antibiotics; furthermore, granulation tissue formation and morphology were restored [100]. Another group used the same method to create a protocol for chronic diabetic wounds. They showed that such an approach could prolong healing to as long as 60 days. Here, however, they used db/db mice on BKS background and the animals were 5–6 months old [101]. Panayi et al. argued that blocking antioxidant enzymes results in high mortality, especially in older animals. They decided to use modified doses of catalase and glutathione peroxidase inhibitors in 47 11-week-old db/db mice and noted no deaths after this procedure. Wounds challenged in such a way showed an arrested inflammatory state during healing [102].

As contraction plays an important role in wound regeneration in rodents, Park et al. investigated the effect of splinting on the healing dynamics. They found that silicone splint application reduced wound contraction in heterozygous and db/db mice, making the process more similar to that in humans, in which wounds heal primarily by granulation [103].

### 3.1.15. Other Studies

The outcomes of several studies do not fit into any of the previous chapters, thus we summarized them here.

NEP (neutral endopeptidase) degrades substance P—a neuropeptide stimulating proliferation and migration of keratinocytes. The activity of NEP is usually increased in patients with chronic wounds, as it is elevated in unwounded skin of db/db mice [104]. HMG-CoA reductase (HMGR) is responsible for keratinocyte angiogenic and proliferative responses, found mainly at the wound margin. Its mRNA expression peaks between day 3 and 5, as well as on day 13. This biphasic expression is not present in ob/ob mice, possibly contributing to wound healing impairment [105]. P38 is phosphorylated (peaks) on days 1 through 7 after wounding in db/db mice, possibly accelerating inflammatory processes. Blocking this protein results in accelerated wound healing (reduced wound width, accelerated re-epithelialization, increased granulation, and reduced inflammatory cell infiltration into the wound) [106].

One group investigated wound healing in db/db mice exposed to healthy peripheral circulation. They performed parabiosis at week 4 and wounding at week 8. Wound healing enhanced by parabiosis with WT animals showed an increased granulation tissue amount and more collagen deposition. Platelet endothelial cell adhesion molecule-1 (PECAM-1) and Ki-67 signals increased in chimeras, compared with db/db control. The blood exchange rate in anastomoses also improved. Cell proliferation increased, though not reaching the level of WT controls. Interestingly, WT fibrocytes may be recruited into the wound from WT circulation and facilitate ECM deposition. Vessel formation, however, relies mainly on



db/db cells. Approximately 20% of total cells in the wound area were derived from WT animals in chimeras. Parabiosis did not influence glycemic control. Improvement in wound healing was also observable when animals were separated 24 h after wound formation [107]. Skin flap tissue re-integration is also impaired under diabetic conditions in ob/ob mice. Flap tissue loses early VEGF expression, as well as wound margin keratinocytes, associated with reduced blood vessel formation. Importantly, HIF-1 $\alpha$  is completely absent in diabetic flap tissue. These findings suggest difficult conditions that may appear when performing reconstructive surgeries under diabetic conditions [108]. Surprisingly, when creating a myocutaneous flap in ob/ob or db/db mice, increased perfusion and revascularization rates are observed, coupled with reduced flap necrosis on day 10, compared with healthy littermates [109].

One group showed that topical application of 11 $\beta$ -hydroxysteroid dehydrogenase (11 $\beta$ -HSD1) enhances wound healing in ob/ob mice, also proving that 11 $\beta$ -HSD1 negatively regulates the proliferation of keratinocytes and fibroblasts [110]. A conflicting study showed that 11 $\beta$ -HSD1 levels in intact db/db murine skin are in fact elevated and argued that it may contribute to impaired wound healing in this model [111]. The issue of corticosteroids' synthesis in the skin under diabetic conditions seems to be unresolved. Another study showed that systemic and topical administration of adiponectin improves wound healing in db/db mice, augmenting proliferation and migration of keratinocytes via AdipoR1/AdipoR2 and the Extracellular signal-regulated kinase (ERK) signaling pathways [112].

Sood et al. aimed to assess the metabolic profile of intact and wounded skin of db/db mice 7 days after injury. They found 62 metabolites, which showed an altered response to injury compared with healthy counterparts. It was the first study pointing to glycine, kynurenate, and OH-phenylpyruvate being dysregulated in the wound healing process [113]. Zhao et al. investigated the role of Epoxyeicosatrienoic acids (EETs)—molecules, whose production is catalyzed by cytochrome P450. Ob/ob mice showed lower mRNA and protein expression of cytochrome P450 2C65 and 2J6 (CYP2C65 and CYP2J6), suggesting low EETs levels. Furthermore, 11,12-EET partially rescued wound healing by modulating inflammation and angiogenesis, posing a potential therapeutic agents in leptin-deficient model [114].

### 3.1.16. Interventions

Innumerable publications have attempted to find an intervention that would be viable in wound healing in the leptin-deficient mice model. However, only a handful of these has passed the preclinical phase and entered human clinical trials (Table 2).

PDGF had shown success in pre-clinical studies and its recombinant form, Becaplermin (REGRANEX<sup>®</sup> Gel) [115], was approved for the topical treatment for lower extremity diabetic neuropathic ulcers that extend beyond the subcutaneous tissue. Unfortunately, in 2008, a black box warning was added to the gel as there had been an increased rate of deaths from systemic malignancies seen in patients who received three or more tubes [116]. Beyond 2008, post-marketing studies have demonstrated no increased safety risk with the use of the gel [117]. Other interventions, which successfully proceeded to clinical trials are displayed in Table 2.

**Table 2.** Interventions studied in leptin-deficient murine models, which progressed to clinical trials.

Intervention	In Vivo Studies	Most Advanced Clinical Trial	Reference
rPDGF-BB (Becaplermin)	[118–124]	Phase 3	[125]
Collagen application (scaffold)	[126,127]	Phase 4	[128]
Chitosan Gel Application	[129–131]	Phase 2	[132]
bFGF	[119,133,134]	Phase 3	[135]
VEGF, HIF1- $\alpha$	[136–139]	Phase 2	[140]
Negative Pressure Wound Therapy	[141]	Phase 2	[142]
Cold Plasma Therapy	[143,144]	Phase 2	[145]
Topical Insulin	[111,146]	Phase 2	[147]
Low Magnitude High-Frequency Vibration Platform	[148]	Phase 2	[149]
Nitric Oxide Releasing Patch	[150–152]	Phase 3	[153]

rPDGF-BB—recombinant human BB homodimeric platelet-derived growth factor; bFGF—basic fibroblast growth factor, VEGF—vascular endothelial growth factor, HIF1- $\alpha$ —hypoxia-inducible factor 1  $\alpha$ .

### 3.2. Discussion

The study intended to comprehensively summarize both the mechanistic and functional aspects of using T2DM murine models of leptin deficiency in wound healing research. The wound healing process relies on numerous molecular and physiological pathways. Thus, the coexistence of DM modulates the process. A vast majority of analyzed papers focused on deepening the knowledge of shifts in molecular pathways as either a systemic or local response to injury. The most prevalently described pathologies in wound healing concerned: extension in complete wound healing time in both excisional and incisional settings, impaired growth factor expression especially via distorted HIF1 $\alpha$  pathway, severely impaired angiogenesis at various stages, distorted macrophage role, prolonged proinflammatory cytokine excretion, and impaired apoptosis. Along with local discrepancies, also systemic alterations are present, such as distorted stem cells function.

Conclusions drawn from the summary are limited by a few factors. The study aimed to address only the leptin-deficient murine model of T2DM. Thus, it lacks findings concerning diabetic wound healing on other rodent models such as Zucker diabetic Sprague Dawley rats, Zucker fatty rat, SHR/N-cp Rat, or JCR/LA-cp Rat [5,154]. In addition, the review did not cover dietary or pharmacologically induced T2DM models—such C57BL/6J mice fed with a high-fat diet [155] or low-dose streptozocin-treated animals [156]. However, small size, cost efficiency, obesity and hyperglycemia, easy availability of those mice, widespread use in wound healing research, and delayed healing are still advantages of the leptin-deficient murine model. The above-mentioned are counterbalanced with unfavourable traits such as loose and hairy skin, wound healing with contraction (overcome by wound splinting), difficulty in inducing partial thickness wounds, limited translational efficiency, and an immune response distinct from that of humans [154]. Additionally, the background strain of leptin-deficient mice influences the phenotype. C57BLKS background leads to an uncontrolled rise in blood sugar, severe depletion of the insulin-producing beta-cells of the pancreatic islets, and death by 10 months of age [157]. Mice with the C57BL/6 background have compensatory hyperplasia of the islet B cells, and continued hyperinsulinemia throughout an 18- to 20-month life span. Eventually, wound healing is delayed and metabolic efficiency is increased [7]. Thus, researchers should be aware of those details when designing a study or analyzing the literature.

Some important distinctions must be underlined between the human and murine skin anatomy, physiology, and molecular signaling. Despite the same layers of cells in the dermis and epidermis, human skin is relatively thick (over 100  $\mu$ m) and adhered to the

underlying tissues, whereas murine skin is thinner than 25  $\mu\text{m}$  and loose. Human epidermis is composed of 5 to 10 cell layers, whereas murine skin contains only 2 or 3. Murine dermis is thicker and 40% firmer in males compared to females, whereas the epidermis and subcutaneous tissue are thicker in the latter. Further, panniculus carnosus found in murine subcutaneous tissue is absent in humans, and thus influences skin biomechanics during wound healing—up to 90% of excisional wounds in mice close by contraction. Histologically, epidermal ridges are present in human skin and absent in mice. However, collagen types I and III, respectively, are similarly distributed in mice and human skin. There are also several differences in skin immunology. The phenotypic markers of macrophages differ between species. F4/80 adhesive glycoprotein, for instance, identifies both murine macrophages and human eosinophils. Conversely, the macrophage mannose receptor (CD206) found in murine M2 macrophages is expressed in human dermal fibroblasts and keratinocytes. Langerhans and CD8-positive T cells populate the human epidermis. Murine epidermis, in addition to these cell types, contains a specific population of  $\gamma\delta$  dendritic epidermal T cells (DETCs). They secrete FGF-9 in injured skin and promote the WNT pathway, upregulating FGF-9 in dermal fibroblasts, finally leading to hair follicle regeneration. Such a mechanism could explain hair follicles formation in mice scars but not in humans. They play an exceptional role in murine wound healing, unlike in humans. Further, IL-8, CXCL-7, CXCL-11, and monocyte chemoattractant were identified in humans but not in mice wound healing. Human skin also specifically expresses CCL-13, CCL-14, CCL-15, and CCL-18, whereas CCL-6, CCL-9, CXCL-15, CXCL-14, and CCL-12 are only expressed in mice [158].

Noteworthy, the monogenic origin of db/db and ob/ob mice do not correspond with the polygenic nature of T2DM in humans. Leptin deficiency is not the main causative mechanism of T2DM. Thus, considering polygenic models such as NONcNZO10 seems worthwhile. Compared with db/db and STZ-induced DM models, only NONcNZO10 preserved impaired wound healing phenotypes in different wound models compared with the healthy origin strain. Db/db were inefficient in ischemia-reperfusion lesions [12].

The multifactorial nature of the wound healing process becomes even more complex with coexisting diabetes. The aforementioned studies, despite their limitations, serve as an important preclinical basis for translational applications. In total, 27 studies served as in vivo preclinical studies, prior to further clinical trials ( $n = 10$ ). The most promising results concerned rPDGF-BB (Becaplermin), Collagen application (scaffold), Trafermin (bFGF spray), and Nitric Oxide Releasing Patch which achieved phase III clinical trial.

The discrepancy between the number of in vivo intervention studies ( $n = 361$ ) and clinical trials confirms the inevitable need for use of the animal model in wound healing studies—both basic and applicatory ones.

#### 4. Conclusions

An impressive number of studies relies on db/db or ob/ob mice as T2DM models for wound healing in both basic and applicatory research. Despite their limitations hindering the transnationality of results into the human setting, they remain reliable and widely studied animal models. Their strength is based on a diligently studied mechanisms of wound healing on both local and systemic levels along with satisfactory reflection on pathologies present in human diabetic wounds. Mechanistic studies revealed some degree of resemblance and discrepancy between the animal models and human physiology. With some precaution, especially concerning the monogenic nature of the model, they may be further used in preclinical studies of wound healing for incisional and excisional lesions with comorbid diabetes mellitus.

**Supplementary Materials:** The following are available online at <https://www.mdpi.com/article/10.3390/ijms23158621/s1>.

**Author Contributions:** Conceptualization, A.S.; methodology, A.S.; software, P.W.; validation, W.P. and P.W.; data curation, A.S.; writing—original draft preparation, A.S., I.K. and P.K.; writing—review and editing, A.S., W.P., P.W., I.K. and P.K.; visualization, I.K. and P.K.; supervision, P.W.; project administration, A.S. All authors have read and agreed to the published version of the manuscript.

**Funding:** This research received no external funding.

**Institutional Review Board Statement:** Not applicable.

**Informed Consent Statement:** Not applicable.

**Conflicts of Interest:** The authors declare no conflict of interest.

## References

1. Boulton, A.J.; Vileikyte, L.; Ragnarson-Tennvall, G.; Apelqvist, J. The global burden of diabetic foot disease. *Lancet* **2005**, *366*, 1719–1724. [[CrossRef](#)]
2. Zheng, Y.; Ley, S.H.; Hu, F.B. Global aetiology and epidemiology of type 2 diabetes mellitus and its complications. *Nat. Rev. Endocrinol.* **2018**, *14*, 88–98. [[CrossRef](#)] [[PubMed](#)]
3. Uivaraseanu, B.; Bungau, S.; Tit, D.M.; Fratila, O.; Rus, M.; Maghiar, T.A.; Maghiar, O.; Pantis, C.; Vesa, C.M.; Zaha, D.C. Clinical, Pathological and Microbiological Evaluation of Diabetic Foot Syndrome. *Medicina* **2020**, *56*, 380. [[CrossRef](#)]
4. Edmonds, M.; Manu, C.; Vas, P. The current burden of diabetic foot disease. *J. Clin. Orthop. Trauma* **2021**, *17*, 88–93. [[CrossRef](#)] [[PubMed](#)]
5. Wang, B.; Chandrasekera, P.C.; Pippin, J.J. Leptin- and leptin receptor-deficient rodent models: Relevance for human type 2 diabetes. *Curr. Diabetes Rev.* **2014**, *10*, 131–145. [[CrossRef](#)] [[PubMed](#)]
6. Hummel, K.P.; Coleman, D.L.; Lane, P.W. The influence of genetic background on expression of mutations at the diabetes locus in the mouse. I. C57BL-KsJ and C57BL-6J strains. *Biochem. Genet.* **1972**, *7*, 1–13. [[CrossRef](#)]
7. Coleman, D.L. Obese and diabetes: Two mutant genes causing diabetes-obesity syndromes in mice. *Diabetologia* **1978**, *14*, 141–148. [[CrossRef](#)]
8. Page, M.J.; McKenzie, J.E.; Bossuyt, P.M.; Boutron, I.; Hoffmann, T.C.; Mulrow, C.D.; Shamseer, L.; Tetzlaff, J.M.; Akl, E.A.; Brennan, S.E.; et al. The PRISMA 2020 statement: An updated guideline for reporting systematic reviews. *BMJ* **2021**, *372*, n71. [[CrossRef](#)]
9. Senter, L.H.; Legrand, E.K.; Laemmerhirt, K.E.; Kiorpes, T.C. Assessment of full-thickness wounds in the genetically diabetic mouse for suitability as a wound healing model. *Wound Repair Regen.* **1995**, *3*, 351–358. [[CrossRef](#)]
10. Brem, H.; Tomic-Canic, M.; Entero, H.; Hanflik, A.M.; Wang, V.M.; Fallon, J.T.; Ehrlich, H.P. The synergism of age and db/db genotype impairs wound healing. *Exp. Gerontol.* **2007**, *42*, 523–531. [[CrossRef](#)]
11. Sullivan, S.R.; Underwood, R.A.; Gibran, N.S.; Sigle, R.O.; Usui, M.L.; Carter, W.G.; Olerud, J.E. Validation of a model for the study of multiple wounds in the diabetic mouse (db/db). *Plast. Reconstr. Surg.* **2004**, *113*, 953–960. [[CrossRef](#)] [[PubMed](#)]
12. Fang, R.C.; Kryger, Z.B.; Buck, D.W., II; De La Garza, M.; Galiano, R.D.; Mustoe, T.A. Limitations of the db/db mouse in translational wound healing research: Is the NONcNZO10 polygenic mouse model superior? *Wound Repair Regen.* **2010**, *18*, 605–613. [[CrossRef](#)]
13. Berdal, M.; Jenssen, T. No association between glycemia and wound healing in an experimental db/db mouse model. *ISRN Endocrinol.* **2013**, *2013*, 307925. [[CrossRef](#)] [[PubMed](#)]
14. Michaels, J.T.; Churgin, S.S.; Blechman, K.M.; Greives, M.R.; Aarabi, S.; Galiano, R.D.; Gurtner, G.C. db/db mice exhibit severe wound-healing impairments compared with other murine diabetic strains in a silicone-splinted excisional wound model. *Wound Repair. Regen.* **2007**, *15*, 665–670. [[CrossRef](#)]
15. Tkalcević, V.I.; Cuzić, S.; Parnham, M.J.; Pasalić, I.; Brajsa, K. Differential evaluation of excisional non-occluded wound healing in db/db mice. *Toxicol. Pathol.* **2009**, *37*, 183–192. [[CrossRef](#)] [[PubMed](#)]
16. Wang, X.T.; McKeever, C.C.; Vonu, P.; Patterson, C.; Liu, P.Y. Dynamic Histological Events and Molecular Changes in Excisional Wound Healing of Diabetic DB/DB Mice. *J. Surg. Res.* **2019**, *238*, 186–197. [[CrossRef](#)]
17. Gnyawali, S.C.; Sinha, M.; El Masry, M.S.; Wulff, B.; Ghatak, S.; Soto-Gonzalez, F.; Wilgus, T.A.; Roy, S.; Sen, C.K. High resolution ultrasound imaging for repeated measure of wound tissue morphometry, biomechanics and hemodynamics under fetal, adult and diabetic conditions. *PLoS ONE* **2020**, *15*, e0241831. [[CrossRef](#)]
18. Trousdale, R.K.; Jacobs, S.; Simhaee, D.A.; Wu, J.K.; Lustbader, J.W. Wound closure and metabolic parameter variability in a db/db mouse model for diabetic ulcers. *J. Surg. Res.* **2009**, *151*, 100–107. [[CrossRef](#)] [[PubMed](#)]
19. Goren, I.; Kämpfer, H.; Podda, M.; Pfeilschifter, J.; Frank, S. Leptin and wound inflammation in diabetic ob/ob mice: Differential regulation of neutrophil and macrophage influx and a potential role for the scab as a sink for inflammatory cells and mediators. *Diabetes* **2003**, *52*, 2821–2832. [[CrossRef](#)]
20. Werner, S.; Breeden, M.; Hübner, G.; Greenhalgh, D.G.; Longaker, M.T. Induction of keratinocyte growth factor expression is reduced and delayed during wound healing in the genetically diabetic mouse. *J. Investig. Dermatol.* **1994**, *103*, 469–473. [[CrossRef](#)]
21. Beer, H.D.; Longaker, M.T.; Werner, S. Reduced expression of PDGF and PDGF receptors during impaired wound healing. *J. Investig. Dermatol.* **1997**, *109*, 132–138. [[CrossRef](#)] [[PubMed](#)]

22. Brown, D.L.; Kane, C.D.; Chernausk, S.D.; Greenhalgh, D.G. Differential expression and localization of insulin-like growth factors I and II in cutaneous wounds of diabetic and nondiabetic mice. *Am. J. Pathol.* **1997**, *151*, 715–724. [[PubMed](#)]
23. Botusan, I.R.; Sunkari, V.G.; Savu, O.; Catrina, A.I.; Grunler, J.; Lindberg, S.; Pereira, T.; Yla-Herttuala, S.; Poellinger, L.; Brismar, K.; et al. Stabilization of HIF-1alpha is critical to improve wound healing in diabetic mice. *Proc. Natl. Acad. Sci. USA* **2008**, *105*, 19426–19431. [[CrossRef](#)] [[PubMed](#)]
24. Frank, S.; Hübner, G.; Breier, G.; Longaker, M.T.; Greenhalgh, D.G.; Werner, S. Regulation of vascular endothelial growth factor expression in cultured keratinocytes. Implications for normal and impaired wound healing. *J. Biol. Chem.* **1995**, *270*, 12607–12613. [[CrossRef](#)] [[PubMed](#)]
25. Qi, W.W.; Yang, C.; Dai, Z.Y.; Che, D.; Feng, J.; Mao, Y.L.; Cheng, R.; Wang, Z.X.; He, X.M.; Zhou, T.; et al. High Levels of Pigment Epithelium-Derived Factor in Diabetes Impair Wound Healing Through Suppression of Wnt Signaling. *Diabetes* **2015**, *64*, 1407–1419. [[CrossRef](#)]
26. Kämpfer, H.; Pfeilschifter, J.; Frank, S. Expressional regulation of angiopoietin-1 and -2 and the tie-1 and -2 receptor tyrosine kinases during cutaneous wound healing: A comparative study of normal and impaired repair. *Lab. Invest.* **2001**, *81*, 361–373. [[CrossRef](#)]
27. Maruyama, K.; Asai, J.; Li, M.; Thorne, T.; Losordo, D.W.; D'Amore, P.A. Decreased macrophage number and activation lead to reduced lymphatic vessel formation and contribute to impaired diabetic wound healing. *Am. J. Pathol.* **2007**, *170*, 1178–1191. [[CrossRef](#)]
28. Goren, I.; Müller, E.; Schiefelbein, D.; Gutwein, P.; Seitz, O.; Pfeilschifter, J.; Frank, S. Akt1 controls insulin-driven VEGF biosynthesis from keratinocytes: Implications for normal and diabetes-impaired skin repair in mice. *J. Invest. Dermatol.* **2009**, *129*, 752–764. [[CrossRef](#)]
29. Zins, S.R.; Amare, M.F.; Tadaki, D.K.; Elster, E.A.; Davis, T.A. Comparative analysis of angiogenic gene expression in normal and impaired wound healing in diabetic mice: Effects of extracorporeal shock wave therapy. *Angiogenesis* **2010**, *13*, 293–304. [[CrossRef](#)] [[PubMed](#)]
30. Kotlinowski, J.; Grochot-Przeczek, A.; Taha, H.; Kozakowska, M.; Pilecki, B.; Skrzypek, K.; Bartelik, A.; Derlacz, R.; Horvoets, A.J.G.; Pap, A.; et al. PPAR gamma activation but not PPAR gamma haploinsufficiency affects proangiogenic potential of endothelial cells and bone marrow-derived progenitors. *Cardiovasc. Diabetol.* **2014**, *13*, 150. [[CrossRef](#)]
31. Langer, S.; Beescho, C.; Ring, A.; Dorfmann, O.; Steinau, H.U.; Spindler, N. A new in vivo model using a dorsal skinfold chamber to investigate microcirculation and angiogenesis in diabetic wounds. *GMS Interdiscip. Plast. Reconstr. Surg. Dgprw* **2016**, *5*, Doc09. [[CrossRef](#)] [[PubMed](#)]
32. Okonkwo, U.A.; Chen, L.; Ma, D.; Haywood, V.A.; Barakat, M.; Urao, N.; Dipietro, L.A. Compromised angiogenesis and vascular integrity in impaired diabetic wound healing. *PLoS ONE* **2020**, *15*, e0231962. [[CrossRef](#)] [[PubMed](#)]
33. Hong, S.J.; Jin, D.P.; Buck, D.W., II; Galiano, R.D.; Mustoe, T.A. Impaired response of mature adipocytes of diabetic mice to hypoxia. *Exp. Cell Res.* **2011**, *317*, 2299–2307. [[CrossRef](#)] [[PubMed](#)]
34. Singh, K.; Sinha, M.; Pal, D.; Tabasum, S.; Gnyawali, S.C.; Khona, D.; Sarkar, S.; Mohanty, S.K.; Soto-Gonzalez, F.; Khanna, S.; et al. Cutaneous Epithelial to Mesenchymal Transition Activator ZEB1 Regulates Wound Angiogenesis and Closure in a Glycemic Status-Dependent Manner. *Diabetes* **2019**, *68*, 2175–2190. [[CrossRef](#)] [[PubMed](#)]
35. Kämpfer, H.; Paulukat, J.; Mühl, H.; Wetzler, C.; Pfeilschifter, J.; Frank, S. Lack of interferon-gamma production despite the presence of interleukin-18 during cutaneous wound healing. *Mol. Med.* **2000**, *6*, 1016–1027. [[CrossRef](#)] [[PubMed](#)]
36. Wetzler, C.; Kämpfer, H.; Stallmeyer, B.; Pfeilschifter, J.; Frank, S. Large and sustained induction of chemokines during impaired wound healing in the genetically diabetic mouse: Prolonged persistence of neutrophils and macrophages during the late phase of repair. *J. Invest. Dermatol.* **2000**, *115*, 245–253. [[CrossRef](#)] [[PubMed](#)]
37. Goren, I.; Kämpfer, H.; Müller, E.; Schiefelbein, D.; Pfeilschifter, J.; Frank, S. Oncostatin M expression is functionally connected to neutrophils in the early inflammatory phase of skin repair: Implications for normal and diabetes-impaired wounds. *J. Invest. Dermatol.* **2006**, *126*, 628–637. [[CrossRef](#)] [[PubMed](#)]
38. Zykova, S.N.; Jenssen, T.G.; Berdal, M.; Olsen, R.; Myklebust, R.; Seljelid, R. Altered cytokine and nitric oxide secretion in vitro by macrophages from diabetic type II-like db/db mice. *Diabetes* **2000**, *49*, 1451–1458. [[CrossRef](#)] [[PubMed](#)]
39. Liu, R.; Desta, T.; He, H.; Graves, D.T. Diabetes alters the response to bacteria by enhancing fibroblast apoptosis. *Endocrinology* **2004**, *145*, 2997–3003. [[CrossRef](#)] [[PubMed](#)]
40. Jun, J.I.; Kim, K.H.; Lau, L.F. The matricellular protein CCN1 mediates neutrophil efferocytosis in cutaneous wound healing. *Nat. Commun.* **2015**, *6*, 7386. [[CrossRef](#)] [[PubMed](#)]
41. Sawaya, A.P.; Stone, R.C.; Brooks, S.R.; Pastar, I.; Jozic, I.; Hasneen, K.; O'Neill, K.; Mehdizadeh, S.; Head, C.R.; Strbo, N.; et al. Deregulated immune cell recruitment orchestrated by FOXM1 impairs human diabetic wound healing. *Nat. Commun.* **2020**, *11*, 4678. [[CrossRef](#)] [[PubMed](#)]
42. Taylor, K.R.; Mills, R.E.; Costanzo, A.E.; Jameson, J.M. Gammadelta T cells are reduced and rendered unresponsive by hyperglycemia and chronic TNFalpha in mouse models of obesity and metabolic disease. *PLoS ONE* **2010**, *5*, e11422. [[CrossRef](#)] [[PubMed](#)]
43. Taylor, K.R.; Costanzo, A.E.; Jameson, J.M. Dysfunctional gamma delta T Cells Contribute to Impaired Keratinocyte Homeostasis in Mouse Models of Obesity. *J. Invest. Dermatol.* **2011**, *131*, 2409–2418. [[CrossRef](#)] [[PubMed](#)]



44. Schürmann, C.; Seitz, O.; Sader, R.; Pfeilschifter, J.; Goren, I.; Frank, S. Role of wound macrophages in skin flap loss or survival in an experimental diabetes model. *Br. J. Surg.* **2010**, *97*, 1437–1451. [[CrossRef](#)] [[PubMed](#)]
45. Kampfer, H.; Schmidt, R.; Geisslinger, G.; Pfeilschifter, J.; Frank, S. Wound inflammation in diabetic ob/ob mice—Functional coupling of prostaglandin biosynthesis to cyclooxygenase-1 activity in diabetes-impaired wound healing. *Diabetes* **2005**, *54*, 1543–1551. [[CrossRef](#)] [[PubMed](#)]
46. Frank, S.; Seitz, O.; Schürmann, C.; Hermes, N.; Müller, E.; Pfeilschifter, J.; Goren, I. Wound healing in mice with high-fat diet- or ob gene-induced diabetes-obesity syndromes: A comparative study. *Exp. Diabetes Res.* **2010**, *2010*, 476969. [[CrossRef](#)]
47. Schürmann, C.; Goren, I.; Linke, A.; Pfeilschifter, J.; Frank, S. Deregulated unfolded protein response in chronic wounds of diabetic ob/ob mice: A potential connection to inflammatory and angiogenic disorders in diabetes-impaired wound healing. *Biochem. Biophys. Res. Commun.* **2014**, *446*, 195–200. [[CrossRef](#)] [[PubMed](#)]
48. Mirza, R.; Koh, T.J. Dysregulation of monocyte/macrophage phenotype in wounds of diabetic mice. *Cytokine* **2011**, *56*, 256–264. [[CrossRef](#)] [[PubMed](#)]
49. Mirza, R.E.; Fang, M.M.; Ennis, W.J.; Koh, T.J. Blocking Interleukin-1 beta Induces a Healing-Associated Wound Macrophage Phenotype and Improves Healing in Type 2 Diabetes. *Diabetes* **2013**, *62*, 2579–2587. [[CrossRef](#)]
50. Rodero, M.P.; Hodgson, S.S.; Hollier, B.; Combadiere, C.; Khosrotehrani, K. Reduced Il17a expression distinguishes a Ly6c(lo)MHCII(hi) macrophage population promoting wound healing. *J. Investig. Dermatol.* **2013**, *133*, 783–792. [[CrossRef](#)]
51. Goren, I.; Pfeilschifter, J.; Frank, S. Uptake of Neutrophil-Derived Ym1 Protein Distinguishes Wound Macrophages in the Absence of Interleukin-4 Signaling in Murine Wound Healing. *Am. J. Pathol.* **2014**, *184*, 3249–3261. [[CrossRef](#)] [[PubMed](#)]
52. Yan, J.; Tie, G.; Wang, S.; Tutto, A.; DeMarco, N.; Khair, L.; Fazzio, T.G.; Messina, L.M. Diabetes impairs wound healing by Dnmt1-dependent dysregulation of hematopoietic stem cells differentiation towards macrophages. *Nat. Commun.* **2018**, *9*, 33. [[CrossRef](#)] [[PubMed](#)]
53. Wood, S.; Jayaraman, V.; Huelsmann, E.J.; Bonish, B.; Burgad, D.; Sivaramakrishnan, G.; Qin, S.S.; DiPietro, L.A.; Zloza, A.; Zhang, C.X.; et al. Pro-Inflammatory Chemokine CCL2 (MCP-1) Promotes Healing in Diabetic Wounds by Restoring the Macrophage Response. *PLoS ONE* **2014**, *9*, e91574. [[CrossRef](#)]
54. Guest, C.B.; Chakour, K.S.; Freund, G.G. Macropinocytosis is decreased in diabetic mouse macrophages and is regulated by AMPK. *BMC Immunol.* **2008**, *9*, 42. [[CrossRef](#)] [[PubMed](#)]
55. Mirza, R.E.; Fang, M.M.; Weinheimer-Haus, E.M.; Ennis, W.J.; Koh, T.J. Sustained inflammasome activity in macrophages impairs wound healing in type 2 diabetic humans and mice. *Diabetes* **2014**, *63*, 1103–1114. [[CrossRef](#)]
56. Stallmeyer, B.; Kämpfer, H.; Podda, M.; Kaufmann, R.; Pfeilschifter, J.; Frank, S. A novel keratinocyte mitogen: Regulation of leptin and its functional receptor in skin repair. *J. Investig. Dermatol.* **2001**, *117*, 98–105. [[CrossRef](#)] [[PubMed](#)]
57. Zhang, J.; Li, L.M.; Li, J.; Liu, Y.; Zhang, C.Y.; Zhang, Y.J.; Zen, K. Protein Tyrosine Phosphatase 1B Impairs Diabetic Wound Healing Through Vascular Endothelial Growth Factor Receptor 2 Dephosphorylation. *Arterioscler. Thromb. Vasc. Biol.* **2015**, *35*, 163–174. [[CrossRef](#)] [[PubMed](#)]
58. Goren, I.; Pfeilschifter, J.; Frank, S. Determination of leptin signaling pathways in human and murine keratinocytes. *Biochem. Biophys. Res. Commun.* **2003**, *303*, 1080–1085. [[CrossRef](#)]
59. Ring, B.D.; Scully, S.; Davis, C.R.; Baker, M.B.; Cullen, M.J.; Pelleymounter, M.A.; Danilenko, D.M. Systemically and topically administered leptin both accelerate wound healing in diabetic ob/ob mice. *Endocrinology* **2000**, *141*, 446–449. [[CrossRef](#)] [[PubMed](#)]
60. Cao, Y.; Gao, F.; Li, C.Z.; Xue, Y.M. Expression of leptin and its long-form receptor in the marginal cutaneous tissues of diabetic foot ulcers. *Acta Diabetol.* **2012**, *49*, S205–S214. [[CrossRef](#)]
61. Kämpfer, H.; Pfeilschifter, J.; Frank, S. Expression and activity of arginase isoenzymes during normal and diabetes-impaired skin repair. *J. Investig. Dermatol.* **2003**, *121*, 1544–1551. [[CrossRef](#)] [[PubMed](#)]
62. Goodson, W.H., III; Hunt, T.K. Wound collagen accumulation in obese hyperglycemic mice. *Diabetes* **1986**, *35*, 491–495. [[CrossRef](#)] [[PubMed](#)]
63. Kern, P.A.; Saghizadeh, M.; Ong, J.M.; Bosch, R.J.; Deem, R.; Simsolo, R.B. The expression of tumor necrosis factor in human adipose tissue. Regulation by obesity, weight loss, and relationship to lipoprotein lipase. *J. Clin. Investig.* **1995**, *95*, 2111–2119. [[CrossRef](#)] [[PubMed](#)]
64. Goren, I.; Muller, E.; Pfeilschifter, J.; Frank, S. Severely impaired insulin signaling in chronic wounds of diabetic ob/ob mice—A potential role of tumor necrosis factor-alpha. *Am. J. Pathol.* **2006**, *168*, 765–777. [[CrossRef](#)] [[PubMed](#)]
65. Wang, X.Q.; Lee, S.; Wilson, H.; Seeger, M.; Iordanov, H.; Gatla, N.; Whittington, A.; Bach, D.; Lu, J.Y.; Paller, A.S. Ganglioside GM3 depletion reverses impaired wound healing in diabetic mice by activating IGF-1 and insulin receptors. *J. Investig. Dermatol.* **2014**, *134*, 1446–1455. [[CrossRef](#)]
66. Peppas, M.; Zhang, J.G.; Cai, W.J.; Brem, H.; Vlassara, H. Wound healing in diabetic db/db(+/+) mice is regulated by dietary content in glycotoxins under stable hyperglycemia. *Diabetes* **2002**, *51*, A17–A18.
67. Ji, X.Y.; Chen, Y.; Ye, G.H.; Dong, M.W.; Lin, K.Z.; Han, J.G.; Feng, X.P.; Li, X.B.; Yu, L.S.; Fan, Y.Y. Detection of RAGE expression and its application to diabetic wound age estimation. *Int. J. Leg. Med.* **2017**, *131*, 691–698. [[CrossRef](#)]
68. Kim, J.H.; Yoon, N.Y.; Kim, D.H.; Jung, M.; Jun, M.; Park, H.Y.; Chung, C.H.; Lee, K.; Kim, S.; Park, C.S.; et al. Impaired permeability and antimicrobial barriers in type 2 diabetes skin are linked to increased serum levels of advanced glycation end-product. *Exp. Dermatol.* **2018**, *27*, 815–823. [[CrossRef](#)] [[PubMed](#)]

69. Goova, M.T.; Li, J.; Kislinger, T.; Qu, W.; Lu, Y.; Bucciarelli, L.G.; Nowygrod, S.; Wolf, B.M.; Caliste, X.; Yan, S.F.; et al. Blockade of receptor for advanced glycation end-products restores effective wound healing in diabetic mice. *Am. J. Pathol.* **2001**, *159*, 513–525. [[CrossRef](#)]
70. Lerman, O.Z.; Galiano, R.D.; Armour, M.; Levine, J.P.; Gurtner, G.C. Cellular dysfunction in the diabetic fibroblast—Impairment in migration, vascular endothelial growth factor production, and response to hypoxia. *Am. J. Pathol.* **2003**, *162*, 303–312. [[CrossRef](#)]
71. Liu, R.K.; Bal, H.S.; Desta, T.; Behl, Y.; Graves, D.T. Tumor necrosis factor-alpha mediates diabetes-enhanced apoptosis of matrix-producing cells and impairs diabetic healing. *Am. J. Pathol.* **2006**, *168*, 757–764. [[CrossRef](#)]
72. Siqueira, M.F.; Li, J.; Chehab, L.; Desta, T.; Chino, T.; Krothpali, N.; Behl, Y.; Alikhani, M.; Yang, J.; Braasch, C.; et al. Impaired wound healing in mouse models of diabetes is mediated by TNF- $\alpha$  dysregulation and associated with enhanced activation of forkhead box O1 (FOXO1). *Diabetologia* **2010**, *53*, 378–388. [[CrossRef](#)] [[PubMed](#)]
73. Peng, C.; Chen, B.; Kao, H.K.; Murphy, G.; Orgill, D.P.; Guo, L.F. Lack of FGF-7 Further Delays Cutaneous Wound Healing in Diabetic Mice. *Plast. Reconstr. Surg.* **2011**, *128*, 673E–684E. [[CrossRef](#)] [[PubMed](#)]
74. Jung, N.; Yu, J.; Um, J.; Dubon, M.J.; Park, K.S. Substance P modulates properties of normal and diabetic dermal fibroblasts. *Tissue Eng. Regen. Med.* **2016**, *13*, 155–161. [[CrossRef](#)] [[PubMed](#)]
75. Yu, J.; Choi, S.; Um, J.; Park, K.S. Reduced Expression of YAP in Dermal Fibroblasts is Associated with Impaired Wound Healing in Type 2 Diabetic Mice. *Tissue Eng. Regen. Med.* **2017**, *14*, 49–55. [[CrossRef](#)] [[PubMed](#)]
76. Al-Mashat, H.A.; Kandru, S.; Liu, R.K.; Behl, Y.; Desta, T.; Graves, D.T. Diabetes enhances mRNA levels of proapoptotic genes and caspase activity, which contribute to impaired healing. *Diabetes* **2006**, *55*, 487–495. [[CrossRef](#)]
77. Guo, Y.Y.; Lin, C.; Xu, P.; Wu, S.; Fu, X.J.; Xia, W.D.; Yao, M. AGEs Induced Autophagy Impairs Cutaneous Wound Healing via Stimulating Macrophage Polarization to M1 in Diabetes. *Sci. Rep.* **2016**, *6*, 36416. [[CrossRef](#)]
78. Brown, D.L.; Kao, W.W.; Greenhalgh, D.G. Apoptosis down-regulates inflammation under the advancing epithelial wound edge: Delayed patterns in diabetes and improvement with topical growth factors. *Surgery* **1997**, *121*, 372–380. [[CrossRef](#)]
79. Shin, L.; Peterson, D.A. Impaired therapeutic capacity of autologous stem cells in a model of type 2 diabetes. *Stem Cells Transl. Med.* **2012**, *1*, 125–135. [[CrossRef](#)]
80. Fiorina, P.; Pietramaggiore, G.; Scherer, S.S.; Jurewicz, M.; Mathews, J.C.; Vergani, A.; Thomas, G.; Orsenigo, E.; Staudacher, C.; La Rosa, S.; et al. The mobilization and effect of endogenous bone marrow progenitor cells in diabetic wound healing. *Cell Transpl.* **2010**, *19*, 1369–1381. [[CrossRef](#)]
81. Tepper, O.M.; Carr, J.; Allen, R.J., Jr.; Chang, C.C.; Lin, C.D.; Tanaka, R.; Gupta, S.M.; Levine, J.P.; Saadeh, P.B.; Warren, S.M. Decreased circulating progenitor cell number and failed mechanisms of stromal cell-derived factor-1alpha mediated bone marrow mobilization impair diabetic tissue repair. *Diabetes* **2010**, *59*, 1974–1983. [[CrossRef](#)] [[PubMed](#)]
82. Bermudez, D.M.; Xu, J.W.; Herdrich, B.J.; Radu, A.; Mitchell, M.E.; Liechty, K.W. Inhibition of stromal cell-derived factor-1 alpha further impairs diabetic wound healing. *J. Vasc. Surg.* **2011**, *53*, 774–784. [[CrossRef](#)] [[PubMed](#)]
83. Wang, P.; Yang, X.; Zhang, Z.; Song, J.; Guan, Y.F.; Zou, D.J.; Miao, C.Y. Depletion of NAD pool contributes to impairment of endothelial progenitor cell mobilization in diabetes. *Metab. Clin. Exp.* **2016**, *65*, 852–862. [[CrossRef](#)] [[PubMed](#)]
84. Barman, P.K.; Urao, N.; Koh, T.J. Diabetes induces myeloid bias in bone marrow progenitors associated with enhanced wound macrophage accumulation and impaired healing. *J. Pathol.* **2019**, *249*, 435–446. [[CrossRef](#)] [[PubMed](#)]
85. Hoyer, F.F.; Zhang, X.Y.; Coppin, E.; Vasamsetti, S.B.; Modugu, G.; Schloss, M.J.; Rohde, D.; McAlpine, C.S.; Iwamoto, Y.; Libby, P.; et al. Bone Marrow Endothelial Cells Regulate Myelopoiesis in Diabetes Mellitus. *Circulation* **2020**, *142*, 244–258. [[CrossRef](#)] [[PubMed](#)]
86. Li, H.N.; O'Meara, M.; Zhang, X.; Zhang, K.Z.; Seyoum, B.; Yi, Z.P.; Kaufman, R.J.; Monks, T.J.; Wang, J.M. Ameliorating Methylglyoxal-Induced Progenitor Cell Dysfunction for Tissue Repair in Diabetes. *Diabetes* **2019**, *68*, 1287–1302. [[CrossRef](#)]
87. Wang, J.M.; Tao, J.; Chen, D.D.; Cai, J.J.; Irani, K.; Wang, Q.D.; Yuan, H.; Chen, A.F. MicroRNA miR-27b Rescues Bone Marrow-Derived Angiogenic Cell Function and Accelerates Wound Healing in Type 2 Diabetes Mellitus. *Arterioscler. Thromb. Vasc. Biol.* **2014**, *34*, 99–109. [[CrossRef](#)] [[PubMed](#)]
88. Icli, B.; Nabzdyk, C.S.; Lujan-Hernandez, J.; Cahill, M.; Auster, M.E.; Wara, A.K.M.; Sun, X.H.; Ozdemir, D.; Giatsidis, G.; Orgill, D.P.; et al. Regulation of impaired angiogenesis in diabetic dermal wound healing by microRNA-26a. *J. Mol. Cell. Cardiol.* **2016**, *91*, 151–159. [[CrossRef](#)]
89. Li, X.; Li, D.Q.; Wang, A.X.; Chu, T.B.; Lohcharoenkal, W.; Zheng, X.W.; Grunler, J.; Narayanan, S.; Eliasson, S.; Herter, E.K.; et al. MicroRNA-132 with Therapeutic Potential in Chronic Wounds. *J. Invest. Dermatol.* **2017**, *137*, 2630–2638. [[CrossRef](#)] [[PubMed](#)]
90. Icli, B.; Wu, W.; Ozdemir, D.; Li, H.; Cheng, H.S.; Haemmig, S.; Liu, X.; Giatsidis, G.; Avci, S.N.; Lee, N.; et al. MicroRNA-615-5p Regulates Angiogenesis and Tissue Repair by Targeting AKT/eNOS (Protein Kinase B/Endothelial Nitric Oxide Synthase) Signaling in Endothelial Cells. *Arterioscler. Thromb. Vasc. Biol.* **2019**, *39*, 1458–1474. [[CrossRef](#)]
91. Grice, E.A.; Snitkin, E.S.; Yockey, L.J.; Bermudez, D.M.; Liechty, K.W.; Segre, J.A.; Sequencing, N.C. Longitudinal shift in diabetic wound microbiota correlates with prolonged skin defense response. *Proc. Natl. Acad. Sci. USA* **2010**, *107*, 14799–14804. [[CrossRef](#)] [[PubMed](#)]
92. James, G.A.; Zhao, A.G.; Usui, M.; Underwood, R.A.; Nguyen, H.; Beyenal, H.; Pulcini, E.D.; Hunt, A.A.; Bernstein, H.C.; Fleckman, P.; et al. Microsensor and transcriptomic signatures of oxygen depletion in biofilms associated with chronic wounds. *Wound Repair Regen.* **2016**, *24*, 373–383. [[CrossRef](#)] [[PubMed](#)]

93. Desmet, C.M.; Lafosse, A.; Vériter, S.; Porporato, P.E.; Sonveaux, P.; Dufrane, D.; Levêque, P.; Gallez, B. Application of Electron Paramagnetic Resonance (EPR) Oximetry to Monitor Oxygen in Wounds in Diabetic Models. *PLoS ONE* **2015**, *10*, e0144914. [[CrossRef](#)] [[PubMed](#)]
94. Park, S.; Rich, J.; Hanses, F.; Lee, J.C. Defects in Innate Immunity Predispose C57BL/6J-Lepr(db)/Lepr(db) Mice to Infection by *Staphylococcus aureus*. *Infect. Immun.* **2009**, *77*, 1008–1014. [[CrossRef](#)]
95. Naguib, G.; Al-Mashat, H.; Desta, T.; Graves, D.T. Diabetes prolongs the inflammatory response to a bacterial stimulus through cytokine dysregulation. *J. Investig. Dermatol.* **2004**, *123*, 87–92. [[CrossRef](#)] [[PubMed](#)]
96. Zhao, G.; Bauerle, E.A.; Usui, M.L.; Underwood, R.A.; Singh, P.K.; James, G.A.; Stewart, P.S.; Olerud, J.E.; Fleckman, P. Characterization of biofilm infected wounds in diabetic mice. *J. Investig. Dermatol.* **2010**, *130*, S2. [[CrossRef](#)]
97. Zhao, G.; Hochwalt, P.C.; Usui, M.L.; Underwood, R.A.; Singh, P.K.; James, G.A.; Stewart, P.S.; Fleckman, P.; Olerud, J.E. Delayed wound healing in diabetic (db/db) mice with *Pseudomonas aeruginosa* biofilm challenge: A model for the study of chronic wounds. *Wound Repair Regen.* **2010**, *18*, 467–477. [[CrossRef](#)]
98. Zhao, G.; Usui, M.L.; Underwood, R.A.; Singh, P.K.; James, G.A.; Stewart, P.S.; Fleckman, P.; Olerud, J.E. Time course study of delayed wound healing in a biofilm-challenged diabetic mouse model. *Wound Repair Regen.* **2012**, *20*, 342–352. [[CrossRef](#)]
99. Chen, S.N.; Li, R.R.; Cheng, C.; Xu, J.Y.; Jin, C.X.; Gao, F.R.; Wang, J.; Zhang, J.P.; Zhang, J.F.; Wang, H.; et al. *Pseudomonas aeruginosa* infection alters the macrophage phenotype switching process during wound healing in diabetic mice. *Cell Biol. Int.* **2018**, *42*, 877–889. [[CrossRef](#)]
100. Dhall, S.; Do, D.C.; Garcia, M.; Kim, J.; Mirebrahim, S.H.; Lyubovitsky, J.; Lonardi, S.; Nothnagel, E.A.; Schiller, N.; Martins-Green, M. Generating and reversing chronic wounds in diabetic mice by manipulating wound redox parameters. *J. Diabetes Res.* **2014**, *2014*, 562625. [[CrossRef](#)]
101. Kim, J.H.; Martins-Green, M. Protocol to create chronic wounds in diabetic mice. *J. Vis. Exp.* **2019**, *2019*, e57656. [[CrossRef](#)] [[PubMed](#)]
102. Panayi, A.C.; Endo, Y.; Karvar, M.; Sensharma, P.; Haug, V.; Fu, S.Q.; Mi, B.B.; An, Y.; Orgill, D.P. Low mortality oxidative stress murine chronic wound model. *BMJ Open Diabetes Res. Care* **2020**, *8*, e001221. [[CrossRef](#)] [[PubMed](#)]
103. Park, S.A.; Teixeira, L.B.C.; Raghunathan, V.K.; Covert, J.; Dubielzig, R.R.; Isseroff, R.R.; Schurr, M.; Abbott, N.L.; McAnulty, J.; Murphy, C.J. Full-thickness splinted skin wound healing models in db/db and heterozygous mice: Implications for wound healing impairment. *Wound Repair Regen.* **2014**, *22*, 368–380. [[CrossRef](#)] [[PubMed](#)]
104. Spenny, M.L.; Muangman, P.; Sullivan, S.R.; Bunnett, N.W.; Ansel, J.C.; Olerud, J.E.; Gibran, N.S. Neutral endopeptidase inhibition in diabetic wound repair. *Wound Repair Regen.* **2002**, *10*, 295–301. [[CrossRef](#)] [[PubMed](#)]
105. Schiefelbein, D.; Goren, I.; Fisslthaler, B.; Schmidt, H.; Geisslinger, G.; Pfeilschifter, J.; Frank, S. Biphasic regulation of HMG-CoA reductase expression and activity during wound healing and its functional role in the control of keratinocyte angiogenic and proliferative responses. *J. Biol. Chem.* **2008**, *283*, 15479–15490. [[CrossRef](#)] [[PubMed](#)]
106. Medicherla, S.; Wadsworth, S.; Cullen, B.; Silcock, D.; Ma, J.Y.; Mangadu, R.; Kerr, I.; Chakravarty, S.; Luedtke, G.L.; Dugar, S.; et al. p38 MAPK inhibition reduces diabetes-induced impairment of wound healing. *Diabetes Metab. Syndr. Obes.* **2009**, *2*, 91–100.
107. Pietramaggiore, G.; Scherer, S.S.; Alperovich, M.; Chen, B.; Orgill, D.P.; Wagers, A.J. Improved cutaneous healing in diabetic mice exposed to healthy peripheral circulation. *J. Investig. Dermatol.* **2009**, *129*, 2265–2274. [[CrossRef](#)] [[PubMed](#)]
108. Schurmann, C.; Schmidt, N.; Seitz, O.; Pfeilschifter, J.; Frank, S. Angiogenic response pattern during normal and impaired skin flap re-integration in mice: A comparative study. *J. Cranio-Maxillofac. Surg.* **2014**, *42*, 1710–1716. [[CrossRef](#)] [[PubMed](#)]
109. Clark, R.M.; Coffman, B.; McGuire, P.G.; Howdieshell, T.R. Myocutaneous revascularization following graded ischemia in lean and obese mice. *Diabetes Metab. Syndr. Obes.* **2016**, *9*, 325–336. [[CrossRef](#)] [[PubMed](#)]
110. Terao, M.; Murota, H.; Kimura, A.; Kato, A.; Ishikawa, A.; Igawa, K.; Miyoshi, E.; Katayama, I. 11 beta-Hydroxysteroid Dehydrogenase-1 Is a Novel Regulator of Skin Homeostasis and a Candidate Target for Promoting Tissue Repair. *PLoS ONE* **2011**, *6*, e25039. [[CrossRef](#)]
111. Brazel, C.B.; Simon, J.C.; Tuckermann, J.P.; Saalbach, A. Inhibition of 11 $\beta$ -HSD1 expression by insulin in skin: Impact for diabetic wound healing. *J. Clin. Med.* **2020**, *9*, 3878. [[CrossRef](#)]
112. Shibata, S.; Tada, Y.; Asano, Y.; Hau, C.S.; Kato, T.; Saeki, H.; Yamauchi, T.; Kubota, N.; Kadowaki, T.; Sato, S. Adiponectin regulates cutaneous wound healing by promoting keratinocyte proliferation and migration via the ERK signaling pathway. *J. Immunol.* **2012**, *189*, 3231–3241. [[CrossRef](#)]
113. Sood, R.F.; Gu, H.W.; Djukovic, D.; Deng, L.L.; Ga, M.; Muffley, L.A.; Rafferty, D.; Hocking, A.M. Targeted metabolic profiling of wounds in diabetic and nondiabetic mice. *Wound Repair Regen.* **2015**, *23*, 423–434. [[CrossRef](#)]
114. Zhao, H.C.; Chen, J.C.; Chai, J.C.; Zhang, Y.C.; Yu, C.; Pan, Z.; Gao, P.; Zong, C.; Guan, Q.B.; Fu, Y.Q.; et al. Cytochrome P450 (CYP) epoxygenases as potential targets in the management of impaired diabetic wound healing. *Lab. Investig.* **2017**, *97*, 782–791. [[CrossRef](#)] [[PubMed](#)]
115. Wieman, T.J.; Smiell, J.M.; Su, Y. Efficacy and Safety of a Topical Gel Formulation of Recombinant Human Platelet-Derived Growth Factor-BB (Becaplermin) in Patients with Chronic Neuropathic Diabetic Ulcers: A phase III randomized placebo-controlled double-blind study. *Diabetes Care* **1998**, *21*, 822–827. [[CrossRef](#)]
116. Papanas, N.; Maltezos, E. Benefit-risk assessment of becaplermin in the treatment of diabetic foot ulcers. *Drug Saf.* **2010**, *33*, 455–461. [[CrossRef](#)] [[PubMed](#)]



117. Ziyadeh, N.; Fife, D.; Walker, A.M.; Wilkinson, G.S.; Seeger, J.D. A matched cohort study of the risk of cancer in users of becaplermin. *Adv. Ski. Wound Care* **2011**, *24*, 31–39. [[CrossRef](#)]
118. Greenhalgh, D.G.; Sprugel, K.H.; Murray, M.J.; Ross, R. PDGF and FGF stimulate wound healing in the genetically diabetic mouse. *Am. J. Pathol.* **1990**, *136*, 1235–1246.
119. Albertson, S.; Hummel, R.P., III; Breeden, M.; Greenhalgh, D.G. PDGF and FGF reverse the healing impairment in protein-malnourished diabetic mice. *Surgery* **1993**, *114*, 368–372; discussion 372–373.
120. Brown, R.L.; Breeden, M.P.; Greenhalgh, D.G. PDGF and TGF- $\alpha$  act synergistically to improve wound healing in the genetically diabetic mouse. *J. Surg. Res.* **1994**, *56*, 562–570. [[CrossRef](#)] [[PubMed](#)]
121. Kiritsy, C.P.; Antoniadou, H.N.; Carlson, M.R.; Beaulieu, M.T.; D'Andrea, M.; Lynch, S.E. Combination of platelet-derived growth factor-BB and insulin-like growth factor-I is more effective than platelet-derived growth factor-BB alone in stimulating complete healing of full-thickness wounds in older diabetic mice. *Wound Repair Regen.* **1995**, *3*, 340–350. [[CrossRef](#)]
122. Breitbart, A.S.; Laser, J.; Parrett, B.; Porti, D.; Grant, R.T.; Grande, D.A.; Mason, J.M. Accelerated diabetic wound healing using cultured dermal fibroblasts retrovirally transduced with the platelet-derived growth factor B gene. *Ann. Plast. Surg.* **2003**, *51*, 409–414. [[CrossRef](#)] [[PubMed](#)]
123. Keswani, S.G.; Katz, A.B.; Lim, F.Y.; Zoltick, P.; Radu, A.; Alaei, D.; Herlyn, M.; Crombleholme, T.M. Adenoviral mediated gene transfer of PDGF-B enhances wound healing in type I and type II diabetic wounds. *Wound Repair Regen.* **2004**, *12*, 497–504. [[CrossRef](#)] [[PubMed](#)]
124. Lee, J.A.; Conejero, J.A.; Mason, J.M.; Parrett, B.M.; Wear-Maggitti, K.D.; Grant, R.T.; Breitbart, A.S. Lentiviral transfection with the PDGF-B gene improves diabetic wound healing. *Plast. Reconstr. Surg.* **2005**, *116*, 532–538. [[CrossRef](#)] [[PubMed](#)]
125. Canadian Institute of Health Research. *Study of Combined Topical Growth Factor and Protease Inhibitor in Chronic Wound Healing*; McMaster University: Hamilton, ON, Canada, 2016; NCT02845466.
126. Chikazu, D.; Taguchi, T.; Koyama, H.; Hikiji, H.; Fujihara, H.; Suenaga, H.; Saijo, H.; Mori, Y.; Seto, I.; Iino, M.; et al. Improvement in wound healing by a novel synthetic collagen-gel dressing in genetically diabetic mice. *Asian J. Oral Maxillofac. Surg.* **2010**, *22*, 61–67. [[CrossRef](#)]
127. Kondo, S.; Niiyama, H.; Yu, A.; Kuroyanagi, Y. Evaluation of a wound dressing composed of hyaluronic acid and collagen sponge containing epidermal growth factor in diabetic mice. *J. Biomater. Sci. Polym. Ed.* **2012**, *23*, 1729–1740. [[CrossRef](#)]
128. Steinberg, J. *Use of INTEGRA™ Flowable Wound Matrix to Manage Diabetic Foot Ulcers*; Georgetown University: Washington, DC, USA, 2010; NCT01108263.
129. Murakami, K.; Aoki, H.; Nakamura, S.; Nakamura, S.; Takikawa, M.; Hanzawa, M.; Kishimoto, S.; Hattori, H.; Tanaka, Y.; Kiyosawa, T.; et al. Hydrogel blends of chitin/chitosan, fucoidan and alginate as healing-impaired wound dressings. *Biomaterials* **2010**, *31*, 83–90. [[CrossRef](#)]
130. Yuan, Z.; Zakhaleva, J.; Ren, H.; Liu, J.; Chen, W.; Pan, Y. Noninvasive and high-resolution optical monitoring of healing of diabetic dermal excisional wounds implanted with biodegradable in situ gelable hydrogels. *Tissue Eng. Part C Methods* **2010**, *16*, 237–247. [[CrossRef](#)] [[PubMed](#)]
131. Yanagibayashi, S.; Kishimoto, S.; Ishihara, M.; Murakami, K.; Aoki, H.; Takikawa, M.; Fujita, M.; Sekido, M.; Kiyosawa, T. Novel hydrocolloid-sheet as wound dressing to stimulate healing-impaired wound healing in diabetic db/db mice. *Biomed. Mater. Eng.* **2012**, *22*, 301–310. [[CrossRef](#)]
132. Primex. *Clinical Trial Evaluating the Safety and Efficacy of the Use of Chitosan Gel in Patients with Chronic Wounds*; University of Ljubljana: Ljubljana, Slovenia, 2019; NCT04178525.
133. Tsuboi, R.; Rifkin, D.B. Recombinant basic fibroblast growth factor stimulates wound healing in healing-impaired db/db mice. *J. Exp. Med.* **1990**, *172*, 245–251. [[CrossRef](#)]
134. Tsuboi, R.; Shi, C.M.; Rifkin, D.B.; Ogawa, H. A wound healing model using healing-impaired diabetic mice. *J. Dermatol.* **1992**, *19*, 673–675. [[CrossRef](#)]
135. Olympus Biotech Corporation. *The TRAFermin in Neuropathic Diabetic Foot Ulcer Study—Southern Europe The TRANS-South Study*; Olympus Biotech Corporation: Hopkinton, MA, USA, 2010; NCT01217463.
136. Kirchner, L.M.; Meerbaum, S.O.; Gruber, B.S.; Knoll, A.K.; Bulgrin, J.; Taylor, R.A.; Schmidt, S.P. Effects of vascular endothelial growth factor on wound closure rates in the genetically diabetic mouse model. *Wound Repair Regen.* **2003**, *11*, 127–131. [[CrossRef](#)] [[PubMed](#)]
137. Galiano, R.D.; Tepper, O.M.; Pelo, C.R.; Bhatt, K.A.; Callaghan, M.; Bastidas, N.; Bunting, S.; Steinmetz, H.G.; Gurtner, G.C. Topical vascular endothelial growth factor accelerates diabetic wound healing through increased angiogenesis and by mobilizing and recruiting bone marrow-derived cells. *Am. J. Pathol.* **2004**, *164*, 1935–1947. [[CrossRef](#)]
138. Mace, K.A.; Yu, D.H.; Paydar, K.Z.; Boudreau, N.; Young, D.M. Sustained expression of Hif-1 $\alpha$  in the diabetic environment promotes angiogenesis and cutaneous wound repair. *Wound Repair Regen.* **2007**, *15*, 636–645. [[CrossRef](#)]
139. Brem, H.; Kodra, A.; Golinko, M.S.; Entero, H.; Stojadinovic, O.; Wang, V.M.; Sheahan, C.M.; Weinberg, A.D.; Woo, S.L.; Ehrlich, H.P.; et al. Mechanism of sustained release of vascular endothelial growth factor in accelerating experimental diabetic healing. *J. Invest. Dermatol.* **2009**, *129*, 2275–2287. [[CrossRef](#)]
140. Genentech, Inc. *A Study to Assess the Effect of Topical Recombinant Human Vascular Endothelial Growth Factor for Induction of Healing of Diabetic Foot Ulcers*; Genentech, Inc.: San Francisco, CA, USA, 2006; NCT00351767.

141. Song, H.; Xu, Y.; Chang, W.; Zhuang, J.; Wu, X. Negative pressure wound therapy promotes wound healing by suppressing macrophage inflammation in diabetic ulcers. *Regen. Med.* **2020**, *15*, 2341–2349. [[CrossRef](#)]
142. Ministry of Health and Wellnes. *Negative Pressure Wound Therapy in Diabetic Wounds*; University of Mauritius: Moka, Mauritius, 2021; NCT05041244.
143. Pan, S.; Zhang, S.; Chen, H. Low temperature plasma promotes the healing of chronic wounds in diabetic mice. *J. Phys. D Appl. Phys.* **2020**, *53*, 185205. [[CrossRef](#)]
144. He, R.; Li, Q.; Shen, W.; Wang, T.; Lu, H.; Lu, J.; Lu, F.; Luo, M.; Zhang, J.; Gao, H.; et al. The efficacy and safety of cold atmospheric plasma as a novel therapy for diabetic wound in vitro and in vivo. *Int. Wound J.* **2020**, *17*, 851–863. [[CrossRef](#)] [[PubMed](#)]
145. Tschoepe, D. *Cold Plasma Therapy for Acceleration of Wound Healing in Diabetic Foot*; Ruhr University of Bochum: Bochum, Germany, 2019; NCT04205942.
146. Wei, Q.; Zhang, Z.; Luo, J.; Kong, J.; Ding, Y.; Chen, Y.; Wang, K. Insulin treatment enhances pseudomonas aeruginosa biofilm formation by increasing intracellular cyclic di-GMP levels, leading to chronic wound infection and delayed wound healing. *Am. J. Transl. Res.* **2019**, *11*, 3261–3279.
147. University of Campinas. *Topic Insulin Accelerates Wound Healing in Diabetes*; University of Campinas: Sao Paolo, Brazil, 2011; NCT01295177.
148. Roberts, R.E.; Bilgen, O.; Kineman, R.D.; Koh, T.J. Parameter-Dependency of Low-Intensity Vibration for Wound Healing in Diabetic Mice. *Front. Bioeng. Biotechnol.* **2021**, *9*, 654920. [[CrossRef](#)]
149. King, S.K.K. *Vibration Enhances Diabetic ULCER Healing*; Chinese University of Hong Kong: Hong Kong, China, 2020; NCT04275804.
150. Gonzalez, K.; Salem, K.M.; Methé, B.; Li, K.; Hong, G.; Tzeng, E. Impact of Dietary Tungsten and Topical Nitrite in Diabetic Wound Healing and the Composition of the Wound Microbiome. *JVS-Vasc. Sci.* **2020**, *1*, 257. [[CrossRef](#)]
151. Sindler, A.L.; Cox-York, K.; Reese, L.; Bryan, N.S.; Seals, D.R.; Gentile, C.L. Oral nitrite therapy improves vascular function in diabetic mice. *Diab. Vasc. Dis. Res.* **2015**, *12*, 221–224. [[CrossRef](#)] [[PubMed](#)]
152. Weller, R.; Finnen, M.J. The effects of topical treatment with acidified nitrite on wound healing in normal and diabetic mice. *Nitric Oxide* **2006**, *15*, 395–399. [[CrossRef](#)] [[PubMed](#)]
153. Fundación Cardiovascular de Colombia. *Clinical Trial for the Treatment of Diabetic Foot Ulcers Using a Nitric Oxide Releasing Patch: PATHON*; Fundación Cardiovascular de Colombia: Floridablanca, Colombia, 2007; NCT00428727.
154. Rai, V.; Moellmer, R.; Agrawal, D.K. Clinically relevant experimental rodent models of diabetic foot ulcer. *Mol. Cell Biochem.* **2022**, *477*, 1239–1247. [[CrossRef](#)]
155. Surwit, R.S.; Kuhn, C.M.; Cochrane, C.; McCubbin, J.A.; Feinglos, M.N. Diet-induced type II diabetes in C57BL/6J mice. *Diabetes* **1988**, *37*, 1163–1167. [[CrossRef](#)] [[PubMed](#)]
156. Yu, C.O.; Leung, K.S.; Fung, K.P.; Lam, F.F.; Ng, E.S.; Lau, K.M.; Chow, S.K.; Cheung, W.H. The characterization of a full-thickness excision open foot wound model in n5-streptozotocin (STZ)-induced type 2 diabetic rats that mimics diabetic foot ulcer in terms of reduced blood circulation, higher C-reactive protein, elevated inflammation, and reduced cell proliferation. *Exp. Anim.* **2017**, *66*, 259–269. [[CrossRef](#)]
157. Nord, C.; Eriksson, M.; Dicker, A.; Eriksson, A.; Grong, E.; Ilegems, E.; Marvik, R.; Kulseng, B.; Berggren, P.O.; Gorzsas, A.; et al. Biochemical profiling of diabetes disease progression by multivariate vibrational microspectroscopy of the pancreas. *Sci. Rep.* **2017**, *7*, 6646. [[CrossRef](#)] [[PubMed](#)]
158. Zomer, H.D.; Trentin, A.G. Skin wound healing in humans and mice: Challenges in translational research. *J. Dermatol. Sci.* **2018**, *90*, 3–12. [[CrossRef](#)]



# The Influence of N-Acetylcysteine-Enriched Hydrogels on Wound Healing in a Murine Model of Type II Diabetes Mellitus

Albert Stachura <sup>1,2</sup>, Marcin Sobczak <sup>3</sup>, Karolina Kędra <sup>4</sup>, Michał Kopka <sup>1,2</sup>, Karolina Kopka <sup>1</sup> and Paweł K. Włodarski <sup>1,\*</sup>

<sup>1</sup> Department of Methodology, Medical University of Warsaw, 1 Banacha Street, 02-091 Warsaw, Poland

<sup>2</sup> Doctoral School, Medical University of Warsaw, 1 Banacha Street, 02-091 Warsaw, Poland

<sup>3</sup> Department of Pharmaceutical Chemistry and Biomaterials, Faculty of Pharmacy, Medical University of Warsaw, 1 Banacha Street, 02-097 Warsaw, Poland

<sup>4</sup> Institute of Physical Chemistry, Polish Academy of Sciences, 44/52 Kasprzaka Street, 01-224 Warsaw, Poland

\* Correspondence: pawel.wlodarski@wum.edu.pl

**Abstract:** Diabetes mellitus (DM) severely impairs skin wound healing capacity, yet few treatment options exist to enhance this process. N-acetylcysteine (NAC) is an antioxidant that improves cellular proliferation and enhances wound healing in healthy animals, yet its use in the context of type II DM has not been studied. The aim of our research was to investigate the effect of topically applied NAC-enriched hydrogels on wound healing in a leptin-deficient murine wound model. Four excisional wounds were created on the backs of 20 db/db mice and were subsequently treated with hydrogels containing NAC at concentrations of 5%, 10% and 20% or placebo (control). Healing was monitored for 28 days; photographs of the wounds were taken on every third day. Wound tissues were harvested on days 3, 7, 14 and 28 to undergo histological examinations. Wounds treated with 5% NAC showed improved wound closure speed accompanied by an increased dermal proliferation area on microscopic assessment compared with other groups. Higher concentrations of NAC failed to show a beneficial effect on wound healing. 5% NAC improved early stages of wound healing in a murine model of type II DM by increasing wound closure speed, likely mediated by improved dermal proliferation.

**Keywords:** wound healing; diabetes mellitus; acetylcysteine; biomedical hydrogels; hydrogel drug delivery systems; in vivo; db/db mice; leptin

**Citation:** Stachura, A.; Sobczak, M.; Kędra, K.; Kopka, M.; Kopka, K.; Włodarski, P.K. The Influence of N-Acetylcysteine-Enriched Hydrogels on Wound Healing in a Murine Model of Type II Diabetes Mellitus. *Int. J. Mol. Sci.* **2024**, *25*, 9986. <https://doi.org/10.3390/ijms25189986>

Academic Editor:  
Antonio Lucacchini

Received: 20 July 2024

Revised: 28 August 2024

Accepted: 14 September 2024

Published: 16 September 2024



**Copyright:** © 2024 by the author. Licensee MDPI, Basel, Switzerland. This article is an open access article distributed under the terms and conditions of the Creative Commons Attribution (CC BY) license (<https://creativecommons.org/licenses/by/4.0/>).

## 1. Introduction

N-acetylcysteine (NAC) is an antioxidant and a cysteine prodrug that potently replenishes intracellular glutathione levels [1]. It also regulates the expression of genes via inhibiting c-Jun N-terminal kinase, p38 MAP kinase or nuclear factor kappa B transcription factor [2]. NAC may prevent apoptosis and promote cell survival and directly reduces the activity of several proteins [2]. Though nonspecific, this substance has been widely used: as a mucolytic agent, an antidote to paracetamol intoxication, for doxorubicin cardiotoxicity, ischemia/reperfusion cardiac injury, acute respiratory distress syndrome and bronchitis [3]. Recently, it has been of interest to dermatologists and psychiatrists [4,5]. The dosages and administration routes vary greatly depending on the indication. High doses of up to 3000 mg/day orally or at a 20% concentration applied topically have been used in humans and were tolerated well [6,7].

The use of NAC has also been studied in the context of wound healing. This process comprises four consecutive phases: hemostasis, inflammation, proliferation and remodeling [8]. As NAC may reduce endothelial dysfunction and inflammation, as well as accelerate cellular proliferation [2], it has been considered a candidate intervention for wound

healing enhancement. Topically applied 3% NAC promoted re-epithelialization in a rat model of burn wounds and, at the same concentration, improved angiogenesis and wound healing rate in an incisional wound model [9,10]. Tsai et al. showed the beneficial effect of NAC was dose-dependent and peaked at the maximum concentration of 3% [9]. Also, a single injection of 0.03% NAC decreased scar area and width in an incisional rat wound healing model [11]. This was associated with numerous changes in the gene expression patterns [12].

Diabetes mellitus (DM) severely impairs skin wound healing capacity. Factors contributing to dismal outcomes in patients treated for diabetic foot ulcer are poor angiogenesis and reduced blood flow, altered inflammatory response (often prolonged), proneness to infection, diminished amount of growth factors, accumulation of advanced glycosylation end products (AGEs), increasing oxidative stress, etc. [13]. NAC, with its mechanism of action, could theoretically alleviate some of these issues. It indeed improved the wound-breaking strength in an incisional alloxan-induced diabetic murine wound model following peritoneal NAC administration [14]. When NAC was administered systemically and/or topically to wounds in a rat, streptozotocin (STZ)-induced diabetic excisional wound model, wound areas decreased compared with the control group, which was associated with favorable histological outcomes [15]. Despite showing beneficial effects, these studies were limited by utilizing substance-induced type I DM models, which show relatively smaller wound healing impairment than leptin-deficient db/db type II DM model [16]. The latter model exhibits a wide range of healing dysregulations also seen in humans [17]. Moreover, the translatability of previous research is undermined by not addressing skin contraction—a major healing mechanism only present in rodents. A splinting model has been developed so that wounds heal through granulation and re-epithelialization, resembling the process occurring in patients with DM [18]. In our research, we took these methodological aspects into consideration.

According to the Global Burden of Disease 2021 report, diabetes is the 10th leading cause of death and the 7th leading cause of disease burden worldwide [19]. The lifetime risk of developing a diabetic foot ulcer among people with diabetes mellitus ranges between 19% and 34% [20]. DM is also frequently associated with complicated wound healing [13]. Although surgical debridement remains the gold standard for the management of diabetic wounds [21], adjunct treatments are urgently needed to improve patients' outcomes. Interventions such as growth factors, collagen scaffolds, chitosan gels and cold plasma therapy have been investigated to treat diabetic wounds. These potential therapies are, however, often costly or require specialized equipment. To date, only Becaplermin was approved for topical treatment of diabetic ulcers but was withdrawn soon after registration due to serious side effects [17]. Therefore, new easily accessible and effective alternatives should be investigated. As noted above, NAC was shown to improve wound healing in healthy animals and in some models of DM. It is also theoretically a more appealing molecule than modified growth factors as it is more easily accessible, cheaper and has a well-documented safety record [22]. This study aimed to broaden the understanding of NAC's efficacy in improving diabetic wound healing using a hydrogel-based sustained-release formula.

Polymeric hydrogels are one of the most exciting medical materials for dermatology. One of the main advantages of hydrogels used in the topical treatment of skin diseases is their ease of application and significant minimization of side effects. Various combinations of natural, semi-synthetic and synthetic polymers are made into hydrogel formulations to use their potential as biomaterials. Hydrogels have numerous applications in the medical and pharmaceutical sectors [23–25]. This type of biomaterial can absorb large amounts of water or biological fluids while retaining integrity. Hydrogel drug delivery systems (DDSs) can change their properties in response to external or internal stimuli such as temperature, pH, ionic strength, etc. They are capable of releasing drugs in a prolonged and controlled manner [23–26]. Hydrogels are obtained from natural or synthetic polymers [24,27]. Their use helps maintain adequate wound moisture, which allows cell growth and

migration. In a humid environment, keratinocytes can easily move around the wound's surface, leading to its faster closure, and fibroblasts produce more collagen. A significant advantage of using hydrogels in wound treatment is their limited adhesion, which means they can be easily removed from the wound without causing further injury to the treated tissue [24,28]. Many hydrogel dressings have been developed for the treatment of difficult-to-heal wounds: poly(vinyl alcohol)(PVA)/ $\beta$ -glucan ( $\beta$ -1,6-branched- $\beta$ -1,3-glucan) [29], dextran hydrogel [30], self-crosslink able dextran-isocyanatoethyl methacrylate-ethylamine hydrogel [31], hybrid dextran hydrogel with incorporated curcumin encapsulated (poly(lactide)-block-poly(ethylene glycol)) [32] and many others.

The aim of this study was to discover the effect of topically applied NAC-enriched hydrogels on wound healing rate in a murine db/db excisional wound splinting model. Additionally, morphometric, histological and immunohistochemical staining analyses were performed to help elucidate the potential NAC mechanism of action.

## 2. Results

### 2.1. Hydrogel Characteristics

Hydrogels were obtained using a previously developed and appropriately modified three-step method with some modifications [33]. In the first step,  $\epsilon$ -caprolactone (CL), lactide (LA) and poly(ethylene glycol) (PEG) (CL-LA-PEG 200) copolymer was synthesized. The prepolymer of 1,6-diisocyanatohexane (HDI), CL-LA-PEG 200 copolymer and poly(ethylene adipate) diol (PEA) were obtained in the second step. Next, chitosan (CHIT)-HDI-CL-LA-PEG 200-PEA hydrogel (HYDROGEL-MS1) was prepared in the final step (Figure 1).

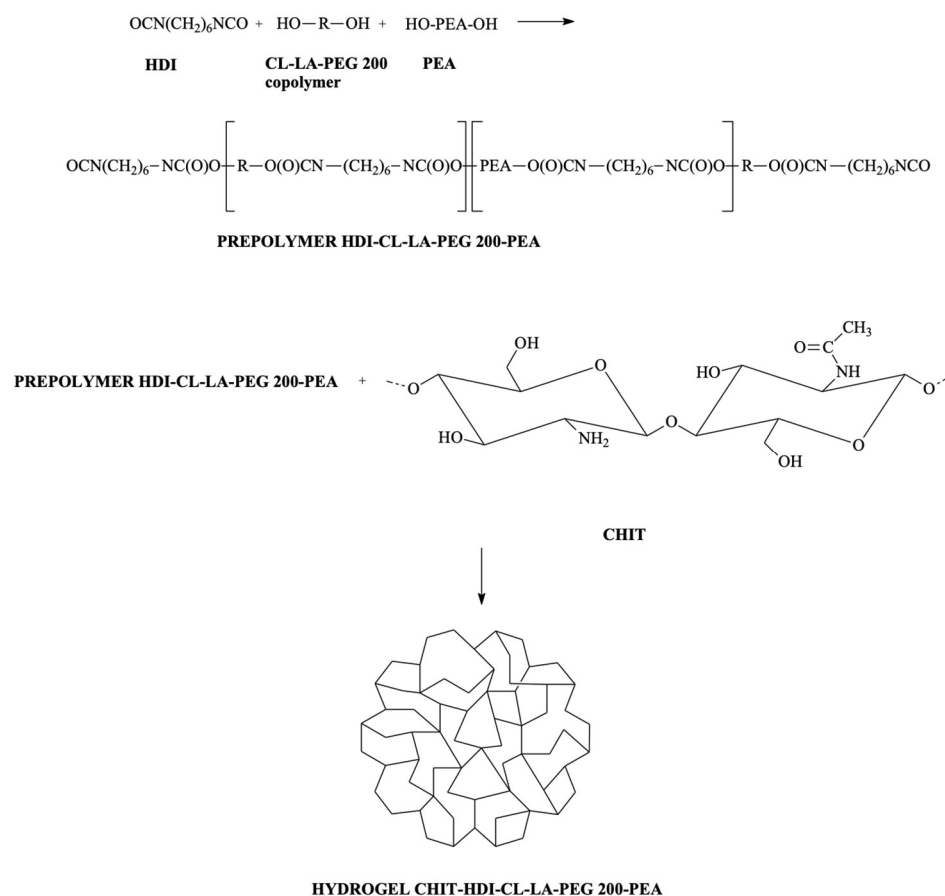


**Figure 1.** CHIT-HDI-CL-LA-PEG 200-PEA hydrogel preparation.

The copolymer was synthesized by ring-opening polymerization (ROP) of CL, rac-LA and PEG 200 in the presence of immobilized lipase B from *Candida antarctica* (CA). The molar mass of the obtained CL-LA-PEG 200 copolymer was  $M_n = 2700$  g/mol ( $D = 1.59$ ). The copolymers' molar content in the chain was 0.57 (CL): 0.38 (LA): 0.05 (PEG 200). The prepolymer was obtained in the polyaddition process of CL-LA-PEG 200 copolymer and PEA with HDI in an NCO/OH molar ratio of 0.9:0.1:2.1. Finally, the hydrogel was reacted with CHT in an NCO (prepolymer)/OH (or  $\text{NH}_2$ ) (CHT) ratio of 1.6:1. The dibutyltin dilaurate (DBDLSn) was used as a polyaddition catalyst. The swelling capacity of the obtained hydrogel was determined. The value of the coefficient of the mass swelling ratio (MSR) was 334%, 387%, 428% and 443% after 2 h, 4 h, 8 h and 24 h. NAC was loaded into hydrogels using the incorporation method. The mean weight of the devices developed was approximately 0.45 g, containing 5%, 10% or 20% of NAC (HYDROGEL-MS1-NAC-5, HYDROGEL-MS1-NAC-10 and HYDROGEL-MS1-NAC-20, respectively). In vitro studies of the release of NAC from obtained hydrogel materials were determined at pH 7.4 and 5.5 and at the temperature of 37 C for 72 h (Figure 2). The plot's ordinate was calculated based on the cumulative amount of NAC released considering its initial amount in the hydrogels.

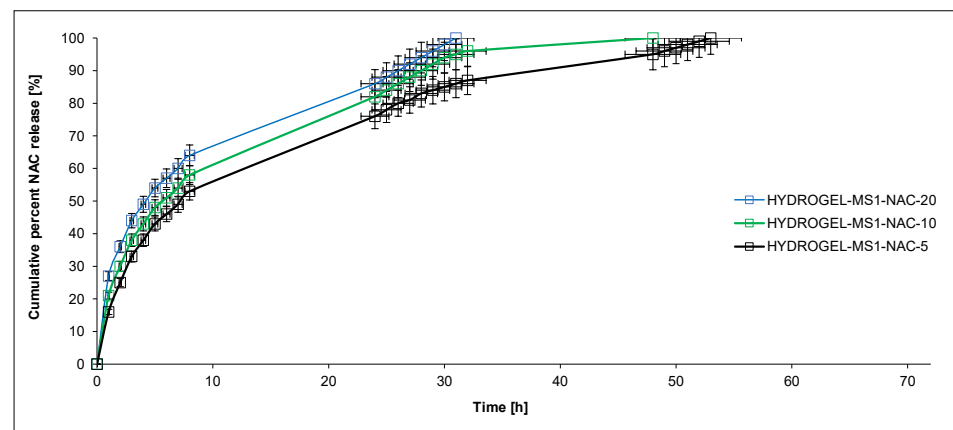


**Figure 2.** NAC release profiles from the obtained hydrogels (at pH 5.5) (each point represents the mean  $\pm$  SD of three points).

The NAC release kinetics from obtained hydrogels were investigated (Figures 2 and 3). The rate of NAC release at pH 7.4 decreased as follows: HYDROGEL-MS1-NAC-20 > HYDROGEL-MS1-NAC-10 > HYDROGEL-MS1-NAC-5. An identical trend was maintained for the experiments conducted at pH 5.5.

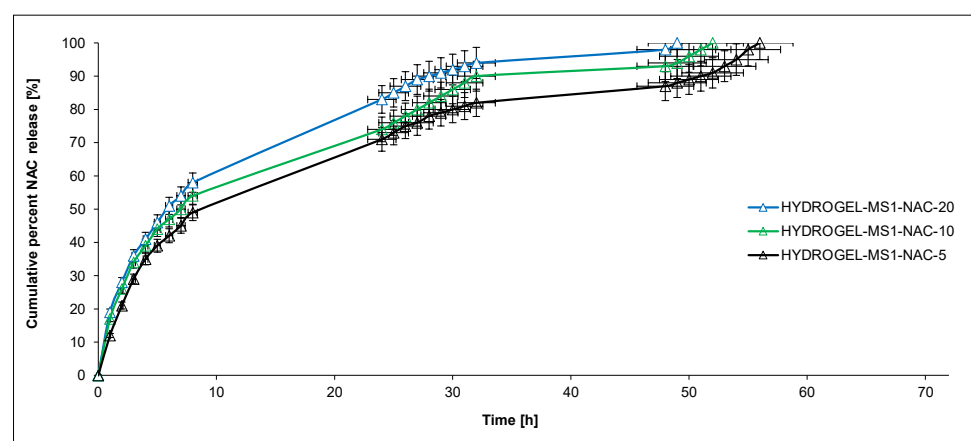


**Figure 3.** NAC release profiles from the obtained hydrogels (at pH 7.4) (each point represents the mean  $\pm$  SD of three points).



The results suggested that the NAC release rate increased as the pH of the solution decreased and the active substance contained in the hydrogel increased. For example, the percentage of the released NAC after 24 h incubation was about 83% from HYDROGEL-MS1-NAC-20 at pH 7.4 and 86% from HYDROGEL-MS1-NAC-20 at pH 5.5. After 24 h incubation, the NAC release was 83% from HYDROGEL-MS1-NAC-20, 74% from HYDROGEL-MS1-NAC-10 and 71% from HYDROGEL-MS1-NAC-5 at pH 7.4.

The data points obtained for the NAC release studies were subjected to zero- and first-order kinetics and the Korsmeyer–Peppas models to evaluate the kinetics and mechanism of NAC release from hydrogels (Table 1). According to the Korsmeyer–Peppas model, for the diffusion–degradation-controlled drug release system, the release exponent value  $n$  is in the range between 0.45 and 0.89 (anomalous, non-Fickian). In contrast, when  $n$  is close to 0.45, the diffusion (Fickian diffusion) predominates in the process, and, in the opposite case,  $n > 0.89$ , the model corresponds to the super case II transport [34].

**Table 1.** Analysis data of NAC release from the obtained hydrogels.

No.	Zero-Order Model	First-Order Model	Korsmeyer–Peppas Model		NAC Transport Mechanism
	R <sup>2</sup>	R <sup>2</sup>	R <sup>2</sup>	n	
HYDROGEL-MS1-NAC-5 pH 7.4	0.912	0.905	0.951	0.561	non-Fickian transport
HYDROGEL-MS1-NAC-10 pH 7.4	0.929	0.903	0.988	0.612	non-Fickian transport
HYDROGEL-MS1-NAC-20 pH 7.4	0.835	0.989	0.998	0.536	non-Fickian transport
HYDROGEL-MS1-NAC-5 pH 5.5	0.918	0.909	0.956	0.540	non-Fickian transport
HYDROGEL-MS1-NAC-10 pH 5.5	0.861	0.954	0.996	0.486	non-Fickian transport
HYDROGEL-MS1-NAC-20 pH 5.5	0.873	0.925	0.997	0.464	non-Fickian transport

The NAC release kinetic at pH 7.4 from HYDROGEL-MS1-NAC-5 and HYDROGEL-MS1-NAC-10 followed the near-zero-order model ( $R^2$  was 0.912 and 0.929, respectively). Furthermore, it was noted that NAC was released at pH 7.4 from HYDROGEL-MS1-NAC-20 with first-order kinetics ( $R^2$  was 0.989). In turn, when conducting the release process at pH 5.5, it was observed that for HYDROGEL-MS1-NAC-5, the NAC release was also close to the zero-order kinetics ( $R^2 = 0.918$ ). Furthermore, it was found that NAC was released from HYDROGEL-MS1-NAC-10 and HYDROGEL-MS1-NAC-20 with first-order kinetics ( $R^2$  was 0.954 and 0.925, respectively). The analysis of NAC release data using the Korsmeyer–Peppas model suggested that all hydrogels were governed rather by non-Fickian transport ( $n = 0.464–0.612$ ).

The biodegradation of the blank hydrogels was also carried out. The hydrolytic degradation test of the resulting hydrogels was conducted under the same conditions as the NAC release experiments. The degradation process was characterized by plotting the weight loss (WL) of hydrogels against time. The results are shown in Figure 4. It was found that the biodegradation rate of hydrogels depended on the pH of the solution. Hydrogels biodegraded faster at pH 5.5 than at pH 7.4, which was found to be consistent with the NAC release experiment data.

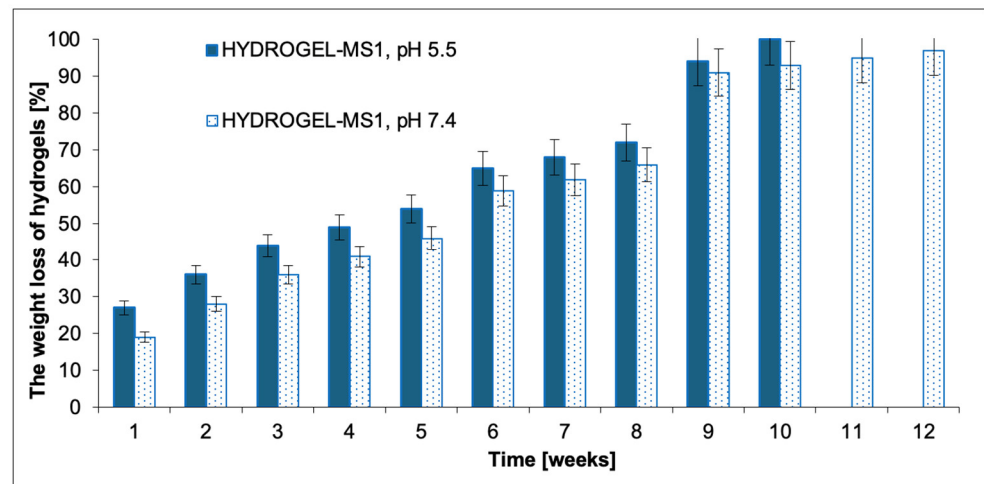


**Figure 4.** The weight loss of the obtained hydrogels over 12 weeks at pH 7.4 and 5.5 (each point represents the mean  $\pm$  SD of three points).

The WL value for HYDROGEL-MS1 was 100% at pH 5.5 after 10 weeks of degradation. In turn, the WL value for HYDROGEL-MS1 was c.a. 100% at pH 7.4 after 12 weeks of degradation. Generally, the degradation process of obtained hydrogels was relatively slow and regular.

## 2.2. Wound Measurements

During the first week, wounds treated with 5% NAC healed faster than those in the control group (Figure 5), and by day 7, their wound area was significantly smaller than those treated with 20% NAC. This difference remained significant until the end of week 2. On day 14, wounds treated with the highest NAC concentration also had bigger wound sizes than in the control group. At the same time, wounds treated with 10% NAC had larger areas than those treated with 5% NAC but not larger than in the control group. During weeks 3 and 4, no significant differences were observed between the groups. At that time, only five animals remained in each cohort (Table 2).

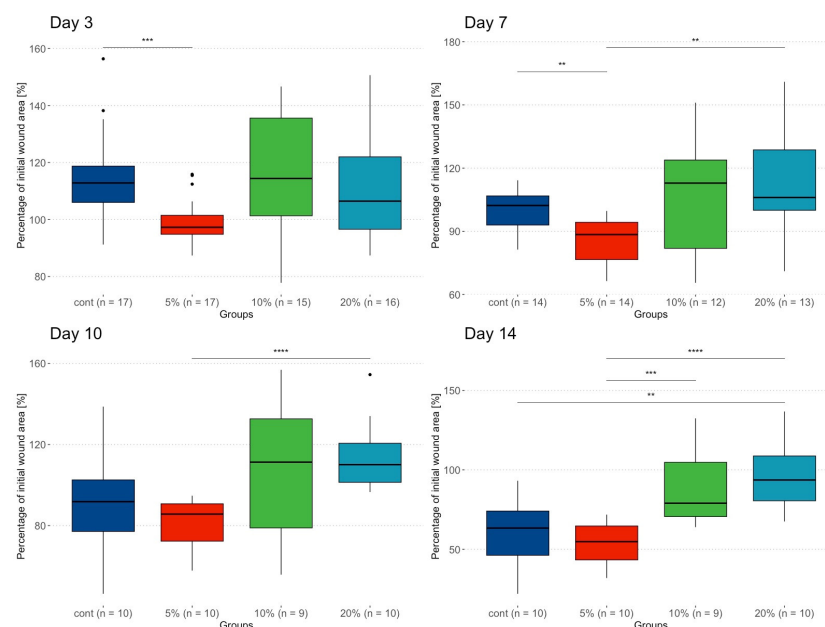


**Figure 5.** Wound area measurements on days 3–14. Displayed values represent the % of initial wound size. Statistically significant between-groups differences are marked with horizontal lines and significance levels (p-value): \*\*  $\leq$  0.01; \*\*\*  $\leq$  0.001; \*\*\*\*  $\leq$  0.0001



**Table 2.** Wound area measurements throughout the study period. Displayed values represent the % of initial wound size.

Timepoint		Control	5% NAC	10% NAC	20% NAC	<i>p</i> -Value *
Day 3	Median (IQR)	112.8 (106–118.7)	97.3 (94.8–101.5)	114.4 (101.3–135.6)	106.4 (96.6–121.9)	0.009
	Min–max	91.2–156.4	87.3–115.9	77.8–146.7	87.4–150.7	
Day 7	Median (IQR)	102.3 (92.9–106.8)	88.5 (76.6–94.3)	112.9 (81.9–123.8)	106 (100–128.7)	0.005
	Min–max	81.3–114.2	66.4–99.7	65.5–151.1	71–160.9	
Day 10	Median (IQR)	91.8 (77.1–102.5)	85.7 (72.3–90.7)	111.3 (78.9–132.6)	110 (101.3–120.6)	0.005
	Min–max	46.3–138.7	57.8–94.7	55.8–156.8	96.5–154.5	
Day 14	Median (IQR)	63.4 (46.2–74.1)	54.8 (43.3–64.7)	79 (70.6–104.7)	93.6 (80.5–108.7)	<0.001
	Min–max	22–93.2	31.9–71.9	63.9–132.4	67.5–136.7	
Day 17	Median (IQR)	52.6 (45.2–67.3)	41.4 (40.7–57.8)	63 (57.9–68.6)	83.5 (60.1–86.5)	0.11
	Min–max	19.7–74.8	24–68.9	50.9–70.8	56.5–100	
Day 21	Median (IQR)	0 (0–9.48)	37.9 (3.76–40.8)	14.3 (6.15–54.9)	57.9 (44.2–57.9)	0.33
	Min–max	0–65.3	0–48.3	3.3–61.2	2.5–59.9	
Day 24	Median (IQR)	0 (0–0)	0 (0–23.5)	0 (0–0)	40.5 (19.3–42)	0.42
	Min–max	0–51.7	0–49.2	0–46.5	0–48.5	
Day 28	Median (IQR)	0 (0–0)	0 (0–0)	0 (0–0)	0 (0–41.9)	0.89
	Min–max	0–56.4	0–59.4	0–44.5	0–57.5	

IQR—interquartile range, NAC—N-acetylcysteine; \* Kruskal–Wallis tests.

### 2.3. Morphometry

Histomorphometric assessment included measurements of three key parameters: epidermal thickness, neoepidermal thickness and dermal proliferation area, i.e., the area of intense cellular proliferation adjacent to the wound (Table 3). Epidermal thickness was comparable between groups at most time points. The epithelium distal to the wounds gradually increased in thickness from day 3 to day 7 through day 14 and came back to near-baseline values on day 28. On day 7, epidermal thickness in the 10% NAC group was smaller than in the 5% NAC group ( $p = 0.006$ ). The newly formed epithelium adjacent to the wounds was thicker than its distal counterpart. Similarly, it became thicker over time, reaching peak values on days 7 and 14. The new epidermis was thinner on day 7 in the group treated with 10% NAC compared with all other groups ( $p < 0.001$ ). The dermal proliferation area was first measured on day 7, but its values became larger on day 14. DPA in the group treated with 5% NAC was more extensive than in the control group and 20% NAC group on day 7 ( $p < 0.006$ ).

**Table 3.** Histomorphometric measurement results in studied groups by time points.

Timepoint	Group	Epidermis Thickness [ $\mu\text{m}$ ]	<i>p</i> -Value	Neoepidermis Thickness [ $\mu\text{m}$ ]	<i>p</i> -Value	Dermal Proliferation Area [ $\mu\text{m}^2$ ]	<i>p</i> -Value
Day 3	Control	32.7 $\pm$ 14.2	0.07	53.9 $\pm$ 26.1	0.6	-	
	5% NAC	21.7 $\pm$ 7.75		57.5 $\pm$ 14.7		-	
	10% NAC	32.3 $\pm$ 19.4		53.8 $\pm$ 14		-	
	20% NAC	31 $\pm$ 11.9		61.3 $\pm$ 15.3		-	
Day 7	Control	31.8 $\pm$ 21.2	0.03	96.9 $\pm$ 22.1	<0.001	57,551 $\pm$ 29,408	0.003
	5% NAC	46 $\pm$ 33.8		104 $\pm$ 39.3		144,333 $\pm$ 28,204 ***	
	10% NAC	24.5 $\pm$ 9.45 *		60.6 $\pm$ 18.1 **		55,845 $\pm$ 33,352	
	20% NAC	40 $\pm$ 24		120 $\pm$ 20.3		50,684 $\pm$ 20,496	
Day 14	Control	45.8 $\pm$ 22.5	0.08	95.1 $\pm$ 33.3	0.4	248,247 $\pm$ 166,097	0.88 **
	5% NAC	49.3 $\pm$ 23.9		92.4 $\pm$ 44.9		379,831 $\pm$ 225,357	
	10% NAC	60.9 $\pm$ 21.9		96.3 $\pm$ 38.7		279,145 $\pm$ 99,181	
	20% NAC	51.7 $\pm$ 17.8		108 $\pm$ 39.2		416,778 $\pm$ 332,634	
Day 28	Control	24.4 $\pm$ 16.7	0.01	55.1 $\pm$ 20.6	0.2	246,033 $\pm$ 111,744	0.54 **
	5% NAC	27.7 $\pm$ 15.1		60 $\pm$ 16.8		441,084 $\pm$ 293,005	
	10% NAC	38 $\pm$ 21		69.7 $\pm$ 34.5		521,948 $\pm$ 468,316	
	20% NAC	26.2 $\pm$ 14		63.4 $\pm$ 27.6		307,195 $\pm$ 323,883	

All *p*-values are for between-groups comparison with ANOVA except DPA comparisons on days 14 and 28, where Kruskal–Wallis test was used due to non-normally distributed data. \*  $p = 0.006$  for comparison between 5% and 10% NAC. \*\*  $p < 0.001$  for comparison between 10% NAC and all other

groups. \*\*\*  $p < 0.006$  for comparisons between 5% NAC and both control and 20% NAC. Remaining differences were insignificant after applying Bonferroni correction.

#### 2.4. IHC and Masson's Trichrome Staining

Both iNOS and CD206 immunohistochemical staining resulted in high percentages of positively stained cells. No differences were detected between the studied groups. The signal from iNOS was least intense on day 7, whereas the CD206 signal was robust at the early stages of wound healing and decreased over time (Table 4).

**Table 4.** Immunohistochemical staining analysis results. Values represent % of positively stained cells.

Timepoint	iNOS					CD206				
	Control	5% NAC	10% NAC	20% NAC	<i>p</i> -Value	Control	5% NAC	10% NAC	20% NAC	<i>p</i> -Value
Day 3	17.6 (13.6–29.9)	16.4 (15.8–40.8)	24.8 (22.2–27.3)	38 (34.5–46.6)	0.46	39.8 (33.9–47.6)	43.8 (24.9–59.8)	53 (50.8–56.2)	44.5 (40.6–52.5)	0.72
Day 7	19.6 (17.7–24.3)	15.3 (11–19.9)	13.7 (13.5–15.8)	10 (9.4–17.1)	0.57	32.4 (22.9–40.3)	30.2 (19.4–41.2)	30.3 (26.6–36.8)	36.1 (31.3–38.2)	0.98
Day 14	19.3 (15.2–22.9)	26.2 (19.4–41.5)	20.1 (16.5–23)	21.6 (19.9–22.9)	0.73	20.3 (16.3–39)	22.6 (19.3–22.8)	14.6 (11.7–27.7)	17.6 (10.6–26.3)	0.59
Day 28	23.8 (16.6–32.1)	29.4 (20.6–45.4)	18 (10.6–23.2)	24.9 (10.6–23.2)	0.39	19.7 (18–33.3)	10.2 (9.1–29.9)	14.8 (8.6–16.5)	18.3 (14.4–19.1)	0.3

Masson's trichrome allowed us to visualize collagen fiber orientation and density (Tables 5 and 6). Throughout the study period, the degree of collagen alignment and density were comparable between groups. Only on day 28, the local directional variance was smaller in the 5% NAC group compared with the 10% NAC group ( $p = 0.007$ ).

**Table 5.** Masson's trichrome staining analysis results in the proximal regions of the wounded tissue. For directional variance, values range from 0 to 1, corresponding to completely aligned and randomly aligned collagen fiber orientation, respectively. For collagen density, higher values indicate higher density.

Timepoint	Group	Directional Variance	<i>p</i> -Value	Local Directional Variance	<i>p</i> -Value	Collagen Density	<i>p</i> -Value
Day 3	Control	0.83 ± 0.05	0.21	0.65 ± 0.04	0.24	0.55 ± 0.12	0.17
	5% NAC	0.76 ± 0.06		0.55 ± 0.13		0.47 ± 0.25	
	10% NAC	0.85 ± 0.12		0.62 ± 0.1		0.45 ± 0.13	
	20% NAC	0.76 ± 0.09		0.61 ± 0.04		0.66 ± 0.08	
Day 7	Control	0.75 ± 0.12	0.15	0.61 ± 0.07	0.19	0.68 ± 0.15	0.25
	5% NAC	0.81 ± 0.05		0.66 ± 0.04		0.61 ± 0.14	
	10% NAC	0.79 ± 0.09		0.61 ± 0.07		0.58 ± 0.09	
	20% NAC	0.86 ± 0.06		0.67 ± 0.04		0.52 ± 0.14	
Day 14	Control	0.72 ± 0.07	0.27	0.59 ± 0.05	0.66	0.45 ± 0.13	0.54
	5% NAC	0.75 ± 0.08		0.58 ± 0.07		0.47 ± 0.18	
	10% NAC	0.79 ± 0.08		0.61 ± 0.06		0.49 ± 0.15	
	20% NAC	0.79 ± 0.09		0.61 ± 0.08		0.57 ± 0.22	
Day 28	Control	0.74 ± 0.13	0.07	0.59 ± 0.06	0.04	0.65 ± 0.13	0.007
	5% NAC	0.73 ± 0.11		0.55 ± 0.06		0.47 ± 0.09	
	10% NAC	0.83 ± 0.05		0.63 ± 0.05 *		0.66 ± 0.15	
	20% NAC	0.7 ± 0.09		0.57 ± 0.06		0.53 ± 0.11	

\*  $p = 0.007$  for comparison with 5% NAC; other pairwise comparisons non-significant after applying the Bonferroni correction.

**Table 6.** Masson’s trichrome staining analysis results in the distal regions of the wounded tissue. For directional variance, values range from 0 to 1, corresponding to completely aligned and randomly aligned collagen fiber orientation, respectively. For collagen density, higher values indicate higher density.

Timepoint	Group	Directional Variance	<i>p</i> -Value	Local Directional Variance	<i>p</i> -Value	Collagen Density	<i>p</i> -Value
Day 3	Control	0.77 ± 0.15	0.05	0.6 ± 0.1	0.18	0.53 ± 0.1	0.95
	5% NAC	0.68 ± 0.03		0.5 ± 0.12		0.48 ± 0.28	
	10% NAC	0.71 ± 0.12		0.53 ± 0.08		0.52 ± 0.09	
	20% NAC	0.87 ± 0.04		0.62 ± 0.05		0.53 ± 0.11	
Day 7	Control	0.72 ± 0.12	0.09	0.59 ± 0.08	0.04	0.59 ± 0.16	0.84
	5% NAC	0.79 ± 0.07		0.65 ± 0.03		0.58 ± 0.1	
	10% NAC	0.84 ± 0.03		0.63 ± 0.03		0.55 ± 0.04	
	20% NAC	0.82 ± 0.08		0.67 ± 0.03		0.54 ± 0.09	
Day 14	Control	0.67 ± 0.06	0.09	0.56 ± 0.05	0.69	0.51 ± 0.08	0.84
	5% NAC	0.77 ± 0.07		0.57 ± 0.07		0.49 ± 0.11	
	10% NAC	0.76 ± 0.11		0.6 ± 0.07		0.52 ± 0.13	
	20% NAC	0.76 ± 0.07		0.59 ± 0.07		0.55 ± 0.19	
Day 28	Control	0.79 ± 0.06	0.66	0.62 ± 0.05	0.23	0.65 ± 0.09	0.72
	5% NAC	0.73 ± 0.11		0.56 ± 0.07		0.64 ± 0.1	
	10% NAC	0.75 ± 0.14		0.56 ± 0.08		0.6 ± 0.14	
	20% NAC	0.77 ± 0.05		0.6 ± 0.05		0.67 ± 0.09	

### 3. Discussion

We found that treatment with 5% NAC improved wound closure speed at early stages of healing—a finding that was linked with an increased dermal proliferation area on a microscopic level. We did not find significant differences in the expression of iNOS and CD206 in wound beds and did not capture significant differences in collagen fibers’ deposition and alignment between groups. Higher concentrations of NAC failed to enhance the wound healing process compared with control. In our project, we used hydrogels, which released NAC in a controlled and extended fashion, facilitating a prolonged action on the wounded tissue. Moreover, using the extended-release formula instead of instant-release administration allowed the delivery of the molecule less frequently, decreasing the amount of stress the animals were subjected to.

This is the first study investigating the effect of NAC on wound healing in an animal model of type II DM that we know of. Previously published research indicated a beneficial role of NAC in wound healing in the context of type I DM and healthy animals, both in excisional and incisional models. In our previous work, we showed that low-dose (0.03%) NAC reduced scar area and width at the early stages of wound healing in an incisional model in healthy rats [11]. This was associated with the persisting elevated expression of numerous genes involved in neoangiogenesis, proliferation and tissue remodeling [12]. Tsai et al. studied the effect of NAC on cell migration and proliferation *in vitro* and wound healing in a burn model *in vivo*. They found that NAC increased glutathione levels, cell viability and migration abilities in a dose-dependent manner. Additionally, topically applied 3% NAC improved re-epithelialization *in vivo*, and the effect was more pronounced in this group compared with lower concentrations [9]. Ozkaya et al. used NAC to treat excisional wounds in a streptozotocin-induced diabetic rat model [15]. They found that using either systemic or topical NAC resulted in improved epithelialization, lower fibrosis scores and reduced oxidative stress markers. Aktunc et al. applied NAC intraperitoneally to treat incisional wounds in two groups: healthy mice and mice with alloxan-induced diabetes [14]. They reported lower oxidative stress marker levels and increased wound-breaking strength in both groups following NAC administration. Our findings align with previous reports suggesting that NAC may improve re-epithelialization, which was reflected by an increased wound closure speed at the early stages of healing and by an

increased dermal proliferation area, indicating improved proliferation and migration rates compared with other groups. Importantly, these effects were lost with NAC concentrations exceeding 5%.

Despite encouraging preliminary *in vivo* reports, selecting an adequate dose and the NAC administration route is challenging. As shown above, NAC has not been repeatedly studied using uniform concentrations (literature reports range from 0.03% to 20%), routes of delivery (topical, intradermal injections or intraperitoneal), wound models (excisional, incisional or burn wound) and DM animal models (alloxan-induced, streptozotocin-induced or leptin-deficient). Though all mentioned studies reported beneficial results using NAC, it remains unclear which approach is optimal when it comes to molecule administration and indications. NAC has been used successfully at high concentrations in the clinical context to treat atopic dermatitis or acne vulgaris [6,35]. Acute treatment with high-dose NAC exhibits strong antioxidative and anti-inflammatory functions [36]—both of which are dysregulated in wound healing in DM [17]. *In vitro* NAC loses its pro-proliferative function in a dose-dependent manner [37]. We did not observe significant differences in iNOS and CD206 positively stained cells between groups at all time points. These are markers of M1 and M2 macrophages, respectively [38,39]. Faster attenuation of inflammation as measured with the density of these cells, as well as a quicker transition from predominant M1 to an M2 phenotype, has not been observed in NAC-treated groups.

Given the pandemic of type II diabetes mellitus and its global burden [40], as well as the scarcity of available topical treatments, future research should maximize its potential for clinical transferability. Excisional models using the splinting method allow the imitation of the natural process of granulation within human wounds and help overcome confounding wound contraction [41]. The diabetes mellitus model itself should also be carefully selected as it has been shown that wound healing in streptozotocin-induced DM (imitating type I DM) is not as impaired as in leptin-deficient mice [16]. Although the leptin-deficient model is not ideal, it has been used in many studies, and its biology is now well understood [17]. The authors of future studies should also consider choosing other animal models depending on available resources. Potential candidates for wound healing research include rabbit and pig models [42].

Our work has limitations. Firstly, murine wound healing models do not fully reflect the processes observed in humans due to the presence of the panniculus carnosus muscle, which plays a potent role in skin contraction. Therefore, excisional wounds heal primarily by this mechanism, not via the formation of granulation tissue, like in humans. We aimed to protect against this limitation by implementing a splinting model [41] and following a previously optimized wound creation protocol [18]. Secondly, large amounts of fat within the subcutaneous tissue made the histological specimens less concise when mounting onto the slides, creating artifacts and hindering analyses. Due to this limitation, we selected only those parameters that could have been measured reliably. Despite this step, the results of secondary analyses should be interpreted with caution. Thirdly, the sample size was sufficient to elucidate differences in the primary outcome measure between groups; however, secondary analyses may have been underpowered to detect small effects. Therefore, it cannot be stated that NAC does not influence the quantity of macrophages in the wound bed or does not have an impact on collagen alignment. These effects are possible, though a large effect is unlikely. Fourthly, splints mounted around the wounds could have fallen off throughout the study period and may have influenced consecutive assessments. We protected against unequal measurements of wound sizes by randomly allocating wounds to receive different treatments within each animal.

## 4. Materials and Methods

### 4.1. Animals, Sample Size Calculation and Study Design

Animal care and handling were carried out under the UK's Animals (Scientific Procedures) Act 1986 and associated guidelines under the EU Directive 2010/63/EU for animal

experiments. The experiment was approved by the Second Local Ethics Committee in Warsaw (protocol code WAW2/029/2021). A total of 20 male 10-week db/db mice (strain BKS(D)-*Lepr<sup>db</sup>*/JorIRj, Janvier, Le Genest-Saint-Isle, France) were used in this experiment. Their baseline mean glucose serum concentration was  $483 \pm 191.9$  mg/dL, and they weighed on average  $50.2 \pm 6.3$  g. The number of animals needed for the experiment was based on a priori sample size calculation using G\*Power 3.1 [43] (ANOVA: fixed effects, omnibus, one-way test) assuming a moderate effect size of 0.55,  $\alpha$  error probability of 0.05, power of 95% and 4 groups. The effect size was estimated for the primary endpoint—wound healing rate. The final sample size was 64, but we increased the number of experimental units (wounds) to 80 (20 animals with 4 wounds each) due to a high risk of infection or early animal deaths.

Four excisional wounds were created on the backs of each animal, and each wound within one animal was randomly assigned to one of the four groups: a control group receiving hydrogel without any active substance or one of three groups receiving hydrogels with different NAC concentrations: 5%, 10% or 20%. Group allocation was based on a computer random number generator. The allocation had been concealed before the experiment commenced by a person from outside of the research team, who tagged the hydrogel containers with one of four letters—A, B, C or D—representing one of the four interventions. Therefore, researchers were blinded to the intervention they were applying to each wound. Unmasking took place after the experiment had been finished. As each animal served as their own control, the risk of confounding was minimized.

## 4.2. NAC Hydrogel Synthesis

### 4.2.1. Reagents

The following reagents were used for subsequent experiments:  $\epsilon$ -Caprolactone (2-Oxepanone, CL, 97%, Aldrich, Poznan, Poland), rac-lactide (3,6-dimethyl-1,4-dioxane-2,5-dione, rac-LA, 96%, Sigma-Aldrich, Poznan, Poland), 1,6-diisocyanatohexane (hexamethylene diisocyanate, HDI, 98%, Aldrich, Poznan, Poland), poly(ethylene glycol) 200 (PEG 200,  $M_n = 200$  g/mol, pure, Sigma-Aldrich, Poznan, Poland), poly(ethylene adipate) diol (PEA) diol,  $M_n = 1000$  g/mol, Sigma-Aldrich, Poznan, Poland), chitosan (CHIT, low molecular weight, 75% deacetylated, Sigma-Aldrich, Poznan, Poland), dibutyltin dilaurate (DBDLSn, >96%, Sigma-Aldrich, Poznan, Poland), immobilized lipase B from *Candida antarctica* (CA) (Sigma-Aldrich, Poznan, Poland), N-Acetyl-L-cysteine (NAC,  $\geq 99.9\%$ , Sigma-Aldrich, Poznan, Poland), dichloromethane (DCM,  $\text{CH}_2\text{Cl}_2$ , 99.8%, POCH, Gliwice, Poland), toluene anhydrous (Acros Organics, 99.8%, Extra Dry, Gdansk, Poland) and N,N-dimethylformamide (DMF, anhydrous, 99.8%, Sigma-Aldrich, Poznan, Poland). PEG 200 was used for copolymer synthesis, and HDI was heated at  $80^\circ\text{C}$  for 2 h in a vacuum to remove water residues. Phosphate buffer solution ( $\text{pH } 7.40 \pm 0.05$ , 0.1 M, PBS, potassium dihydrogen phosphate/di-sodium hydrogen phosphate,  $20^\circ\text{C}$ , Avantor Performance Materials, Gliwice, Poland) and potassium acetate buffer solution (100 mM,  $\text{pH } 5.5$ ,  $0.2 \mu\text{M}$  filtered, Avantor Performance Materials, Gliwice, Poland) were also used as received.

### 4.2.2. Synthesis of $\epsilon$ -Caprolactone, Rac-Lactide and Poly(ethylene glycol) Copolymers

The polymerization reactions were carried out according to our previously described method with some modifications [44–46]. Before the reaction, monomers (CL and rac-LA), PEG and CA were dried under a vacuum at room temperature for 2 h. Next, 0.05 mol CL and 0.05 mol rac-LA were placed in a three-neck flask equipped with a stirrer and thermometer (under argon atmosphere), and 20 mL of toluene was added. The mixture was stirred at  $80^\circ\text{C}$  for 3 h. Next, an appropriate amount of PEG 200 and CA (500 mg) was added to the mixture. Stirring was continued at  $80^\circ\text{C}$  for 72 h under an argon atmosphere. After this time, the enzyme was filtered off. Toluene was removed by evaporation under reduced pressure at room temperature. Next, the cooled product was dissolved in DCM and extracted with cold methanol and distilled water.

Spectroscopy data of obtained copolymers are as follows: The  $^1\text{H}$  NMR: 1.40 ppm (-CO-CH<sub>2</sub>-CH<sub>2</sub>-CH<sub>2</sub>-CH<sub>2</sub>-CH<sub>2</sub>-O-), 1.48 ppm (-CO-CH(CH<sub>3</sub>)-O-), 1.64 ppm (-CO-CH<sub>2</sub>-CH<sub>2</sub>-CH<sub>2</sub>-CH<sub>2</sub>-CH<sub>2</sub>-O-), 2.30 ppm (-CO-CH<sub>2</sub>-CH<sub>2</sub>-CH<sub>2</sub>-CH<sub>2</sub>-CH<sub>2</sub>-O-) in -CO-Cap-Cap- sequences, 2.38 ppm (-CO-CH<sub>2</sub>-CH<sub>2</sub>-CH<sub>2</sub>-CH<sub>2</sub>-CH<sub>2</sub>-O-) in -CO-Lac-Cap- sequences, 3.63 ppm (-CH<sub>2</sub>-CH<sub>2</sub>-O-), 4.05 ppm (-CO-CH<sub>2</sub>-CH<sub>2</sub>-CH<sub>2</sub>-CH<sub>2</sub>-CH<sub>2</sub>-O-) in -CO-Cap-Cap- sequences, 4.13 ppm (-CO-CH<sub>2</sub>-CH<sub>2</sub>-CH<sub>2</sub>-CH<sub>2</sub>-CH<sub>2</sub>-O-) in -CO-Cap-Lac sequences, 4.21 ppm (-CH<sub>2</sub>-CH<sub>2</sub>-O-CH<sub>2</sub>-CH<sub>2</sub>-O-Cap-), 4.27 ppm (-CH<sub>2</sub>-CH<sub>2</sub>-O-CH<sub>2</sub>-CH<sub>2</sub>-O-Lac-), 5.04 ppm (-CO-CH(CH<sub>3</sub>)-O-); the  $^{13}\text{C}$  NMR: 17.02 ppm (-CO-CH(CH<sub>3</sub>)-O-), 20.49 ppm (-CO-CH(CH<sub>3</sub>)-OH) end groups, 24.62 ppm (-CO-CH<sub>2</sub>-CH<sub>2</sub>-CH<sub>2</sub>-CH<sub>2</sub>-CH<sub>2</sub>-O-), 25.57 ppm (-CO-CH<sub>2</sub>-CH<sub>2</sub>-CH<sub>2</sub>-CH<sub>2</sub>-CH<sub>2</sub>-O-), 28.39 ppm (-CO-CH<sub>2</sub>-CH<sub>2</sub>-CH<sub>2</sub>-CH<sub>2</sub>-CH<sub>2</sub>-O-), 32.36 ppm (-CO-CH<sub>2</sub>-CH<sub>2</sub>-CH<sub>2</sub>-CH<sub>2</sub>-CH<sub>2</sub>-OH) end groups, 34.16 ppm (-CO-CH<sub>2</sub>-CH<sub>2</sub>-CH<sub>2</sub>-CH<sub>2</sub>-CH<sub>2</sub>-O-), 62.57 ppm (-CO-CH<sub>2</sub>-CH<sub>2</sub>-CH<sub>2</sub>-CH<sub>2</sub>-CH<sub>2</sub>-OH) end groups, 63.49 ppm (-CH<sub>2</sub>-CH<sub>2</sub>-O-CH<sub>2</sub>-CH<sub>2</sub>-O-CO-), 64.18 ppm (-CO-CH<sub>2</sub>-CH<sub>2</sub>-CH<sub>2</sub>-CH<sub>2</sub>-CH<sub>2</sub>-O-), 66.77 ppm (-CO-CH(CH<sub>3</sub>)-OH) end groups, 69.21 ppm (-CO-CH(CH<sub>3</sub>)-O-) and (-CH<sub>2</sub>-CH<sub>2</sub>-O-CH<sub>2</sub>-CH<sub>2</sub>-O-CO-), 70.60 ppm (-CH<sub>2</sub>-CH<sub>2</sub>-O-), 170.90 ppm (-CO-CH(CH<sub>3</sub>)-O-) in lactyl units (L) in -Cap-L-Cap- sequences and 173.57 ppm (-CO-CH<sub>2</sub>-CH<sub>2</sub>-CH<sub>2</sub>-CH<sub>2</sub>-CH<sub>2</sub>-O-).

#### 4.2.3. Hydrogel Preparation and Characterization

Hydrogels were obtained using a previously developed and appropriately modified three-step method [33,47]. In the first step, the CL-LA-PEG 200 copolymer was synthesized. The prepolymer of DI and CL-LA-PEG 200 copolymer and PEA was obtained in the second step. Next, the CHIT-DI-CL-LA-PEG 200- PEA hydrogel was prepared. The prepolymers were obtained through a polyaddition reaction between HDI, CL-LA-PEG 200 copolymer and PEA in an NCO/OH molar ratio of 2.1: 0.9: 0.1, using 3 drops of 0.1 wt % DBDL<sub>Sn</sub> solution in toluene as a catalyst. The reactions were performed at 80 °C for 3 h under an argon atmosphere to form an isocyanate-terminated prepolymer. Next, the CHIT dispersion into a glacial acetic acid/DMF mixture (30 mL) in a volume ratio of 50/50 was prepared. Next, the obtained prepolymer was added to the dispersion of CHIT. The reactions were carried out in an NCO (prepolymer)/OH (or NH<sub>2</sub>) (CHIT) molar ratio of 1.6:1 at 80 °C for 4 h under an argon atmosphere. The reaction mixture was then transferred to the distilled water. Precipitated products were separated by filtration and washed with DMF, methanol, and acetone. The final products were dried under a vacuum for one week. The mass swelling ratio (MSR) of obtained hydrogels was determined at 37 °C during 80 h of incubation in a buffer. Samples in triplicate were submerged in a buffer solution (20 mL) for a given time, and their weights were taken after removing the excessive surface water. The mass swelling ratio was calculated using the following formula:

$$\text{MSR} = ((W_2 - W_1)/W_1)/100\%$$

where  $W_1$  is the weight of the initial hydrogel and  $W_2$  is the weight of the swollen hydrogel.

To evaluate the percentage of degradation, the hydrogel samples were immersed in a buffer at 37 °C for 8 weeks; most importantly, the medium was replaced with a fresh buffer every week. At the end of the experiment, the samples were dried in a vacuum for 48 h. The degree of degradation of hydrogels (in triplicate) was determined by the weight loss (WL) of the samples according to the following equation:

$$\text{WL} = [(W_1 - W_2)/W_1]/100\%$$

where  $W_1$  is the weight of the dry sample before degradation and  $W_2$  is the weight of the dry sample after degradation.

#### 4.2.4. In Vitro Release Studies of N-Acetyl-L-Cysteine from Hydrogels

NAC was loaded to the hydrogel by physical mixing using the following procedure. A total of 5.0, 10.0 or 20% (m/m) of NAC in distilled water/Tween 80 mixture (2% (w/v)) was added to three hydrogel samples (HYDROGEL-MS1-NAC-5, HYDROGEL-MS1-



NAC-10 and HYDROGEL-MS1-NAC-20). The hydrogels were left sealed for 24 h. The mixtures were dried under vacuum at room temperature to obtain a NAC-loaded hydrogel film. The *in vitro* release of NAC from the hydrogels was performed in a buffer (pH 7.4 or 5.5) containing 2% (*w/v*) Tween 80 at 37 °C under stirring. Vials containing hydrogel films were filled with 5.0 mL of a buffer, sealed and left at 37 °C for 2 h. The solutions were then removed for further testing and replaced by fresh buffer. Subsequent samples were collected at selected intervals. NAC concentration in the *in vitro* samples was also determined by the UV-Vis spectrophotometric method (detected at a wavelength of 593 nm) [48].

The release data points were subjected to zero-order and first-order kinetics and Korsmeyer–Peppas models. Calculations were made based on formulas mentioned below [34]:

$$\text{Zero-order: } F = kt$$

$$\text{First-order: } \log F = \log F_0 - \frac{kt}{2.303}$$

$$\text{Korsmeyer–Peppas model: } F = kt^n \quad (F < 0.6)$$

where  $F$  is the fraction of the drug released from the matrix after time  $t$ ;  $F_0$  is the initial amount of the drug,  $k$  is a model constant, and  $n$  is the drug release exponent in the Korsmeyer–Peppas model.

#### 4.2.5. Measurements

The structure of the obtained copolymers,  $M_n$ , and the monomers conversion were evaluated using  $^1\text{H}$  and  $^{13}\text{C}$  NMR techniques. The spectra were recorded on an Agilent Technologies 400 MHz (Santa Clara, CA, USA) spectrometer. The synthesized copolymers  $M_n$  and  $D$  index values were determined using the GPC technique. The measurements were carried out on a Malvern Viscotek GPCMax TDA 305 (Malvern Panalytical, Malvern, UK) chromatograph equipped with a Jordi Gel DVB mixed bed column (Jordi Labs, Mansfield, MA, USA). The mobile phase flow (DCM) was set to 1.0 mL/min, and the column temperature was set to 30 °C. The system was calibrated using polystyrene standards. The amount of released NAC was determined by UV–Vis spectrophotometry (UV-1202 Shimadzu, Shimadzu, Kyoto, Japan) using a 1 cm quartz cell.

#### 4.3. Surgical Procedure and NAC Administration

All surgical procedures were performed using aseptic techniques. Male db/db mice aged 10 weeks ( $n = 20$ ) were acclimatized to a 12 h light/dark cycle at 19 Celsius degrees, with water and high-energy-density food *ad libitum*. The animals were housed in a specific-pathogen-free room at the Central Laboratory of Experimental Animals, Medical University of Warsaw.

All steps of the surgical procedure were performed according to a previously published protocol with slight modifications [18]. Briefly, a few days before the experiment, 0.5 mm-thick silicone splinting rings with an 8 mm inner and 18 mm outer diameter were prepared. They were first washed with a detergent, rinsed with water, then incubated in sodium hypochlorite (20,000 p.p.m.) for 30 min, washed with sterile water and incubated in 70% ethanol for 30 min. They were air-dried on sterile gauze and kept in a sterile bottle before the surgical part commenced. On the day of surgery, all mice had the hair on their back cut, and removal cream was applied for 3–5 min and gently removed. Prior to surgery, grease was removed from the skin with a mild detergent.

The same anesthesia protocol was applied to all animals. Firstly, 2–3% isoflurane was used for induction in an anesthesia chamber, and later, anesthesia was maintained with 1–2% isoflurane mixed with normal air delivered via a mask. The skin was disinfected with octenidine dihydrochloride and phenoxyethanol, and four full-thickness 6 mm excisional wounds were created on the backs of each animal with a sterile single-use punch

biopsy tool. This approach enables minimizing the number of animals used for the experiment and was previously validated in a leptin-deficient murine model [49]. An instant-bonding adhesive was used to mount the silicone splint so that the wound was centered within the splint. All splints were secured with three sutures of 6.0 nylon. Following the surgical procedure, all animals received an intramuscular injection with enrofloxacin 10 mg/kg and metamizole 30 mg/kg and a subcutaneous injection with buprenorphine 0.03 mg/kg. To avoid the drying of the cornea, Vidisic gel was applied topically on the eyeballs of all animals. All above-mentioned steps were performed by a surgeon unaware of the intervention allocation.

Photographs of the wounds were taken with a digital camera (Figure 6), and hydrogels were applied to the wounds according to the pre-determined allocation based on letters representing study groups (A, B, C or D). The person applying hydrogels was blinded to the intervention used. The wounds and splints were covered with Tegaderm sterile transparent dressings, and mice were placed in separate cages with environmental enrichment to avoid biting wounds by cohabitants.

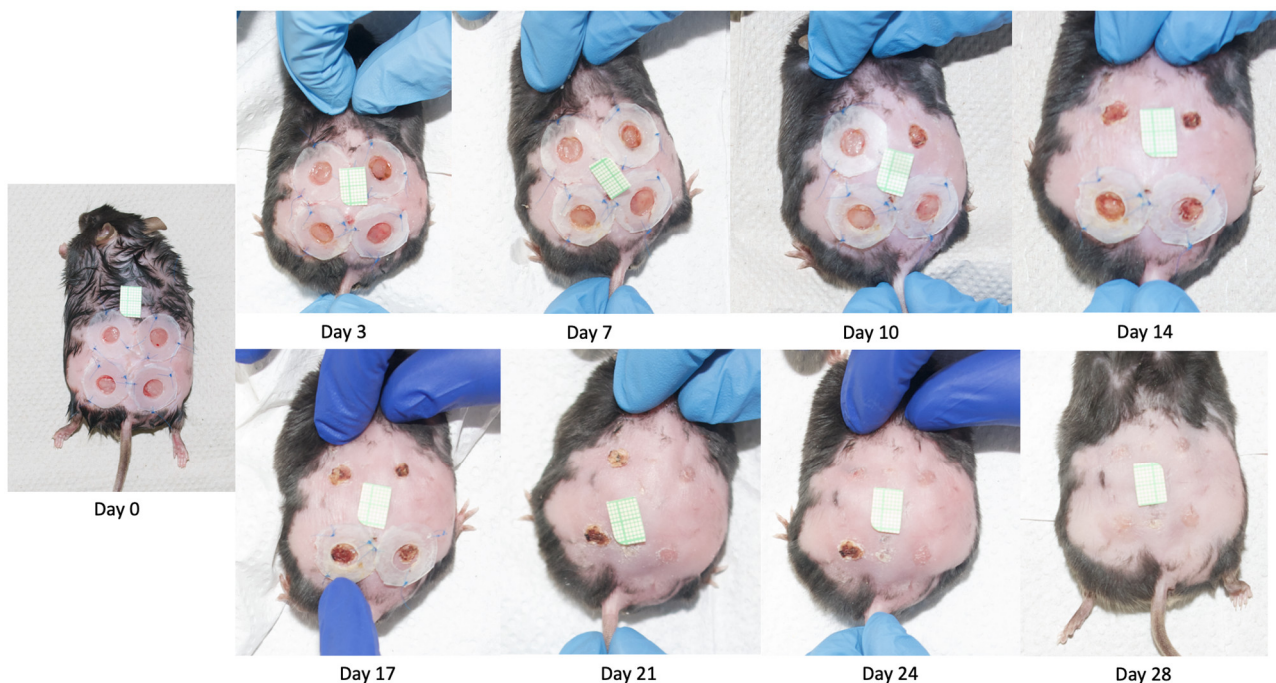


**Figure 6.** Examples of photographs taken to monitor the wound healing process throughout the experimental period.

NAC was topically applied on the wounds on the day of the surgery and subsequently on days 3, 6, 9 and 12 as the hydrogels were expected to gradually release active substances for approximately 2–3 days. All hydrogels were removed on day 14, and from that time, all wounds continued healing without any additional interventions.

#### 4.4. Tissue Harvesting and Histological Staining

Five animals chosen at random were sacrificed on days 3, 7, 14 and 28. These days were selected to reflect different stages of wound healing. Typically, day 3 reflects the inflammatory phase, day 7 the proliferative phase and days 14 and 28 the remodeling phases; however, in diabetic wounds, these phases are usually delayed and may overlap. Wounds/scars were excised, divided into two equal parts and preserved for histologic and further analyses. One half was fixed in 10% formalin and embedded in paraffin using an automated tissue processor (ASP 6026, Leica, Buffalo Grove, IL, USA). Samples were sectioned into 3–5  $\mu\text{m}$  slices, mounted on the histological slides and stained (1) with hematoxylin and eosin (Sigma-Aldrich, Saint Louis, MO, USA) using an automatic tissue stainer



(Autostainer XL, Leica, Buffalo Grove, IL, USA); as shown in Figure 7, (2) with Masson's trichrome (Sigma-Aldrich, Saint Louis, MO, USA) to visualize collagen fiber alignment (Figure 8); and using immunohistochemistry, described in a separate section. Manual staining protocols were followed according to the manufacturer's instructions. All stained sections were scanned at 40x magnification using NanoZoomer XR C9600-12 (Hamamatsu, Iwata City, Japan).

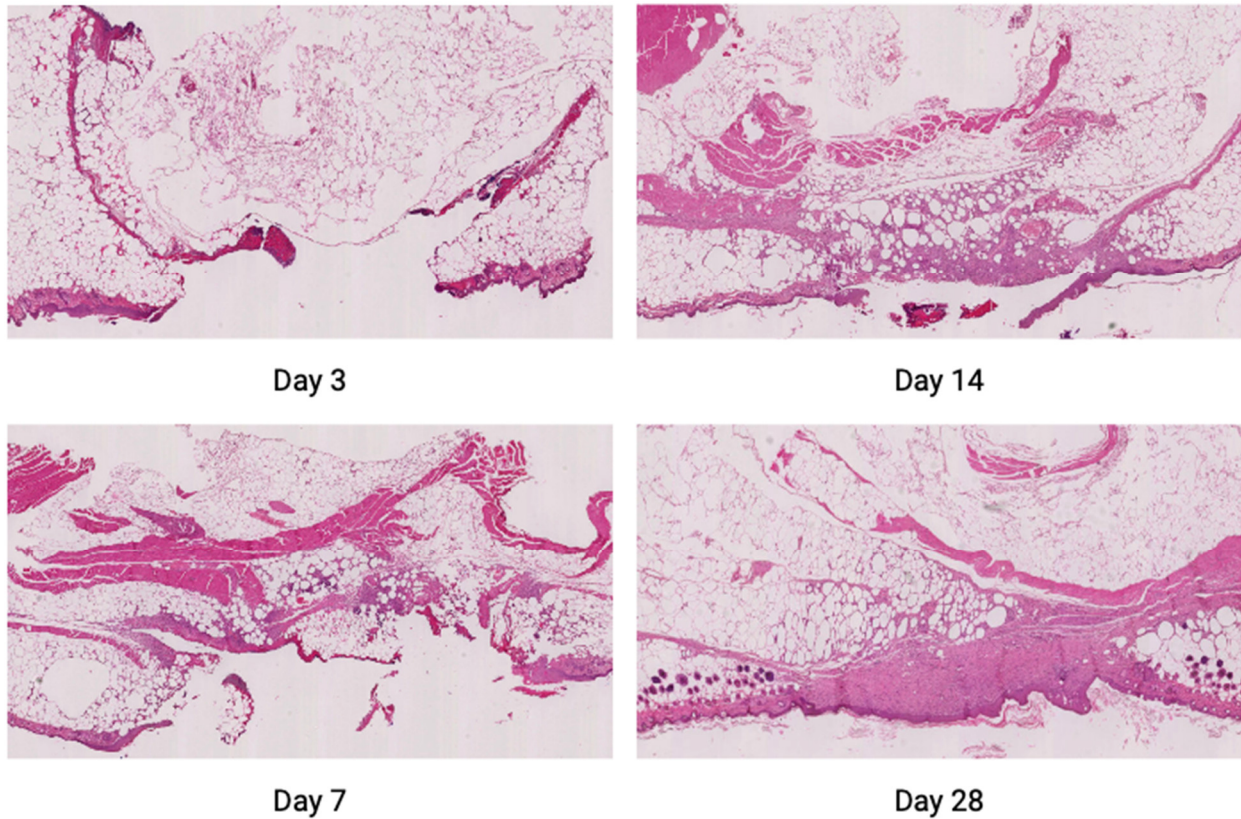


**Figure 7.** Examples of hematoxylin and eosin tissue staining images on days 3, 7, 14 and 28.

Some wounds were excluded from analyses due to early animal death post-anesthesia (2 mice) or wound ulceration extending towards other wounds. Therefore, a total of 15 experimental units were excluded from subsequent analyses.

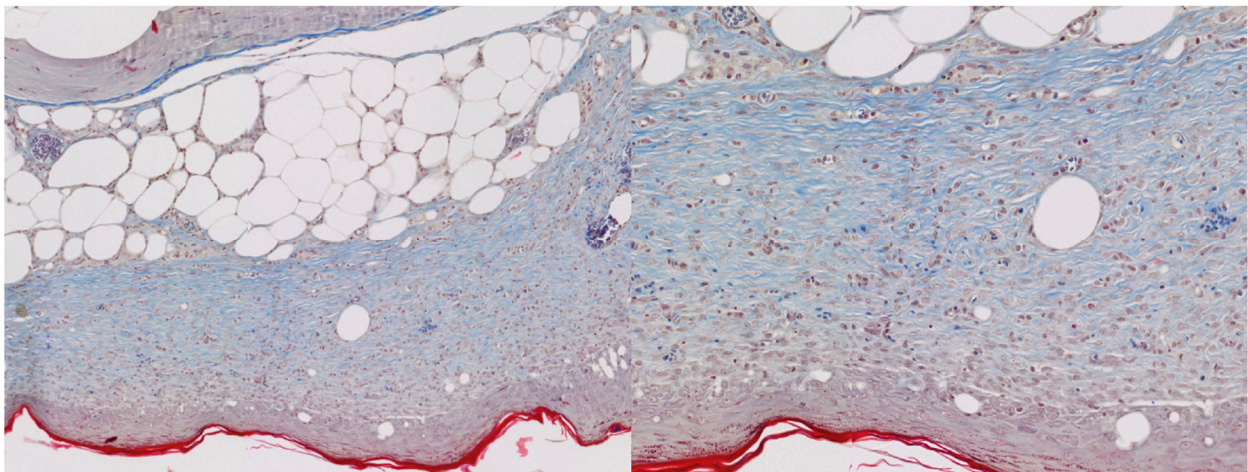


**Figure 8.** Examples of Masson's trichrome staining images at two magnifications.

#### 4.5. Macroscopic Wound Healing Assessment

Standardized photographic documentation of wounds was performed on the day of surgery and on days 3, 7, 10, 14, 17, 21, 24 and 28 following surgeries (Figure 6). The camera was placed on a stand 30 cm above the dorsal side of the animal. In each photo, there was a 1 cm-long millimeter scale placed on the skin. Photos were uploaded to ImageJ 1.48 v. software (National Institutes of Health, Bethesda, MD, USA) by a blinded researcher who measured the total wound areas. Results at each time point were presented as percentages of the baseline wound areas.

#### 4.6. Histomorphometry

Initially, we aimed to measure all critical wound parameters as described in our previous work [11]. However, as the subcutaneous tissue of leptin-deficient mice contains huge amounts of fat and the dermis is relatively thin, obtaining intact histological slides was challenging, particularly at the early stages of healing. To ascertain robust and reliable measurements and to reduce the chance of spurious findings, we decided to limit histomorphometric assessments to three parameters: thickness of the epidermis (measured thrice on each side of the wound), thickness of the newly formed epidermis (measured similarly) and dermal proliferation area excluding day 3. Measurements were performed as described in our previous work based on methods that had been introduced in works by Lemo et al. [50] and Schencke et al. [51].

#### 4.7. Immunohistochemical Staining and Analysis

Following deparaffinization, immunohistochemistry staining was performed with REAL EnVision™ Detection System (DAKO, Agilent, Santa Clara, CA, USA, Code Number K5007). The following primary antibodies were used: anti-iNOS (Abcam ab115819) and anti-CD206 (Abcam ab64693) to visualize inflammatory cells, particularly different phenotypes of macrophages [38,39]. Two distinct staining methods were used as pro-inflammatory macrophages persist through day 10 following excisions in diabetic wounds and the macrophage polarization is skewed towards the M1 phenotype [17]. We aimed to assess whether NAC would improve the transition from the M1 to the M2 phenotype. Anti-iNOS antibodies were diluted 1:100 and incubated for 2 h, whereas anti-CD206 antibodies were diluted 1:20,000 and incubated for 15 min. The following reagents from DAKO were utilized during immunohistochemical staining: Wash Buffer (Code Number S3006); Peroxidase-Blocking Solution (Code Number S2023); Dako REAL™ Antibody Diluent (Code Number S2022); and Target Retrieval Solution, Citrate pH 6 (Code Number S2369). Staining procedures were carried out manually according to the manufacturer's guidelines. All stained sections were scanned at 40× magnification with NanoZoomer XR C9600-12 (Hamamatsu, Iwata City, Japan) to obtain WSI (whole slide image) scans (Figure 9). WSIs underwent automated analysis in QuPath [52]. Uploaded files were manually checked for artifacts (stain traces, blood clots, folded tissue, etc.), and ROIs (regions of interest) were outlined. The process of nuclei identification was optimized, and the type of staining (intra- or extracellular) was selected. Results were presented as % of positively stained cells.



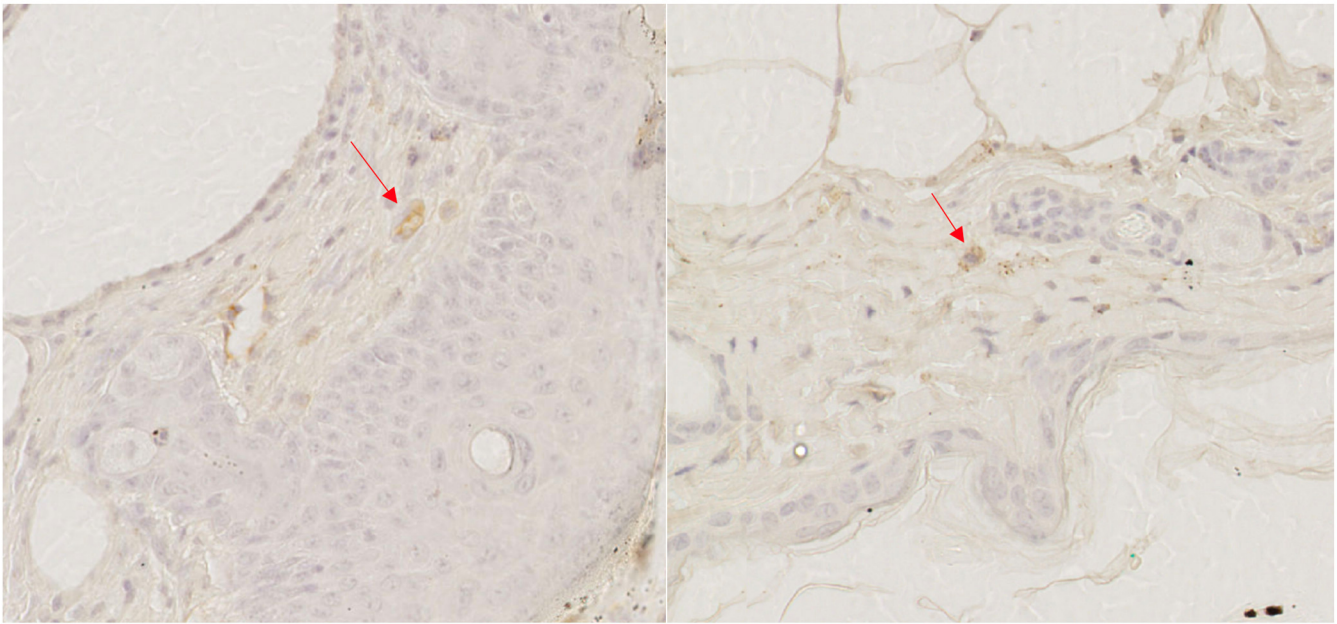


**Figure 9.** Examples of immunohistochemical staining images—anti-iNOS staining on the left and anti-CD206 staining on the right. Stained cells were marked with red arrows.

#### 4.8. Statistical Analysis.

For all variables, data distribution was verified using the Shapiro–Wilk test and double-checked if in doubt using QQ plots. For non-parametric data distribution, we used the Kruskal–Wallis test with the post hoc Wilcoxon test. For parametric data distribution, ANOVA was used with post hoc *t*-tests. All data were presented as means  $\pm$  standard deviations for normally distributed data and as medians and IQR (interquartile ranges) for non-normally distributed data unless otherwise indicated. In the case of multiple comparisons, the Bonferroni correction was applied to avoid overstating significant differences. All statistical analyses were carried out in R version 4.2.3.

## 5. Conclusions

Topically applied hydrogel releasing 5% N-acetylcysteine improved the diabetic wound closure speed at early stages of healing, accompanied by an increased dermal proliferation area adjacent to the wound on histological assessment compared with the control hydrogel. Higher concentrations of NAC did not have a beneficial effect on the wound healing process in the leptin-deficient murine model of type 2 diabetes mellitus. We did not identify substantial changes in collagen fiber alignment or macrophage phenotype transition speed following NAC treatment.

Future research should focus on optimizing the NAC concentration and the route of delivery in diabetic wound healing. In vivo studies should focus on exploring the mechanism of action of NAC, especially its potential to improve cellular proliferation. Experiments should closely reflect the wound healing conditions in humans. Therefore, if performed in murine models, they should apply splinting to counteract the robust contraction mechanism present in rodents.

**Author Contributions:** Conceptualization, A.S. and P.K.W.; methodology, A.S. and M.S.; software, A.S. and P.K.W.; validation, P.K.W.; formal analysis, A.S., P.K.W., M.S. and K.K.; investigation, A.S., M.K., K.K.; M.S. and K.K.; resources, P.K.W.; data curation, A.S.; writing—original draft preparation, A.S.; writing—review and editing, M.K., K.K. and P.K.W.; visualization, A.S.; supervision, P.K.W.; project administration, A.S.; funding acquisition, A.S. All authors have read and agreed to the published version of the manuscript.

**Funding:** This research was funded by the Medical University of Warsaw, grant number 1MN/2/MG/N/20.

**Institutional Review Board Statement:** The animal study protocol was approved by the Second Local Ethics Committee in Warsaw (protocol code WAW2/029/2021 on 24 February 2021).

**Informed Consent Statement:** Not applicable.

**Data Availability Statement:** The data that support the findings of this study are available from the corresponding author, P.K.W., upon reasonable request.

**Acknowledgments:** We would like to thank Klaudia Klicka for help with allocation concealment and unmasking after the study had finished. We also thank Agata Czapla for her technical support.

**Conflicts of Interest:** The authors declare no conflicts of interest.

## References

- Atkuri, K.R.; Mantovani, J.J.; Herzenberg, L.A.; Herzenberg, L.A. N-Acetylcysteine—a safe antidote for cysteine/glutathione deficiency. *Curr. Opin. Pharmacol.* **2007**, *7*, 355–359. <https://doi.org/10.1016/j.coph.2007.04.005>.
- Zafarullah, M.; Li, W.Q.; Sylvester, J.; Ahmad, M. Molecular mechanisms of N-acetylcysteine actions. *Cell Mol. Life Sci.* **2003**, *60*, 6–20. <https://doi.org/10.1007/s000180300001>.
- Samuni, Y.; Goldstein, S.; Dean, O.M.; Berk, M. The chemistry and biological activities of N-acetylcysteine. *Biochim. Biophys. Acta* **2013**, *1830*, 4117–4129. <https://doi.org/10.1016/j.bbagen.2013.04.016>.
- Dean, O.; Giorlando, F.; Berk, M. N-acetylcysteine in psychiatry: Current therapeutic evidence and potential mechanisms of action. *J. Psychiatry Neurosci.* **2011**, *36*, 78–86. <https://doi.org/10.1503/jpn.100057>.
- Janeczek, M.; Moy, L.; Riopelle, A.; Vetter, O.; Reserva, J.; Tung, R.; Swan, J. The Potential Uses of N-acetylcysteine in Dermatology: A Review. *J. Clin. Aesthet. Dermatol.* **2019**, *12*, 20–26.
- Nakai, K.; Yoneda, K.; Murakami, Y.; Koura, A.; Maeda, R.; Tamai, A.; Ishikawa, E.; Yokoi, I.; Moriue, J.; Moriue, T.; et al. Effects of Topical N-Acetylcysteine on Skin Hydration/Transepidermal Water Loss in Healthy Volunteers and Atopic Dermatitis Patients. *Ann. Dermatol.* **2015**, *27*, 450–451. <https://doi.org/10.5021/ad.2015.27.4.450>.
- Calverley, P.; Rogliani, P.; Papi, A. Safety of N-Acetylcysteine at High Doses in Chronic Respiratory Diseases: A Review. *Drug Saf.* **2021**, *44*, 273–290. <https://doi.org/10.1007/s40264-020-01026-y>.
- Guo, S.; Dipietro, L.A. Factors affecting wound healing. *J. Dent. Res.* **2010**, *89*, 219–229. <https://doi.org/10.1177/0022034509359125>.
- Tsai, M.L.; Huang, H.P.; Hsu, J.D.; Lai, Y.R.; Hsiao, Y.P.; Lu, F.J.; Chang, H.R. Topical N-acetylcysteine accelerates wound healing in vitro and in vivo via the PKC/Stat3 pathway. *Int. J. Mol. Sci.* **2014**, *15*, 7563–7578. <https://doi.org/10.3390/ijms15057563>.
- Oguz, A.; Uslukaya, O.; Alabalik, U.; Turkoglu, A.; Kapan, M.; Bozdag, Z. Topical N-acetylcysteine improves wound healing comparable to dexpanthenol: An experimental study. *Int. Surg.* **2015**, *100*, 656–661. <https://doi.org/10.9738/INTSURG-D-14-00227.1>.
- Paskal, W.; Paskal, A.M.; Pietruski, P.; Stachura, A.; Pelka, K.; Woessner, A.E.; Quinn, K.P.; Kopka, M.; Galus, R.; Wejman, J.; et al. N-Acetylcysteine Added to Local Anesthesia Reduces Scar Area and Width in Early Wound Healing—An Animal Model Study. *Int. J. Mol. Sci.* **2021**, *22*, 7549. <https://doi.org/10.3390/ijms22147549>.
- Paskal, W.; Kopka, M.; Stachura, A.; Paskal, A.M.; Pietruski, P.; Pelka, K.; Woessner, A.E.; Quinn, K.P.; Galus, R.; Wejman, J.; et al. Single Dose of N-Acetylcysteine in Local Anesthesia Increases Expression of HIF1alpha, MAPK1, TGFbeta1 and Growth Factors in Rat Wound Healing. *Int. J. Mol. Sci.* **2021**, *22*, 8659. <https://doi.org/10.3390/ijms22168659>.
- Greenhalgh, D.G. Wound healing and diabetes mellitus. *Clin. Plast. Surg.* **2003**, *30*, 37–45. [https://doi.org/10.1016/s0094-1298\(02\)00066-4](https://doi.org/10.1016/s0094-1298(02)00066-4).
- Aktunc, E.; Ozacmak, V.H.; Ozacmak, H.S.; Barut, F.; Buyukates, M.; Kandemir, O.; Demircan, N. N-acetyl cysteine promotes angiogenesis and clearance of free oxygen radicals, thus improving wound healing in an alloxan-induced diabetic mouse model of incisional wound. *Clin. Exp. Dermatol.* **2010**, *35*, 902–909. <https://doi.org/10.1111/j.1365-2230.2010.03823.x>.
- Ozkaya, H.; Omma, T.; Bag, Y.M.; Uzunoglu, K.; Isildak, M.; Duymus, M.E.; Kismet, K.; Senes, M.; Fidanci, V.; Celepli, P.; et al. Topical and Systemic Effects of N-acetyl Cysteine on Wound Healing in a Diabetic Rat Model. *Wounds* **2019**, *31*, 91–96.
- Michaels, J.t.; Churgin, S.S.; Blechman, K.M.; Greives, M.R.; Aarabi, S.; Galiano, R.D.; Gurtner, G.C. db/db mice exhibit severe wound-healing impairments compared with other murine diabetic strains in a silicone-splinted excisional wound model. *Wound Repair. Regen.* **2007**, *15*, 665–670. <https://doi.org/10.1111/j.1524-475X.2007.00273.x>.
- Stachura, A.; Khanna, I.; Krysiak, P.; Paskal, W.; Wlodarski, P. Wound Healing Impairment in Type 2 Diabetes Model of Leptin-Deficient Mice—A Mechanistic Systematic Review. *Int. J. Mol. Sci.* **2022**, *23*, 8621. <https://doi.org/10.3390/ijms23158621>.
- Wang, X.; Ge, J.; Tredget, E.E.; Wu, Y. The mouse excisional wound splinting model, including applications for stem cell transplantation. *Nat. Protoc.* **2013**, *8*, 302–309. <https://doi.org/10.1038/nprot.2013.002>.
- Institute for Health Metrics and Evaluation (IHME). Global Burden of Disease 2021: Findings from the GBD 2021 Study. Seattle, WA: IHME, 2024.



20. Edmonds, M.; Manu, C.; Vas, P. The current burden of diabetic foot disease. *J. Clin. Orthop. Trauma* **2021**, *17*, 88–93. <https://doi.org/10.1016/j.jcot.2021.01.017>.
21. Everett, E.; Mathioudakis, N. Update on management of diabetic foot ulcers. *Ann. N. Y. Acad. Sci.* **2018**, *1411*, 153–165. <https://doi.org/10.1111/nyas.13569>.
22. Schwalfenberg, G.K. N-Acetylcysteine: A Review of Clinical Usefulness (an Old Drug with New Tricks). *J. Nutr. Metab.* **2021**, *2021*, 9949453. <https://doi.org/10.1155/2021/9949453>.
23. Kasinski, A.; Zielinska-Pisklak, M.; Oledzka, E.; Sobczak, M. Smart Hydrogels—Synthetic Stimuli-Responsive Antitumor Drug Release Systems. *Int. J. Nanomed.* **2020**, *15*, 4541–4572. <https://doi.org/10.2147/IJN.S248987>.
24. Zagorska-Dziok, M.; Sobczak, M. Hydrogel-Based Active Substance Release Systems for Cosmetology and Dermatology Application: A Review. *Pharmaceutics* **2020**, *12*, 396. <https://doi.org/10.3390/pharmaceutics12050396>.
25. Kasinski, A.; Swierczek, A.; Zielinska-Pisklak, M.; Kowalczyk, S.; Plichta, A.; Zgadzaj, A.; Oledzka, E.; Sobczak, M. Dual-Stimuli-Sensitive Smart Hydrogels Containing Magnetic Nanoparticles as Antitumor Local Drug Delivery Systems-Synthesis and Characterization. *Int. J. Mol. Sci.* **2023**, *24*, 6906. <https://doi.org/10.3390/ijms24086906>.
26. Agarwal, P.; Greene, D.G.; Sherman, S.; Wendl, K.; Vega, L.; Park, H.; Shimanovich, R.; Reid, D.L. Structural characterization and developability assessment of sustained release hydrogels for rapid implementation during preclinical studies. *Eur. J. Pharm. Sci.* **2021**, *158*, 105689. <https://doi.org/10.1016/j.ejps.2020.105689>.
27. Steffens, D.; Braghirolli, D.I.; Maurmann, N.; Pranke, P. Update on the main use of biomaterials and techniques associated with tissue engineering. *Drug Discov. Today* **2018**, *23*, 1474–1488. <https://doi.org/10.1016/j.drudis.2018.03.013>.
28. Kamoun, E.A.; Kenawy, E.S.; Chen, X. A review on polymeric hydrogel membranes for wound dressing applications: PVA-based hydrogel dressings. *J. Adv. Res.* **2017**, *8*, 217–233. <https://doi.org/10.1016/j.jare.2017.01.005>.
29. Muthuramalingam, K.; Choi, S.I.; Hyun, C.; Kim, Y.M.; Cho, M. beta-Glucan-Based Wet Dressing for Cutaneous Wound Healing. *Adv. Wound Care* **2019**, *8*, 125–135. <https://doi.org/10.1089/wound.2018.0843>.
30. Sun, G.; Zhang, X.; Shen, Y.I.; Sebastian, R.; Dickinson, L.E.; Fox-Talbot, K.; Reinblatt, M.; Steenbergen, C.; Harmon, J.W.; Gerecht, S. Dextran hydrogel scaffolds enhance angiogenic responses and promote complete skin regeneration during burn wound healing. *Proc. Natl. Acad. Sci. USA* **2011**, *108*, 20976–20981. <https://doi.org/10.1073/pnas.1115973108>.
31. Sun, G. Pro-Regenerative Hydrogel Restores Scarless Skin during Cutaneous Wound Healing. *Adv. Healthcare Mater.* **2017**, *6*, 1700659. <https://doi.org/10.1002/adhm.201700659>.
32. Alibolandi, M.; Mohammadi, M.; Taghdisi, S.M.; Abnous, K.; Ramezani, M. Synthesis and preparation of biodegradable hybrid dextran hydrogel incorporated with biodegradable curcumin nanomicelles for full thickness wound healing. *Int. J. Pharm.* **2017**, *532*, 466–477. <https://doi.org/10.1016/j.ijpharm.2017.09.042>.
33. Zagorska-Dziok, M.; Kleczkowska, P.; Oledzka, E.; Figat, R.; Sobczak, M. Poly(chitosan-ester-ether-urethane) Hydrogels as Highly Controlled Genistein Release Systems. *Int. J. Mol. Sci.* **2021**, *22*, 3339. <https://doi.org/10.3390/ijms22073339>.
34. Dash, S.; Murthy, P.N.; Nath, L.; Chowdhury, P. Kinetic modeling on drug release from controlled drug delivery systems. *Acta Pol. Pharm.* **2010**, *67*, 217–223.
35. Montes, L.F.; Wilborn, W.H.; Montes, C.M. Topical acne treatment with acetylcysteine: Clinical and experimental effects. *Skinmed* **2012**, *10*, 348–351.
36. Montero, P.; Roger, I.; Estornut, C.; Milara, J.; Cortijo, J. Influence of dose and exposition time in the effectiveness of N-Acetyl-L-cysteine treatment in A549 human epithelial cells. *Heliyon* **2023**, *9*, e15613. <https://doi.org/10.1016/j.heliyon.2023.e15613>.
37. Parasassi, T.; Brunelli, R.; Bracci-Laudiero, L.; Greco, G.; Gustafsson, A.C.; Krasnowska, E.K.; Lundeberg, J.; Lundeberg, T.; Pittaluga, E.; Romano, M.C.; et al. Differentiation of normal and cancer cells induced by sulfhydryl reduction: Biochemical and molecular mechanisms. *Cell Death Differ.* **2005**, *12*, 1285–1296. <https://doi.org/10.1038/sj.cdd.4401663>.
38. Fan, W.; Yang, X.; Huang, F.; Tong, X.; Zhu, L.; Wang, S. Identification of CD206 as a potential biomarker of cancer stem-like cells and therapeutic agent in liver cancer. *Oncol. Lett.* **2019**, *18*, 3218–3226. <https://doi.org/10.3892/ol.2019.10673>.
39. Wilmes, V.; Kur, I.M.; Weigert, A.; Verhoff, M.A.; Gradhand, E.; Kaufenstein, S. iNOS expressing macrophages co-localize with nitrotyrosine staining after myocardial infarction in humans. *Front. Cardiovasc. Med.* **2023**, *10*, 1104019. <https://doi.org/10.3389/fcvm.2023.1104019>.
40. Khan, M.A.B.; Hashim, M.J.; King, J.K.; Govender, R.D.; Mustafa, H.; Al Kaabi, J. Epidemiology of Type 2 Diabetes—Global Burden of Disease and Forecasted Trends. *J. Epidemiol. Glob. Health* **2020**, *10*, 107–111. <https://doi.org/10.2991/jegh.k.191028.001>.
41. Davidson, J.M.; Yu, F.; Opalenik, S.R. Splinting Strategies to Overcome Confounding Wound Contraction in Experimental Animal Models. *Adv. Wound Care* **2013**, *2*, 142–148. <https://doi.org/10.1089/wound.2012.0424>.
42. Hu, Y.; Xiong, Y.; Tao, R.; Xue, H.; Chen, L.; Lin, Z.; Panayi, A.C.; Mi, B.; Liu, G. Advances and perspective on animal models and hydrogel biomaterials for diabetic wound healing. *Biomater. Transl.* **2022**, *3*, 188–200. <https://doi.org/10.12336/biomater-transl.2022.03.003>.
43. Faul, F.; Erdfelder, E.; Lang, A.G.; Buchner, A. G\*Power 3: a flexible statistical power analysis program for the social, behavioral, and biomedical sciences. *Behav. Res. Methods* **2007**, *39*, 175–191. <https://doi.org/10.3758/bf03193146>.
44. Sobczak, M. Enzyme-catalyzed ring-opening polymerization of cyclic esters in the presence of poly (ethylene glycol). *J. Appl. Polym. Sci.* **2012**, *125*, 3602–3609.
45. Piotrowska, U.; Oledzka, E.; Zgadzaj, A.; Bauer, M.; Sobczak, M. A novel delivery system for the controlled Release~ of antimicrobial peptides: Citropin 1.1 and temporin A. *Polymers* **2018**, *10*, 489.

46. Piotrowska, U.; Sobczak, M.; Oledzka, E.; Combes, C. Effect of ionic liquids on the structural, thermal, and in vitro degradation properties of poly ( $\epsilon$ -caprolactone) synthesized in the presence of *Candida antarctica* lipase B. *J. Appl. Polym. Sci.* **2016**, *133*, doi: 10.1002/app.43728.
47. Mahanta, A.K.; Mittal, V.; Singh, N.; Dash, D.; Malik, S.; Kumar, M.; Maiti, P. Polyurethane-grafted chitosan as new biomaterials for controlled drug delivery. *Macromolecules* **2015**, *48*, 2654–2666.
48. Kukoc-Modun, L.; Radić, N. Spectrophotometric Determination of N-Acetyl-L-Cysteine and N-(2-Mercaptopropionyl)-Glycine in Pharmaceutical Preparations. *Int. J. Anal. Chem.* **2011**, *2011*, 140756.
49. Sullivan, S.R.; Underwood, R.A.; Gibran, N.S.; Sigle, R.O.; Usui, M.L.; Carter, W.G.; Olerud, J.E. Validation of a model for the study of multiple wounds in the diabetic mouse (db/db). *Plast. Reconstr. Surg.* **2004**, *113*, 953–960. <https://doi.org/10.1097/01.prs.0000105044.03230.f4>.
50. Lemo, N.; Marignac, G.; Reyes-Gomez, E.; Lilin, T.; Crosaz, O.; Ehrenfest, D.D. Cutaneous reepithelialization and wound contraction after skin biopsies in rabbits: A mathematical model for healing and remodelling index. *VETERINARSKI ARHIV* **2010**, *80*, 637–652.
51. Schencke, C.; Vasconcellos, A.; Sandoval, C.; Torres, P.; Acevedo, F.; Del Sol, M. Morphometric evaluation of wound healing in burns treated with Ulmo (*Eucryphia cordifolia*) honey alone and supplemented with ascorbic acid in guinea pig (*Cavia porcellus*). *Burn. Trauma.* **2016**, *4*, 25. <https://doi.org/10.1186/s41038-016-0050-z>.
52. Bankhead, P.; Loughrey, M.B.; Fernandez, J.A.; Dombrowski, Y.; McArt, D.G.; Dunne, P.D.; McQuaid, S.; Gray, R.T.; Murray, L.J.; Coleman, H.G.; et al. QuPath: Open source software for digital pathology image analysis. *Sci. Rep.* **2017**, *7*, 16878. <https://doi.org/10.1038/s41598-017-17204-5>.

**Disclaimer/Publisher's Note:** The statements, opinions and data contained in all publications are solely those of the individual author(s) and contributor(s) and not of MDPI and/or the editor(s). MDPI and/or the editor(s) disclaim responsibility for any injury to people or property resulting from any ideas, methods, instructions or products referred to in the content.

---

## 7. Podsumowanie i wnioski

Wiele badań nowych interwencji w gojeniu ran opiera się na mysim modelu db/db lub ob/ob jako imitujących fenotyp cukrzycy typu II. Pomimo ich ograniczeń utrudniających przenoszenie wyników na ludzi, pozostają one wiarygodnymi i szeroko badanymi modelami zwierzęcymi. Ich siła opiera się na starannie zbadanych mechanizmach gojenia ran zarówno na poziomie lokalnym, jak i ogólnoustrojowym, wraz z zadowalającym odzwierciedleniem patologii występujących w ludzkich ranach cukrzycowych. Badania mechanistyczne ujawniły pewien stopień podobieństwa i rozbieżności między modelami zwierzęcymi a fizjologią człowieka. Przy zachowaniu pewnych środków ostrożności, zwłaszcza w odniesieniu do monogenowej natury modelu, mogą one być dalej wykorzystywane w przedklinicznych badaniach gojenia się ran.

W przeprowadzonym badaniu oryginalnym miejscowo stosowany hydrożel uwalniający 5% N-acetylocysteinę poprawił szybkość zamykania się rany cukrzycowej na wczesnych etapach gojenia, czemu towarzyszyła zwiększona proliferacja skóry przylegającej do rany w ocenie histologicznej w porównaniu z hydrożelem kontrolnym. Wyższe stężenia NAC nie miały korzystnego wpływu na proces gojenia się ran w mysim modelu cukrzycy typu II z niedoborem leptyny. Przyszłe badania powinny koncentrować się na optymalizacji stężenia NAC i drogi podawania w procesie gojenia ran cukrzycowych. Badania *in vivo* powinny koncentrować się na badaniu mechanizmu działania NAC, zwłaszcza jej potencjału do poprawy proliferacji komórek. Eksperymenty powinny ściśle odzwierciedlać warunki gojenia się ran u ludzi. Dlatego też, jeśli są przeprowadzane na modelach mysich, należy zastosować szynowanie (*splinting*), aby przeciwdziałać silnemu mechanizmowi skurczu skóry, obecnemu u gryzoni. Wobec korzystnych wyników wspomagania gojenia oraz braku ewidentnych działań niepożądanych potencjalnie możliwa jest translacja badań na organizm ludzki.

## 8. Opinia komisji etycznej

Poniżej znajduje się zgoda komisji etycznej na przeprowadzenie opisanego wyżej doświadczenia.

# UCHWAŁA NR WAW2/029/2021

z dnia 24 lutego 2021 r.

II Lokalnej Komisji Etycznej do Spraw Doświadczeń na Zwierzętach w Warszawie

## § 1

Na podstawie art. 48 ust. 1 pkt. 1<sup>1</sup> ustawy z dnia 15 stycznia 2015r. o ochronie zwierząt wykorzystywanych do celów naukowych lub edukacyjnych (Dz. U. z 2019 r. poz. 1392), zwanej dalej „ustawą” po rozpatrzeniu wniosku pt.: „**Wpływ N-acetylocysteiny na gojenie ran w modelu cukrzycy u myszy db/db**” z dnia 15 stycznia 2021 roku, złożonego przez Centrum Badań Przedklinicznych CBP WUM, adres: ul. Banacha 1B, 02-097 Warszawa, zaplanowanego przez Pawła Włodarskiego<sup>2</sup> przy udziale:<sup>3</sup> (nie dotyczy)

Lokalna Komisja Etyczna:

## WYRAŻA ZGODĘ

na przeprowadzenie doświadczeń na zwierzętach w zakresie wniosku.

## § 2

W wyniku rozpatrzenia wniosku o którym mowa w § 1, Lokalna Komisja Etyczna ustaliła, że:

1. Wniosek należy przypisać do kategorii: badania podstawowe: układ wewnątrzwydzielniczy lub metabolizm.
2. Najwyższy stopień dotkliwości proponowanych procedur to: dotkliwe.
3. Doświadczenia będą przeprowadzane na gatunkach lub grupach gatunków<sup>4</sup>:

Gatunek	Wiek/stadium	Liczba
Mysz domowa ( <i>Mus musculus</i> ) szczepu BKS(D)- <i>Lepr<sup>db</sup></i> /JorlRj	10 tygodni	20

4. Doświadczenia będą przeprowadzane przez: Paweł Włodarski, Wiktor Paskal, Albert Stachura, Agata Gondek, Robert Wrzesień.
5. Doświadczenie będzie przeprowadzane w terminie<sup>5</sup> od 01.04.2021 do 01.04.2025.
6. Doświadczenie będzie przeprowadzone w ośrodku<sup>6</sup>: nie dotyczy.
7. Doświadczenie będzie przeprowadzone poza ośrodkiem, w: nie dotyczy.
8. Użyte do procedur zwierzęta dzikie zostaną odłowione przez: nie dotyczy.
9. Doświadczenie zostanie/~~nie zostanie~~ poddane ocenie retrospektywnej na podstawie art. 53 ust. 1 ustawy w terminie do 6 miesięcy od dnia przekazania przez użytkownika dokumentacji, mającej stanowić podstawę dokonania oceny retrospektywnej. Użytkownik jest zobowiązany do przekazania ww. dokumentacji niezwłocznie, tj. w terminie, o którym mowa w art. 52 ust. 2 ustawy.

<sup>1</sup> Niewłaściwy zapis usunąć

<sup>2</sup> imię i nazwisko osoby, która zaplanowała i jest odpowiedzialna za przeprowadzenie doświadczenia

<sup>3</sup> Wypełnić w przypadku dopuszczenia do postępowania organizacji społecznej.

<sup>4</sup> Podać liczbę, szczep/stado, wiek/stadium rozwoju

<sup>5</sup> Nie dłużej niż 5 lat

<sup>6</sup> Podać jeśli jest to inny ośrodek niż użytkownik

### § 3


#### Uzasadnienie:

Komisja oceniła wniosek zgodnie z art. 47 ust. 1 i 2 ustawy z dnia 15 stycznia 2015 r. o ochronie zwierząt wykorzystywanych do celów naukowych lub edukacyjnych (Dz. U. z 2019 r. poz. 1392). Po zapoznaniu się z problematyką badawczą przedstawioną we wniosku komisja stwierdza, że przedstawiony projekt spełnia zasady dopuszczenia doświadczeń na zwierzętach pod kątem oceny etycznej. Na podstawie art. 107 § 4 ustawy z dnia 14 czerwca 1960 r. – Kodeks postępowania administracyjnego z późniejszymi zmianami (Dz. U. 2020 r. poz. 256) odstąpiono od sporządzania uzasadnienia decyzji, gdyż decyzja jest zgodna z wnioskiem strony.

### § 4

Integralną część niniejszej uchwały stanowi kopia wniosku, o którym mowa w § 1.

Szkoła Główna Gospodarstwa Wiejskiego  
w Warszawie  
II Lokalna Komisja Etyczna  
ds. Doświadczeń na Zwierzętach  
02-786 Warszawa, ul. Ciszewskiego 8  
tel. 22 59-35622  
(Pieczęć lokalnej komisji etycznej)

PRZEWODNICZĄCA  
II Lokalnej Komisji Etycznej  
ds. Doświadczeń na Zwierzętach przy SGGW  
  
/ Prof. dr hab. Joanna Gromadzka-Ustrowska /  
(Podpis Przewodniczącej Komisji)

#### Pouczenie:

Zgodnie z art. 33 ust. 3 i art. 40 ustawy w zw. z art. 127 § 1 i 2 oraz 129 § 2 ustawy z dnia z dnia 14 czerwca 1960 r. Kodeks postępowania administracyjnego (Dz. U. 2017, poz. 1257 – tj.; dalej KPA) od uchwały Lokalnej Komisji Etycznej strona może wnieść, za jej pośrednictwem, odwołanie do Krajowej Komisji Etycznej do Spraw Doświadczeń na Zwierzętach w terminie 14 od dnia doręczenia uchwały.

Na podstawie art. 127a KPA w trakcie biegu terminu do wniesienia odwołania strona może zrzec się prawa do jego wniesienia, co należy uczynić wobec Lokalnej Komisji Etycznej, która wydała uchwałę. Z dniem doręczenia Lokalnej Komisji Etycznej oświadczenia o zrzeczeniu się prawa do wniesienia odwołania przez ostatnią ze stron postępowania, decyzja staje się ostateczna i prawomocna.

#### Otrzymuje:

- 1) Użytkownik,
- 2) Organizacja społeczna dopuszczona do udziału w postępowaniu (jeśli dotyczy)
- 3) a/a

#### Użytkownik kopie przekazuje:

- Osoba planująca doświadczenie
- Zespół ds. dobrostanu

---

## **9. Oświadczenia współautorów publikacji**

Poniżej znajdują się oświadczenia współautorów publikacji, określające indywidualny wkład każdego z nich w ich powstanie.



Warszawa, 18.09.2024r.  
(miejsowość, data)

Ishani Khanna  
(imię i nazwisko)

## OŚWIADCZENIE

Jako współautorka pracy pt. *Wound Healing Impairment in Type 2 Diabetes Model of Leptin-Deficient Mice—A Mechanistic Systematic Review* oświadczam, iż mój własny wkład merytoryczny w przygotowanie, przeprowadzenie i opracowanie badań oraz przedstawienie pracy w formie publikacji stanowi:  
pisanie części manuskryptu, edycję tekstu, przegląd literatury.

Mój udział procentowy w przygotowaniu publikacji określam jako 20%.

Wkład Alberta Stachury w powstawanie publikacji określam jako 60%,

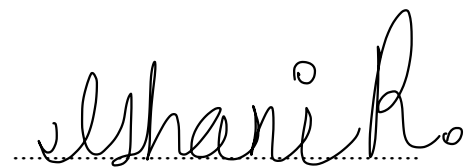
(imię i nazwisko kandydata do stopnia)

obejmował on: przygotowanie koncepcji, opracowanie tematu pracy, opracowanie metodologii, przegląd literatury, ekstrakcję danych, interpretację wyników, pisanie manuskryptu, edycję tekstu.

(merytoryczny opis wkładu kandydata do stopnia w powstanie publikacji)\*

Jednocześnie wyrażam zgodę na wykorzystanie w/w pracy jako część rozprawy doktorskiej  
lek. Alberta Stachury

(imię i nazwisko kandydata do stopnia)



(podpis oświadczającego)

\*w szczególności udziału w przygotowaniu koncepcji, metodyki, wykonaniu badań, interpretacji wyników

Warszawa, 18.09.2024r.  
(miejsowość, data)

Piotr Krysiak  
(imię i nazwisko)

## OŚWIADCZENIE

Jako współautor pracy pt. *Wound Healing Impairment in Type 2 Diabetes Model of Leptin-Deficient Mice—A Mechanistic Systematic Review* oświadczam, iż mój własny wkład merytoryczny w przygotowanie, przeprowadzenie i opracowanie badań oraz przedstawienie pracy w formie publikacji stanowi:  
pisanie części manuskryptu, edycję tekstu, przegląd literatury.

Mój udział procentowy w przygotowaniu publikacji określam jako 10%.

Wkład Alberta Stachury w powstawanie publikacji określam jako 60%,

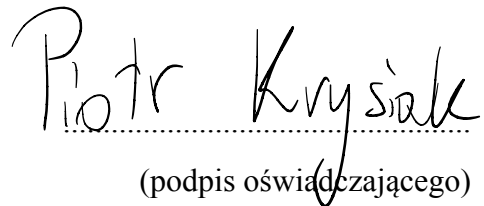
(imię i nazwisko kandydata do stopnia)

obejmował on: przygotowanie koncepcji, opracowanie tematu pracy, opracowanie metodologii, przegląd literatury, ekstrakcję danych, interpretację wyników, pisanie manuskryptu, edycję tekstu.

(merytoryczny opis wkładu kandydata do stopnia w powstanie publikacji)\*

Jednocześnie wyrażam zgodę na wykorzystanie w/w pracy jako część rozprawy doktorskiej lek. Alberta Stachury

(imię i nazwisko kandydata do stopnia)

  
(podpis oświadczającego)

\*w szczególności udziału w przygotowaniu koncepcji, metodyki, wykonaniu badań, interpretacji wyników

Warszawa, 18.09.2024r.  
(miejsowość, data)

Wiktor Pascal  
(imię i nazwisko)

## OŚWIADCZENIE

Jako współautor pracy pt. *Wound Healing Impairment in Type 2 Diabetes Model of Leptin-Deficient Mice—A Mechanistic Systematic Review* oświadczam, iż mój własny wkład merytoryczny w przygotowanie, przeprowadzenie i opracowanie badań oraz przedstawienie pracy w formie publikacji stanowi:

superwizja projektu, edycja tekstu, opracowanie metodologii.

Mój udział procentowy w przygotowaniu publikacji określam jako 5%.

Wkład Alberta Stachury w powstawanie publikacji określam jako 60%,

(imię i nazwisko kandydata do stopnia)

obejmował on: przygotowanie koncepcji, opracowanie tematu pracy, opracowanie metodologii, przegląd literatury, ekstrakcję danych, interpretację wyników, pisanie manuskryptu, edycję tekstu.

(merytoryczny opis wkładu kandydata do stopnia w powstanie publikacji)\*

Jednocześnie wyrażam zgodę na wykorzystanie w/w pracy jako część rozprawy doktorskiej lek. Alberta Stachury

(imię i nazwisko kandydata do stopnia)



.....  
(podpis oświadczającego)

\*w szczególności udziału w przygotowaniu koncepcji, metodyki, wykonaniu badań, interpretacji wyników

Warszawa, 18.09.2024

prof. Paweł Włodarski

## OŚWIADCZENIE


Jako współautor pracy pt. *Wound Healing Impairment in Type 2 Diabetes Model of Leptin-Deficient Mice—A Mechanistic Systematic Review* oświadczam, iż mój własny wkład merytoryczny w przygotowanie, przeprowadzenie i opracowanie badań oraz przedstawienie pracy w formie publikacji stanowi:  
superwizja projektu, edycja tekstu, opracowanie metodologii.

Mój udział procentowy w przygotowaniu publikacji określam jako 5%.

Wkład lek. Alberta Stachury w powstawanie publikacji określam jako 60%.

Wkład lek. Alberta Stachury obejmował: przygotowanie koncepcji, opracowanie tematu pracy, opracowanie metodologii, przegląd literatury, ekstrakcję danych, interpretację wyników, pisanie manuskryptu, edycję tekstu.

Jednocześnie wyrażam zgodę na wykorzystanie w/w pracy jako część rozprawy doktorskiej lek. Alberta Stachury

  
(podpis oświadczającego)

Warszawa, 18.09.2024 r.

prof. Marcin Sobczak  
(imię i nazwisko)

## OŚWIADCZENIE

Jako współautor pracy pt. *The Influence of N-Acetylcysteine-Enriched Hydrogels on Wound Healing in a Murine Model of Type II Diabetes Mellitus* oświadczam, iż mój własny wkład merytoryczny w przygotowanie, przeprowadzenie i opracowanie badań oraz przedstawienie pracy w formie publikacji stanowi:

opracowanie metodologii, analizę danych, wykonanie badań (dot. syntezy hydrożelu), wizualizacja danych, pisanie manuskryptu, edycja tekstu.

Mój udział procentowy w przygotowaniu publikacji określam jako 15%.

Wkład Alberta Stachury w powstawanie publikacji określam jako 50%.

(imię i nazwisko kandydata do stopnia)

obejmował on: przygotowanie koncepcji, opracowanie tematu pracy, opracowanie metodologii, wykonanie badań, analiza danych, interpretacja danych, wizualizacja danych, pisanie manuskryptu, edycja tekstu.

(merytoryczny opis wkładu kandydata do stopnia w powstanie publikacji)\*

Jednocześnie wyrażam zgodę na wykorzystanie w/w pracy jako część rozprawy doktorskiej lek. Alberta Stachury.

(imię i nazwisko kandydata do stopnia)

Podpisany elektronicznie przez  
Marcin Andrzej Sobczak  
25.09.2024  
19:31:00 +02'00'

.....

\*w szczególności udziału w przygotowaniu koncepcji, metodyki, wykonaniu badań, interpretacji wyników

Warszawa, 18.09.2024r.  
(miejsowość, data)

Karolina Kędra  
(imię i nazwisko)

## OŚWIADCZENIE

Jako współautorka pracy pt. *The Influence of N-Acetylcysteine-Enriched Hydrogels on Wound Healing in a Murine Model of Type II Diabetes Mellitus* oświadczam, iż mój własny wkład merytoryczny w przygotowanie, przeprowadzenie i opracowanie badań oraz przedstawienie pracy w formie publikacji stanowi:  
opracowanie metodologii, analiza danych, wykonanie badań (dot. syntezy hydrożelu), wizualizacja danych, pisanie manuskryptu, edycja tekstu

Mój udział procentowy w przygotowaniu publikacji określam jako 15%.

Wkład Alberta Stachury w powstawanie publikacji określam jako 50%,

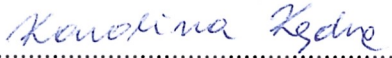
(imię i nazwisko kandydata do stopnia)

obejmował on: przygotowanie koncepcji, opracowanie tematu pracy, opracowanie metodologii, wykonanie badań, analiza danych, interpretacja danych, wizualizacja danych, pisanie manuskryptu, edycja tekstu

(merytoryczny opis wkładu kandydata do stopnia w powstanie publikacji)\*

Jednocześnie wyrażam zgodę na wykorzystanie w/w pracy jako część rozprawy doktorskiej lek. Alberta Stachury

(imię i nazwisko kandydata do stopnia)



(podpis oświadczającego)

\*w szczególności udziału w przygotowaniu koncepcji, metodyki, wykonaniu badań, interpretacji wyników



Warszawa, 18.09.2024r. [1] [2] (miejsowość, data)

Karolina Kopka  
(imię i nazwisko) [1] [2]

## OŚWIADCZENIE

Jako współautorka pracy pt. *The Influence of N-Acetylcysteine-Enriched Hydrogels on Wound Healing in a Murine Model of Type II Diabetes Mellitus* oświadczam, iż mój własny wkład merytoryczny w przygotowanie, przeprowadzenie i opracowanie badań oraz przedstawienie pracy w formie publikacji stanowi:  
analiza danych, wykonanie badań, wizualizacja danych

Mój udział procentowy w przygotowaniu publikacji określam jako 8%.

Wkład Alberta Stachury w powstawanie publikacji określam jako 50%,

(imię i nazwisko kandydata do stopnia)

obejmował on: przygotowanie koncepcji, opracowanie tematu pracy, opracowanie metodologii, wykonanie badań, analiza danych, interpretacja danych, wizualizacja danych, pisanie manuskryptu, edycja tekstu

(merytoryczny opis wkładu kandydata do stopnia w powstanie publikacji)\*

Jednocześnie wyrażam zgodę na wykorzystanie w/w pracy jako część rozprawy doktorskiej lek. Alberta Stachury

(imię i nazwisko kandydata do stopnia)



PODPIS ZAUFANY  
KAROLINA  
KOPKA  
18.09.2024 17:58:16 (GMT+2)  
Dokument podpisany elektronicznie  
podpisem zaufanym

[1] [2]  
.....[SEP]

(podpis  
oświadczającego)

\*w szczególności udziału w przygotowaniu koncepcji, metodyki, wykonaniu badań, interpretacji wyników

**Warszawa, 18.09.2024r.** <sup>17</sup> <sub>SEP</sub> <sup>17</sup> (miejsowość, data)

Michał Kopka  
(imię i nazwisko) <sup>17</sup> <sub>SEP</sub> <sup>17</sup>

## OŚWIADCZENIE

Jako współautor pracy pt. *The Influence of N-Acetylcysteine-Enriched Hydrogels on Wound Healing in a Murine Model of Type II Diabetes Mellitus* oświadczam, iż mój własny wkład merytoryczny w przygotowanie, przeprowadzenie i opracowanie badań oraz przedstawienie pracy w formie publikacji stanowi:  
analiza danych, wykonanie badań, wizualizacja danych

Mój udział procentowy w przygotowaniu publikacji określam jako 8%.

Wkład Alberta Stachury w powstawanie publikacji określam jako 50%,

(imię i nazwisko kandydata do stopnia)

obejmował on: przygotowanie koncepcji, opracowanie tematu pracy, opracowanie metodologii, wykonanie badań, analiza danych, interpretacja danych, wizualizacja danych, pisanie manuskryptu, edycja tekstu

(merytoryczny opis wkładu kandydata do stopnia w powstanie publikacji)\*

Jednocześnie wyrażam zgodę na wykorzystanie w/w pracy jako część rozprawy doktorskiej lek. Alberta Stachury

(imię i nazwisko kandydata do stopnia)

..... <sup>17</sup> <sub>SEP</sub> <sup>17</sup>

(podpis  
oświadczającego)



\*w szczególności udziału w przygotowaniu koncepcji, metodyki, wykonaniu badań, interpretacji wyników

Warszawa, 18.09.2024

prof. Paweł Włodarski

## OŚWIADCZENIE


Jako współautor pracy pt. *The Influence of N-Acetylcysteine-Enriched Hydrogels on Wound Healing in a Murine Model of Type II Diabetes Mellitus* oświadczam, iż mój własny wkład merytoryczny w przygotowanie, przeprowadzenie i opracowanie badań oraz przedstawienie pracy w formie publikacji stanowi:  
przygotowanie koncepcji, superwizja projektu, opracowanie metodologii

Mój udział procentowy w przygotowaniu publikacji określam jako 4%.

Wkład lek. Alberta Stachury w powstawanie publikacji określam jako 50%,

Wkład lek. Alberta Stachury obejmował: przygotowanie koncepcji, opracowanie tematu pracy, opracowanie metodologii, wykonanie badań, analiza danych, interpretacja danych, wizualizacja danych, pisanie manuskryptu, edycja tekstu

Jednocześnie wyrażam zgodę na wykorzystanie w/w pracy jako część rozprawy doktorskiej lek. Alberta Stachury

  
(podpis oświadczającego)

---

## 10. Referencje

- 1 Harris, M. I. Impaired glucose tolerance in the U.S. population. *Diabetes Care* **12**, 464-474 (1989). <https://doi.org:10.2337/diacare.12.7.464>
- 2 Saeedi, P. *et al.* Global and regional diabetes prevalence estimates for 2019 and projections for 2030 and 2045: Results from the International Diabetes Federation Diabetes Atlas, 9(th) edition. *Diabetes Res Clin Pract* **157**, 107843 (2019). <https://doi.org:10.1016/j.diabres.2019.107843>
- 3 Engelgau, M. M. *et al.* The evolving diabetes burden in the United States. *Ann Intern Med* **140**, 945-950 (2004). <https://doi.org:10.7326/0003-4819-140-11-200406010-00035>
- 4 Sullivan, P. W., Morrato, E. H., Ghushchyan, V., Wyatt, H. R. & Hill, J. O. Obesity, inactivity, and the prevalence of diabetes and diabetes-related cardiovascular comorbidities in the U.S., 2000-2002. *Diabetes Care* **28**, 1599-1603 (2005). <https://doi.org:10.2337/diacare.28.7.1599>
- 5 Institute for Health Metrics and Evaluation (IHME). Global Burden of Disease 2021: Findings from the GBD 2021 Study. Seattle, WA: IHME, 2024.
- 6 Edmonds, M., Manu, C. & Vas, P. The current burden of diabetic foot disease. *J Clin Orthop Trauma* **17**, 88-93 (2021). <https://doi.org:10.1016/j.jcot.2021.01.017>
- 7 Greenhalgh, D. G. Wound healing and diabetes mellitus. *Clin Plast Surg* **30**, 37-45 (2003). [https://doi.org:10.1016/s0094-1298\(02\)00066-4](https://doi.org:10.1016/s0094-1298(02)00066-4)
- 8 Everett, E. & Mathioudakis, N. Update on management of diabetic foot ulcers. *Ann N Y Acad Sci* **1411**, 153-165 (2018). <https://doi.org:10.1111/nyas.13569>
- 9 Tsourdi, E., Barthel, A., Rietzsch, H., Reichel, A. & Bornstein, S. R. Current aspects in the pathophysiology and treatment of chronic wounds in diabetes mellitus. *Biomed Res Int* **2013**, 385641 (2013). <https://doi.org:10.1155/2013/385641>
- 10 Hennessey, P. J., Ford, E. G., Black, C. T. & Andrassy, R. J. Wound collagenase activity correlates directly with collagen glycosylation in diabetic rats. *J Pediatr Surg* **25**, 75-78 (1990). [https://doi.org:10.1016/s0022-3468\(05\)80167-8](https://doi.org:10.1016/s0022-3468(05)80167-8)
- 11 Spravchikov, N. *et al.* Glucose effects on skin keratinocytes: implications for diabetes skin complications. *Diabetes* **50**, 1627-1635 (2001). <https://doi.org:10.2337/diabetes.50.7.1627>
- 12 Marhoffer, W., Stein, M., Maeser, E. & Federlin, K. Impairment of polymorphonuclear leukocyte function and metabolic control of diabetes. *Diabetes care* **15**, 256-260 (1992).

- 
- 13 Fahey III, T. J. *et al.* Diabetes impairs the late inflammatory response to wound healing. *Journal of Surgical Research* **50**, 308-313 (1991).
- 14 Stachura, A., Khanna, I., Krysiak, P., Paskal, W. & Włodarski, P. Wound Healing Impairment in Type 2 Diabetes Model of Leptin-Deficient Mice-A Mechanistic Systematic Review. *Int J Mol Sci* **23** (2022). <https://doi.org:10.3390/ijms23158621>
- 15 Stachura, A. *et al.* The Influence of N-Acetylcysteine-Enriched Hydrogels on Wound Healing in a Murine Model of Type II Diabetes Mellitus. *International Journal of Molecular Sciences* **25**, 9986 (2024).
- 16 Sanapalli, B. K. R., Yele, V., Singh, M. K., Thaggikuppe Krishnamurthy, P. & Karri, V. V. S. R. Preclinical models of diabetic wound healing: A critical review. *Biomedicine & Pharmacotherapy* **142**, 111946 (2021). <https://doi.org:https://doi.org/10.1016/j.biopha.2021.111946>
- 17 Remoué, N., Bonod, C., Fromy, B. & Sigaucho-Roussel, D. in *Innovations and Emerging Technologies in Wound Care* (ed Amit Gefen) 197-224 (Academic Press, 2020).
- 18 Ahn, S. T. & Mustoe, T. A. Effects of Ischemia on Ulcer Wound Healing: A New Model in the Rabbit Ear. *Annals of Plastic Surgery* **24** (1990).
- 19 Zhao, L. L., Davidson, J. D., Chin Wee, S., Roth, S. I. & Mustoe, T. A. Effect of Hyperbaric Oxygen and Growth Factors on Rabbit Ear Ischemic Ulcers. *Archives of Surgery* **129**, 1043-1049 (1994). <https://doi.org:10.1001/archsurg.1994.01420340057010>
- 20 Cohen, I. K., Moore, C. D. & Diegelmann, R. F. Onset and Localization of Collagen Synthesis during Wound Healing in Open Rat Skin Wounds. *Proceedings of the Society for Experimental Biology and Medicine* **160**, 458-462 (1979). <https://doi.org:10.3181/00379727-160-40470>
- 21 Singh, R., Gholipourmalekabadi, M. & Shafikhani, S. H. Animal models for type 1 and type 2 diabetes: advantages and limitations. *Frontiers in Endocrinology* **15** (2024). <https://doi.org:10.3389/fendo.2024.1359685>
- 22 Brem, H. *et al.* The synergism of age and db/db genotype impairs wound healing. *Exp Gerontol* **42**, 523-531 (2007). <https://doi.org:10.1016/j.exger.2006.11.018>
- 23 Michaels, J. t. *et al.* db/db mice exhibit severe wound-healing impairments compared with other murine diabetic strains in a silicone-splinted excisional wound model. *Wound Repair Regen* **15**, 665-670 (2007). <https://doi.org:10.1111/j.1524-475X.2007.00273.x>

- 
- 24 Wieman, T. J., Smiell, J. M. & Su, Y. Efficacy and Safety of a Topical Gel Formulation of Recombinant Human Platelet-Derived Growth Factor-BB (Becaplermin) in Patients With Chronic Neuropathic Diabetic Ulcers: A phase III randomized placebo-controlled double-blind study. *Diabetes Care* **21**, 822-827 (1998). <https://doi.org:10.2337/diacare.21.5.822>
- 25 Papanas, D. & Maltezos, E. Benefit-Risk Assessment of Becaplermin in the Treatment of Diabetic Foot Ulcers. *Drug Safety* **33**, 455-461 (2010). <https://doi.org:10.2165/11534570-000000000-00000>
- 26 Lebrun, E., Tomic-Canic, M. & Kirsner, R. S. The role of surgical debridement in healing of diabetic foot ulcers. *Wound Repair Regen* **18**, 433-438 (2010). <https://doi.org:10.1111/j.1524-475X.2010.00619.x>
- 27 Karavan, M., Olerud, J., Bouldin, E., Taylor, L. & Reiber, G. E. Evidence-based chronic ulcer care and lower limb outcomes among Pacific Northwest veterans. *Wound Repair Regen* **23**, 745-752 (2015). <https://doi.org:10.1111/wrr.12341>
- 28 Liu, Z. *et al.* Negative pressure wound therapy for treating foot wounds in people with diabetes mellitus. *Cochrane Database Syst Rev* **10**, Cd010318 (2018). <https://doi.org:10.1002/14651858.CD010318.pub3>
- 29 Santema, T. B., Poyck, P. P. & Ubbink, D. T. Skin grafting and tissue replacement for treating foot ulcers in people with diabetes. *Cochrane Database Syst Rev* **2**, Cd011255 (2016). <https://doi.org:10.1002/14651858.CD011255.pub2>
- 30 Stoekenbroek, R. M. *et al.* Hyperbaric oxygen for the treatment of diabetic foot ulcers: a systematic review. *Eur J Vasc Endovasc Surg* **47**, 647-655 (2014). <https://doi.org:10.1016/j.ejvs.2014.03.005>
- 31 Liu, R., Li, L., Yang, M., Boden, G. & Yang, G. Systematic review of the effectiveness of hyperbaric oxygenation therapy in the management of chronic diabetic foot ulcers. *Mayo Clin Proc* **88**, 166-175 (2013). <https://doi.org:10.1016/j.mayocp.2012.10.021>
- 32 Wu, L., Norman, G., Dumville, J. C., O'Meara, S. & Bell-Syer, S. E. Dressings for treating foot ulcers in people with diabetes: an overview of systematic reviews. *Cochrane Database Syst Rev* **2015**, Cd010471 (2015). <https://doi.org:10.1002/14651858.CD010471.pub2>
- 33 Atkin, L. *et al.* Implementing TIMERS: the race against hard-to-heal wounds. *J Wound Care* **23**, S1-s50 (2019). <https://doi.org:10.12968/jowc.2019.28.Sup3a.S1>



- 
- 34 Atkuri, K. R., Mantovani, J. J., Herzenberg, L. A. & Herzenberg, L. A. N-Acetylcysteine--a safe antidote for cysteine/glutathione deficiency. *Curr Opin Pharmacol* **7**, 355-359 (2007). <https://doi.org:10.1016/j.coph.2007.04.005>
- 35 Zafarullah, M., Li, W. Q., Sylvester, J. & Ahmad, M. Molecular mechanisms of N-acetylcysteine actions. *Cell Mol Life Sci* **60**, 6-20 (2003). <https://doi.org:10.1007/s000180300001>
- 36 Samuni, Y., Goldstein, S., Dean, O. M. & Berk, M. The chemistry and biological activities of N-acetylcysteine. *Biochim Biophys Acta* **1830**, 4117-4129 (2013). <https://doi.org:10.1016/j.bbagen.2013.04.016>
- 37 Dean, O., Giorlando, F. & Berk, M. N-acetylcysteine in psychiatry: current therapeutic evidence and potential mechanisms of action. *J Psychiatry Neurosci* **36**, 78-86 (2011). <https://doi.org:10.1503/jpn.100057>
- 38 Janeczek, M. *et al.* The Potential Uses of N-acetylcysteine in Dermatology: A Review. *J Clin Aesthet Dermatol* **12**, 20-26 (2019).
- 39 Nakai, K. *et al.* Effects of Topical N-Acetylcysteine on Skin Hydration/Transepidermal Water Loss in Healthy Volunteers and Atopic Dermatitis Patients. *Ann Dermatol* **27**, 450-451 (2015). <https://doi.org:10.5021/ad.2015.27.4.450>
- 40 Calverley, P., Rogliani, P. & Papi, A. Safety of N-Acetylcysteine at High Doses in Chronic Respiratory Diseases: A Review. *Drug Saf* **44**, 273-290 (2021). <https://doi.org:10.1007/s40264-020-01026-y>
- 41 Guo, S. & Dipietro, L. A. Factors affecting wound healing. *J Dent Res* **89**, 219-229 (2010). <https://doi.org:10.1177/0022034509359125>
- 42 Tsai, M. L. *et al.* Topical N-acetylcysteine accelerates wound healing in vitro and in vivo via the PKC/Stat3 pathway. *Int J Mol Sci* **15**, 7563-7578 (2014). <https://doi.org:10.3390/ijms15057563>
- 43 Oguz, A. *et al.* Topical N-acetylcysteine improves wound healing comparable to dexpanthenol: an experimental study. *Int Surg* **100**, 656-661 (2015). <https://doi.org:10.9738/INTSURG-D-14-00227.1>
- 44 Paskal, W. *et al.* N-Acetylcysteine Added to Local Anesthesia Reduces Scar Area and Width in Early Wound Healing-An Animal Model Study. *Int J Mol Sci* **22** (2021). <https://doi.org:10.3390/ijms22147549>